

UCLA

UCLA Electronic Theses and Dissertations

Title

Strength of Chimeric Antigen Receptor Signaling Determines T versus Type 2 Innate Lymphoid Cell Lineage Differentiation from Pluripotent Stem Cells

Permalink

<https://escholarship.org/uc/item/0190x8b8>

Author

Li, Suwen

Publication Date

2022

Peer reviewed|Thesis/dissertation

UNIVERSITY OF CALIFORNIA

Los Angeles

Strength of Chimeric Antigen Receptor Signaling Determines
T versus Type 2 Innate Lymphoid Cell Lineage Differentiation
from Pluripotent Stem Cells

A dissertation submitted in partial satisfaction of the
requirements for the degree Doctor of Philosophy
in Molecular and Medical Pharmacology

by

Suwen Li

2022

© Copyright by

Suwen Li

2022

ABSTRACT OF THE DISSERTATION

Strength of Chimeric Antigen Receptor Signaling Determines
T versus Type 2 Innate Lymphoid Cell Lineage Differentiation
from Pluripotent Stem Cells

by

Suwen Li

Doctor of Philosophy in Molecular and Medical Pharmacology

University of California, Los Angeles, 2022

Professor Gay M. Crooks, Co-Chair

Professor Caius Gabriel Radu, Co-Chair

T cells and Type 2 innate lymphoid cells (ILC2) are closely related lymphoid lineages which share certain developmental and transcriptional programs, including a requirement for Notch and IL-7 signaling during differentiation. The recently described artificial thymic organoid (ATO) system supports *in vitro* differentiation of human pluripotent stem cells (PSCs) to mature $\alpha\beta$ T cells. Unexpectedly, PSCs transduced with a CD19-targeted chimeric antigen receptor (CAR) resulted in ILC2-biased lymphopoiesis and a block in T cell differentiation in ATOs. PSC-derived CAR-ILC2s expressed classical ILC2 markers and gene expression, and surprisingly responded to both cytokine stimuli and antigen-induced CAR signaling.

Mechanistically, single cell RNA-seq of early lymphoid precursors in ATOs revealed evidence of CAR activation in ILC2 precursors, and rational modulation of CAR signaling could restore generation of functional CAR-T cells from PSCs or, conversely, divert CAR-T cell differentiation to ILC2 and, to a lesser extent, NK/ILC1 lineages. Taken together, our findings shed light on human T and ILC2 lineage development and provide a framework for applying CAR technology to the generation of multiple lymphoid lineages from PSCs.

The dissertation of Suwen Li is approved.

Kenneth A. Dorshkind

Donald Barry Kohn

Caius Gabriel Radu, Committee Co-Chair

Gay M. Crooks, Committee Co-Chair

University of California, Los Angeles

2022

TABLE OF CONTENTS

ABSTRACT OF THE DISSERTATION	ii
TABLE OF CONTENTS.....	v
LIST OF FIGURES	viii
ACKNOWLEDGMENTS	x
CURRICULUM VITAE.....	xii
CHAPTER 1: Introduction	1
1.1 Human thymic T cell development.....	1
1.2 T cell-based immunotherapies	2
1.3 In vitro T cell generation from HSPC.....	4
1.4 In vitro generation of engineered T cells from HSPC	6
1.5 In vitro generation of T cells from PSC.....	7
1.6 In vitro generation of antigen specific T cells from PSC.....	9
1.7 In vitro generation of CAR-T cell from PSC.....	11
1.8 Human innate lymphoid cell subsets	14
1.9 ILC development	15
1.10 ILC2s in the thymus.....	16
1.11 In vitro generation of ILC2s	18
1.12 Role of ILC2 in cancer.....	19

CHAPTER 2: Strength of CAR Signaling Determines T versus ILC2 Lineage Differentiation

from Pluripotent Stem Cells.....	20
2.1 Introduction.....	20
2.2 Materials and Methods.....	22
2.2.1 Experimental models and subject details	22
2.2.1.1 Cell lines	22
2.2.1.2 Human pluripotent cell lines	22
2.2.2 Methods details	23
2.2.2.1 Generation and isolation of human embryonic mesodermal progenitors (hEMPs)	23
2.2.2.2 Pluripotent stem cell-derived embryonic mesoderm organoids (EMO) and reaggregated artificial thymic organoid (ATO) cultures	23
2.2.2.3 Lentiviral vectors and transduction.....	25
2.2.2.4 Flow Cytometry	26
2.2.2.5 In vitro proliferation assays	27
2.2.2.6 Intracellular cytokine assays	27
2.2.2.7 In vitro ILC2 plasticity assay	28
2.2.2.8 In vitro cytotoxicity assays	29
2.2.2.9 Bulk RNA sequencing	29
2.2.2.10 Bulk RNA sequencing data processing.....	30
2.2.2.11 Single cell RNA sequencing	30
2.2.2.12 Single cell RNA sequencing data processing	31
2.2.2.13 Gene set enrichment analysis (GSEA).....	32

2.2.2.14 Quantification and statistical analysis.....	32
2.2.2.15 Data and code availability.....	33
2.3 Results.....	33
2.3.1 CAR-induced inhibition of T cell differentiation from PSCs	33
2.3.2 CAR-induced ILC2-biased innate lymphoid differentiation from PSCs.....	34
2.3.3 CAR-ILC2 cells are type 2 cells by immunophenotype and transcriptional profiles ..	35
2.3.4 CAR-ILC2 are type 2 cells subject to functional plasticity	36
2.3.5 scRNA-seq revealed multilineage hematopoiesis in early ATOs	37
2.3.6 scRNA-seq revealed multi-lymphoid differentiation in early ATOs.....	38
2.3.7 CAR activation in early lymphoid progenitors precedes ILC2-biased differentiation	40
2.3.8 Tuning CAR expression level controls T versus ILC2 lineage output	41
2.3.9 Tuning CAR expression level affects CAR activation potential	42
2.3.10 Antigen-dependent CAR activation during early ATO diverts T to ILC2 lineage	43
2.3.11 CAR costimulatory domain substitution permits CAR-T cell development	43
2.3.12 4-1BB costimulatory domain substitution permits functional CAR-T cell development.....	45
2.3.13 CAR activation via 4-1BB during early ATO diverts T to ILC2 lineage.....	45
CHAPTER 3: Concluding Remarks	76
3.1 Conclusions.....	76
3.2 Discussion.....	77
3.3 Future studies	80
REFERENCES	84

LIST OF FIGURES

Figure 1. Generation of H1-CD19-CAR PSC and ATO differentiation scheme.....	61
Figure 2. CAR-induced inhibition of T cell differentiation from PSCs	62
Figure 3. CAR-induced innate lymphoid differentiation from PSCs	63
Figure 4. Gating strategy for lymphoid differentiation in the ATOs	64
Figure 5. CAR-induced ILC2 differentiation from PSCs	65
Figure 6. Immunophenotypes and transcription factor expression of CAR induced ILC2s.....	66
Figure 7. CAR induced ILC2s present type 2 transcriptional profile	67
Figure 8. Selected gene expressions of CAR induced ILC2s	68
Figure 9. CAR-ILC2 are type 2 cells subject to functional plasticity.....	69
Figure 10. CAR had little effect on hematopoietic differentiation in early ATOs	71
Figure 11. scRNA-seq revealed multilineage hematopoiesis in early ATOs	72
Figure 12. scRNA-seq comparing early ATO multilineage hematopoiesis in H1 and H1-CAR .	73
Figure 13. scRNA-seq comparing early ATO multilineage hematopoiesis in H1 and H1-CAR at different time points	74
Figure 14. Immunophenotyping early lymphoid differentiation in ATOs	75
Figure 15. scRNA-seq revealed multilymphoid differentiation in early ATOs.....	76
Figure 16. scRNA-seq comparing early ATO multilymphoid differentiation in H1 and H1-CAR	77
Figure 17. scRNA-seq comparing early ATO multilymphoid differentiation in H1 and H1-CAR at different time points	78
Figure 18. Transcription factor patterns of the early lymphoid cells in ATOs.....	79
Figure 19. Gene set enrichment analysis comparing ILC2 versus T lineage.....	80

Figure 20. CAR induced ILC2 development in the ATO is antigen independent	81
Figure 21. Generation of H1-CAR PSC lines with lower CAR surface expression levels	82
Figure 22. Tuning CAR expression level controls T versus ILC2 lineage.	83
Figure 23. Tuning CAR expression level affects CAR activation potential.....	84
Figure 24. Antigen-dependent CAR activation during development diverts T to ILC2 lineage ..	85
Figure 25. Antigen-dependent CAR activation during development diverts T to innate lineages	86
Figure 26. Generation of H1-CAR PSC lines with different CAR architectures	88
Figure 27. CAR costimulatory domain substitution permits CAR-T cell development.....	89
Figure 28. CAR costimulatory domain substitution generates mature naïve CAR-T cell with similar level of surface CAR expression	90
Figure 29. ATO derived 4-1BB CAR-T cells have antigen-specific cytokine response and in vitro tumor killing capacity	92
Figure 30. Early CAR activation in ATOs inhibits CAR-T cell development	93

ACKNOWLEDGMENTS

First and foremost, I would like to express my sincere gratitude to my advisor, Dr. Gay Crooks, for being a wonderful mentor over the past six years. Dr. Crooks is a passionate scientist, a supportive mentor, and a thoughtful leader. I thank her for offering me the opportunity to explore in the developmental immunology field, for preparing me in scientific research and critical thinking, for training me in public speaking and professional writing, and for understating and supporting me with all her love and patience when I was going through hardships in life. Without her, I would not have achieved what I have today, and I would not have been who I am now.

I would like to thank my committee members, Dr. Caius Radu, Dr. Donald Kohn, and Dr Kenneth Dorshkind. I want to thank Caius specifically for being my first mentor in science and leading me into the scientific research world. All my thesis committee have always been supportive and encouraging and have provided valuable insights and generous assistance with my dissertation.

I am glad and proud to be a member of the Crooks lab. It has been a great pleasure to meet everyone and work together in the lab. I thank Dr. Chris Seet for his greatest mentorship and support over these years. Chris is an enthusiastic scientist, a dedicated supervisor, a pleasant collaborator, and a cheerful friend. Chris has taught me essentially everything in and outside lab, given me suggestions from experimental design to good restaurants, and helped me grow in professional career and personal life. I enjoyed and will pleasantly continue exploring science with Chris. I thank Judy Zhu, our best lab manager and friend, for always being caring and supportive. Like everyone else says, Judy is the mom of the lab who I can always go to when I need any help in experiments, when I want to chitchat, or when I hope to share my joy or have someone listen to my upset. Judy had made my graduate life far away from home easier with her love and patience. I thank Dr. Julia Chin, my first supervisor during rotation who taught me a lot in stem cell research

and gave me insights in career development. I thank Dr. Amelie Montel-Hagen and Dr. Stephanie De Barros for their superior knowledge in immunology as well as in dessert and pastries. I thank my fellow graduate students, Dr. Victoria Sun, Patrick Chang, Alex Yoo, and Julia Gensheimer for going through grad school together. I thank those that helped me greatly for my dissertation, including but not exclusively to Chloe Wang, Shawn Lopez, Olivia Zhou, William Satyadi, Carlos Botero, Steven Tsai, and lab alumni Edward He, Brent Chick, Howard Chen, Claudia Wong, and everyone else in the lovely Crooks lab family.

Furthermore, I would like to thank the staff of the BSCRC Flow Cytometry Core: Jessica Scholes, Felicia Codrea, and Jeffery Calimlim for their assistance in flow sorting and analysis. I thank Dr. David Casero for collaboration in bioinformatics analysis. I would like to acknowledge my home area the Molecular and Pharmacology Program at UCLA. My research was supported by Eli & Edythe Broad Stem Cell Research Center Pre-Doctoral Fellowship (2017-2019) and Tobacco-Related Disease Research Program Pre-Doctoral Fellowship (2020-2022).

Last but not least, I want to thank my friends and family. I thank Dr. Yinyu Wu, Dr. Kun Lyu, and almost Dr. Jie Tang for our long-term and long-distance friendship since college that helped me incredibly in making through graduate school. I thank my significant other, almost Dr. Nathanael Bangayan, for his constant support and love. I appreciate our endless memories of joy and happiness, but what I value more is his continuous patience in listening to me venting, his enormous support in me both in science and personal life, and that he never gives up on me. Lastly, I thank my beloved parents for their love and support. They don't always understand yet they fully support my decisions, encourage me in pursuing my dreams, and care about me and love me unconditionally.

CURRICULUM VITAE

Suwen Li

Education

- 2015 – Present Ph.D. Candidate, Molecular Pharmacology (expected graduation 6/2022)
University of California, Los Angeles, Los Angeles, CA
- 2011 – 2015 B.A., Biological Sciences
Nanjing University, Nanjing, Jiangsu, China

Research Experience

- 2015 – Present Graduate Student Researcher
Dept of Molecular and Molecular Pharmacology, David Geffen School of Medicine
at UCLA, University of California, Los Angeles
Mentor: Gay M. Crooks, M.B.B.S.
- 2014 – 2015 Undergraduate Researcher
School of Life Sciences, Nanjing University, Nanjing, Jiangsu, China
Mentor: Junfeng Zhang, Ph.D.
- 2014 Undergraduate Summer Intern
Dept of Molecular and Molecular Pharmacology, David Geffen School of Medicine
at UCLA, University of California, Los Angeles
Mentor: Caius G. Radu, M.D.

Fellowships and Awards

- 2022 American Association of Immunologists Trainee Poster Award, AAI Annual
Meeting
- 2020 – 2022 Tobacco-Related Disease Research Program Pre-Doctoral Fellowship
- 2017 - 2019 Eli & Edythe Broad Stem Cell Research Center Pre-Doctoral Fellowship
- 2014 Cross-Disciplinary Scholars in Science and Technology Program
Scholarship, UCLA
- 2013 Temasek Foundation Leadership Enrichment and Regional Network (TF LEaRN)
Programme Scholarship, National University of Singapore
- 2012 National Scholarship at Nanjing University, Ministry of Education of the People's
Republic of China

Relevant Skills

Bioinformatics: Processing and analysis of single cell RNAseq data using R-Studio packages e.g. Seurat.

Cell Biology: Pluripotent stem cell culture, stem cell differentiation methods, lentiviral production, isolation of primary human cells from tissue samples, primary T cell culture and expansion, MACS cell sorting.

Immunology: Multiparametric flow cytometry, flow data analysis using FlowJo, CAR-T and TCR-T T cell functional assays including cytokine assays, flow and Incucyte-based immune cell cytotoxicity assays.

Molecular Biology: Molecular cloning of plasmids and lentiviral vectors, plasmid design using Benchling, qPCR, Western blots, processing of cells and RNA samples for RNAseq.

Publications

- **Li, S.**, Wang, S.C., Montel-Hagen, A., Chen, H., Lopez, S., Zhou, O., Satyadi, W., Botero, C., Wong, C., Tsai, S., Casero, D., Crooks, G.M., Seet, C.S. (2022). Strength of CAR signaling determines T versus ILC2 lineage differentiation from pluripotent stem cells. Manuscript in preparation
- Abt, E.R., Rashid, K., Le, T.M., **Li, S.**, Lee, H.R., Lok, V., Li, L., Creech, A.L., Labora, A., Lam, A., Cho, A., Rezek, V., Abril-Rodriguez, G., Rosser, E.W., Mittelman, S.D., Mehrling, T., Bantia, S., Ribas, A., Donahue, T.R., Crooks, G.M., Wu, T., Radu, C.G. (2022). Guanine nucleoside catabolism guards against immune deficiency and autoimmunity. Manuscript in revision
- Montel-Hagen, A., Sun, V., Casero, D., Tsai, S., Zampieri, A., Jackson, N., **Li, S.**, Lopez, S., Zhu, Y., Chick, B., He, C., de Barros, S.C., Seet, C.S., & Crooks, G.M. (2020). In vitro recapitulation of murine thymopoiesis from single hematopoietic stem cells. Cell reports, 33(4), 108320.
- Montel-Hagen, A.*, Seet C.S.*, **Li, S.**, Chick, B., Zhu, Y., Chang, P., Tsai, S., Sun, V., Lopez, S., Chen, H., He, C., Chin, C.J., Casero, D., Crooks, G.M., (2019) Organoid-induced differentiation of conventional T cells from human pluripotent stem cells, Cell Stem Cell. Mar 7;24(3):376-389.e8.
- Chin, C. J., **Li, S.**, Corselli, M., Casero, D., Zhu, Y., He, C. B., ... & Crooks, G. M. (2018). Transcriptionally and functionally distinct mesenchymal subpopulations are generated from human pluripotent stem cells. Stem cell reports, 10(2), 436-446.
- Seet, C. S., He, C., Bethune, M. T., **Li, S.**, Chick, B., Gschweng, E. H., Zhu Y., Kim K., Kohn D.B., Baltimore D., Montel-Hagen, A. & Crooks, G.M. (2017). Generation of mature T cells from human hematopoietic stem and progenitor cells in artificial thymic organoids. Nature methods, 14(5), 521-530.

Selected Presentations

- Li, S., Wang, S.C., Montel-Hagen, A., Casero, D., Lopez, S., Chen, H., Zhou, O., Botero, C., Tsai, S., Wong, C., Crooks, G.M., Seet, C.S. (2022). Strength of CAR signaling reveals bifurcation of T and ILC2 lineage differentiation from pluripotent stem cells, Poster presentation (Trainee poster award), American Association of Immunologists (AAI) Annual Meeting, Portland, OR, May 2022.
- Wang, C.S., Li, S., Mao, Z., Zhou, O., Botero, C., Chang, P., Yoo, S., Chen, H., Lopez, S., McLaughlin, J., Montel-Hagen, A., Witte, O.N., Crooks, G.M., Seet, C.S. (2022) PSC-derived T cells as a novel source of tumor antigen-specific T cell receptors. Oral Presentation, AACR Annual Meeting, New Orleans, LA, April 2022

CHAPTER 1: Introduction

1.1 Human thymic T cell development

Hematopoietic stem cells (HSCs), the origin of all blood cells, mainly reside in the bone marrow during steady state in adulthood. Unlike other major hematopoietic lineages that develop in the bone marrow, T cell lineage commitment occurs only after the bone marrow-derived lymphoid progenitors seed the thymus from circulation. The exact identity of the human thymus seeding progenitors (TSPs) remained unclear for decades, candidates of which include the self-renewing HSC, multipotent progenitors (MPP), lymphoid-primed multipotent progenitors (LMPPs) [1], and common lymphoid progenitors (CLPs) [2]. Recently, the rapid development of single cell RNA sequencing (scRNA-seq) technology enabled characterization of these rare populations in high resolution at single cell level. Two groups performed scRNA-seq on human postnatal thymic CD34⁺ progenitors, respectively [3, 4]. Comparing the thymic CD34⁺ cells with bone marrow CD34⁺, Lavaert et al. confirmed the presence of the canonical Lin⁻ CD34⁺ CD44^{hi} CD7⁻ CD10⁺ TSP1 expressing thymic homing molecules CCR7 and CCR9 but high levels of HSPC genes, and a newly identified and presumably Notch-primed population CD7⁻ CD10⁺ TSP2.

After entering the thymus, TSPs encounter a combination of spatiotemporally organized signals from the thymic microenvironment and the majority of TSPs commit exclusively to a T lineage fate. Among these signals, Notch ligand Delta-like-4 (DLL4) expressed by the thymic epithelia cells (TECs) and the cytokine IL-7 play indispensable roles [5-7]. The earliest thymic progenitors express CD34 and sequentially gain expression of CD7 and CD1a or CD5 while progressively losing potential of other lineages (B, T, NK, and DC) [8, 9]. The committed T cell progenitors progress to CD34⁻CD4⁻CD8⁻ (double negative; DN) precursors through the cortex.

Beta-selection, the rearrangement of the $V\beta$ locus of the T-cell receptor (TCR), happens during the transition from DN to CD4 immature single positive (ISP4) stage [10, 11]. ISP4s rapidly gain expression of CD8 in the form of the CD8 $\alpha\beta$ heterodimer and become CD8⁺ CD4⁺ double positive (DP) T cells. Successful rearranged $V\alpha$ loci enables CD3 and TCR $\alpha\beta$ to form a TCR complex on the cell surface for signaling.

Thymocytes undergo two separate selection processes, positive selection and negative selection, guided by TECs before exiting the thymus to the peripheral [12]. Positive selection happens where low affinity interactions of a TCR $\alpha\beta$ ⁺ DP with cortical TEC (cTEC) presented peptide-MHC (pMHC) complex send the DPs a survival signal to mature into either a CD8 single positive (CD8SP) or CD4 single positive (CD4SP) T cells according to their MHC recognition [10, 13]. Before entering the circulation, CD8SP or CD4SP then encounter medullary TECs (mTECs) to remove self-reacting T cells [14]. Self-antigens presented by mTECs (sometimes also by thymic dendritic cells) which bind to TCR in high affinity induce central tolerance, including apoptosis or diversion to regulatory cell lineages. Negative selection prevents autoreactive T cells from entering the peripheral to avoid autoimmune diseases.

1.2 T cell-based immunotherapies

Adoptive T cell transfer (ACT) has achieved durable clinical responses in cancer treatment. Initially, tumor-infiltrating lymphocyte (TIL) therapy has demonstrated complete responses in clinical trials with metastatic melanoma [15, 16]. But the requirement for highly personalized manufacturing process, variations during *ex vivo* expansion, and the dependence on high neoantigen load makes it less widely applicable. Gene transfer technology enabled ectopic expression of antigen receptors in any effector T cells to potentiate their anti-tumor capacity [17].

Expression of a fully rearranged T cell receptor (TCR) or chimeric antigen receptor (CAR) in peripheral blood T cells conveyed antigen specific cytotoxicity to the recipient T cells [18, 19].

Adoptive transfer of CAR-T cells has achieved profound efficacy in treating relapsed B cell leukemia, leading to complete remission in most patients [20]. CARs are synthetic receptors consisting of an extracellular antigen recognition domain single-chain variable fragment (scFv), an extracellular spacer domain (hinge), a transmembrane (TM) domain, one or more costimulatory domains, and a T cell-receptor-derived-CD3 ζ signaling domain. Despite the inability to target intracellular proteome, CAR T cells offer various advantages over TCR engineered T cells, the biggest of which is the HLA independence of antigen recognition, allowing a variety of patients to be treated with the same CAR. The modular nature of CARs also enables easier adaptation in different tumor antigens.

Functionality and efficacy of CAR T cells can be affected by various intrinsic and extrinsic cues, including the structural variations of the CAR and the interactions between CAR T cells with other cells within the tumor microenvironment (TME). One considerable negative factor is the tonic signaling that drives T cells to differentiate into terminal effector phenotype in the absence of antigen which hinders T cell effector function and survival. CAR tonic signaling is defined as the constitutive activation of T cells in the absence of their cognate antigen and it can be influenced by essentially every element of the CAR architecture. Certain scFvs have been reported to have higher potential to tonic signal including ones that target the disialoganglioside GD2 and c-mesenchymal–epithelial transition (c-Met) [21, 22]. Moreover, CARs with the IgG4-CH2-CH3 hinge/ spacer widely used in initial studies was found to perform poorly *in vivo* despite their optimal *in vitro* efficacy and it was later identified due to the tonic signaling driven by the Fc binding domain in the CH2 spacer [21, 23-25]. Even the CD28 transmembrane domain was

reported to have enhanced CAR signaling strength compared to that derived from CD8a [26-28]. The most well characterized here was the costimulatory domain. Multiple groups have shown that CD28 costimulation drives augmented tonic signaling compared to 4-1BB [21, 29, 30]. Last but not least, the CD3 ζ signaling domain can also be modulated for differential signaling strength [31]. Thus, for any given tumor target, CAR design requires rational tuning to achieve optimal potency and persistency in cancer treatment.

Beside mature primary T cells, generation of antigen specific T cells from stem cells, either hematopoietic stem and progenitor cells (HSPC) or ultimately, human pluripotent stem cells (PSC), to make universal, off-the-shelf cell products for ACT has been a popular research area in the development of cellular immunotherapies [20, 32]. The use of stem cells as starting materials offers advantages including the ability to generate naïve antigen-specific T cells with improved efficacy and *in vivo* persistency, the possibility to genetically disrupt endogenous TCR and MHC expression to mitigate rejection during transfer, or to incorporate additional characteristics to improve T cell potency, and the reduced cost from large scale production.

1.3 *In vitro* T cell generation from HSPC

An *in vitro* system that fully and faithfully recapitulates different stages of thymopoiesis is essential for better understanding the molecular regulation of human T cell development. It is also of therapeutic interest to develop standardized, reproducible, and scalable platforms to produce functional T cells from HSPCs for cancer immunotherapy.

The use of fetal thymic organoid cultures (FTOCs) first demonstrated the feasibility of modeling thymic T cell differentiation *in vitro* [33]. HSPCs from fetal or neonatal mouse seeded into T cell depleted thymic fragments could develop into mature T cells. Later, FTOCs were further

developed into reaggregated thymic organoid cultures (RTOCs) in which primary mouse stroma were reaggregated with HSPCs and this enabled manipulation of the thymic stromal environment [34]. However, the large variation, low efficiency, high dependency on substantial amounts of primary tissues, and technical difficulty made it not preferable to be used experimentally as well as challenging to be widely applied in large scale manufacture [35].

The discovery of OP9-DL1 coculture system was a breakthrough that significantly sped up the progress in understanding T cell development. In 2002, Schmitt and Zuniga-Pflucker reported the use of a mouse bone marrow stroma cell line (OP9) retrovirally expressing a murine Notch ligand Dll1 supplemented with IL-7 and FLT3L as a monolayer coculture to support T cell differentiation from mouse HSPCs [36]. Shortly after, in 2005, the same group adapted the OP-DL1 system into primary human cord blood (CB) CD34⁺ HSPCs and illustrated its capacity to support human T cell commitment and early development into CD8⁺ CD4⁺ DPs. The OP9-DL1 became the gold standard in the T cell development field since then [37]. However, it is yet not the perfect system due to the long-term maintenance of labor-intensive stroma culture, the high experimental variations from the usage of high amount of serum, and most importantly, its limited support of late-stage maturation and positive selection of T cells, especially into CD4SPs.

In preparation for a system that is more readily scalable and more clinically relevant, researchers have also attempted to develop stroma-free platforms to generate T cells *in vitro*. Plate-bound DL4 and the more recent microbead-based approach reported to support differentiation from CD34⁺ cells to CD34⁺CD7⁺CD5⁺ pro-T cells to CD3⁺ $\alpha\beta$ T cells [38, 39]. These systems, however, lacked the capacity to support positive selection and relied on *in vivo* transfer for further maturation of the pro-T cells generated, thus not yet ready for translational application.

The artificial thymic organoid (ATO) system developed in the Crooks Lab made another step forward. The ATO system is a serum-free, three-dimensional (3D) culture system that faithfully recapitulated the full-span of human thymopoiesis efficiently and reproducibly. The ATO used an alternative murine stroma cell line MS5 transduced with either DLL1 or DLL4. The use of a membrane based organoid culture created a 3D architecture on an air-fluid interface which likely better facilitated interactions between stroma and hematopoietic cells compared to the loose monolayer cultures. The serum-free medium also reduced experimental variations. Kinetic study showed timely development of CD34+ progenitors, followed by T precursors DN, ISP4, DP, CD3+ TCR $\alpha\beta$ + DP, and finally positively selected CD8SPs and CD4SPs. Moreover, the ATO supported T cell differentiation from all sources of CD34+ HSPCs including CB, adult bone marrow (ABM), postnatal thymus (PNT), and mobilized peripheral blood (MPB) [40]. Thus, the development of the ATO system provided an alternative to the long-standing OP9-DL1 culture, especially for studies involving T cell maturation and positive selection.

It is so far still challenging to model human thymic negative selection *in vitro* due to the lack of mTEC or other alternative antigen presenting cells (APC). Incorporation of TEC or TEC-like stroma cells could be a direction for further development.

1.4 *In vitro* generation of engineered T cells from HSPC

It has been shown in mouse models that ectopic expression of a fully rearranged TCR in HSPCs enables the differentiation of T cells carrying that single TCR [41, 42]. The early expression of a TCR at the stem and progenitor stage cells induced allelic exclusion where TCR rearrangement and beta-selection was bypassed and the rearrangement of the TCR V β loci was suppressed [43, 44]. *In vitro* differentiation of TCR-transduced human HSPCs using the OP9-DL1

system generated TCR-expressing T lineage progenitor and precursor cells, with the same limitations as mentioned above that the maturation and positive selection were largely impaired thus not ideal for large scale manufacture [45]. The ATO system, on contrary, demonstrated feasibility of robust and scalable production of engineered antigen specific mature and functional effector T cells from human HSPCs [40].

The use of chimeric antigen receptor (CAR) offers several advantages over TCR based cell therapies, including the ease of changing target recognition from its modular architecture, the broader patient applicability from its independence of MHC restriction, and the potential of enhancing anti-tumor efficacy by additional layers of engineering, making it preferable in various situations. In contrast to TCR engineering, however, constitutive expression of CARs in HSPCs was shown to perturb critical stages of early T cell differentiation due to either tonic or antigen-specific CAR activation during development. It has been reported that CAR expression suppressed T cell development and induced generation of CAR expressing NK like innate effector cells instead due to the early suppression of the transcription factor critical to T cell commitment *BCL11B* [46]. We have also independently verified this in the CB ATO system with a second-generation CAR targeting CD19 (unpublished data). Modulation of the CAR tonic signaling or timely regulated expression could be potential solutions.

1.5 *In vitro* generation of T cells from PSC

Despite the success in generating T cells from HSPCs, it is yet not the ideal source for cellular immunotherapies due to the difficulty in finding perfect matching donor, the potential risk of graft-versus-host disease (GVHD), the limit in getting enough starting material, the high

biological batch-to-batch variability, and the relative high cost. Human pluripotent stem cells (PSCs) can serve as an alternative source to overcome these challenges [32].

T cell development induced from PSCs adds layers of complexity compared to that from HSPCs. PSCs first need to be directed to differentiate into mesoderm lineage. The specified mesodermal cells then undergo hematopoietic induction to generate hematopoietic progenitor cells (HPCs) with T cell potential [47]. These HPCs are then enriched and transferred to T cell induction condition. Pioneer studies exploring the potential of inducing T lineage commitment from human pluripotent stem cells initiated in the early 2000s.

In 2006, Galic et.al illustrated possible T cell lineage development from human PSCs using a sequential *in vitro* and *in vivo* combined method [48]. Human embryonic stem cells (ESCs) were first cocultured on the murine bone marrow stroma cell OP9 and then engrafted into human thymic tissues in immunodeficient SCID-hu (Thy/Liv) mice. CD45⁺ CD7⁺ CD3⁺ TCR $\alpha\beta$ + T lymphocytes were isolated from the implant and responded to TCR-mediated signals. This marked the success of inducing early T-cell commitment from PSCs.

In 2009, Timmermans et al. demonstrated for the first time of *in vitro* induction of T lineage committed cells from PSCs via a three-step differentiation protocol [49]. Firstly, ESCs were cultured on OP9 stroma to induce hematopoietic zone (HZ) differentiation. HZs were then manually picked and transferred to OP9-DL1 culture in the presence of SCF, FLT3L, and IL-7 for hematopoietic progenitor cell (HPC) induction. Lastly, HPCs were cultured on fresh OP9-DL1 for T cell induction. The final product presented CD7⁺, CD3⁺, TCR $\alpha\beta$ + (and minor TCR $\gamma\delta$ +) and CD4⁺CD8 β + but didn't show convincing evidence of positive selection.

Later other studies also reported similar PSC – HPC – T differentiation protocols. HPCs were generated either using an embryonic body (EB)-based method or feeder cell (OP9) supporting

coculture. The subsequent T cell differentiation stage was induced in OP9-DL1/ OP9-DL4 stroma coculture supplemented with T cell supporting cytokines. Again, positive selection and further maturation of T cells beyond the DP stage was not clear in these studies, possibly due to the limitation of the OP9-DL1/4 system used [47].

In 2019, following the ATO study, the Crooks lab extended the use of ATO to generate positively selected mature T cells using human PSCs [50, 51]. Human ESCs or induced pluripotent stem cells (iPSCs) were first induced into differentiation of human embryonic mesoderm progenitors (EMPs) using a serum-free, feeder-free method developed in the lab. The EMPs were then aggregated with MS5-hDLL4 stroma to form the embryonic mesoderm organoids (EMOs) for hematopoietic specification. After two weeks of induction, non-adherent HPCs were isolated and reaggregated with fresh MS5-hDLL4 into the ATO culture for T cell differentiation and maturation. This PSC-ATO method efficiently generated mature, functional effector T cells with diverse T cell receptor (TCR) repertoires comparable to their thymic counterpart. The PSC-ATO-derived T cells presented predominantly a CD3⁺ TCR $\alpha\beta$ + CD8 $\alpha\beta$ + conventional phenotype and were highly functional. Interestingly, the PSC-ATO T cells demonstrated shorter CDR3 lengths in relative to the T cells from the postnatal thymus or peripheral blood, and this observation was confirmed by the absence of DNTH expression in DPs from PSC-ATOs, suggesting fetal-like T cell properties of PSC-derived T cells [52, 53].

1.6 *In vitro* generation of antigen specific T cells from PSC

The goal of using PSCs in T-cell immunotherapy is to generate cytotoxic antigen specific T cells as treatment for cancer and other infections and this requires the T cells to express an antigen receptor for target recognition instead of a polyclonal TCR repertoire. Studies taking

advantage of T-iPSCs (iPSCs programmed from primary T cells) have shown in proof-of-concept that the expression of a single TCR in PSCs would lead to differentiation of T lineage cells carrying the parent TCR via allelic exclusion [54, 55]. In the OP9-DL1 monolayer system, insufficient positive selection or maturation was obtained unless the DP cells were isolated and stimulated with anti-CD3 antibody post culture. Interestingly, in 2018, the Kaneko group reported generation of TCR expressing innate lymphoid – like helper cells from T-iPSCs reprogrammed from an HLA-DR9-restricted leukemia antigen (b3a2) – specific CD4⁺ Th1 clone (SK). Under their T cell differentiation condition, they obtained lymphocytes with CD45⁺ CD3⁺ CD5^{dim} CD7⁺ CD8 α ^{dim} CD8 β - phenotype. The cells didn't express CD4 despite the constitutive expression of the class II TCR. Instead, the cells had heterogenous expression of NK/ILC1 markers CD56, CD161, NKG2D, c-Kit, NKp30, NKp44, NKp46, and DNAM-1. After comparing their transcriptional profile to that of the primary lymphoid cells including ILC1, ILC2, ILC3, NK, $\alpha\beta$ T cells and $\gamma\delta$ T cells, they concluded that these cells presented group 1 ILC-like properties with expression of innate transcription factors *ID2*, *PLZF*, and *TBX21* and secretion of interferon- γ upon activation [56], again suggesting the importance of having an optimized *in vitro* T differentiation system to ensure PSC to T development.

Using the PSC-ATO system, the Crooks lab illustrated the feasibility of generating antigen specific mature effector T cells from PSCs. Using a UBC promoter that has been proven to maintain stable expression during differentiation in PSCs, we introduced a TCR that targeted NY-ESO1 tumor associated antigen into embryonic stem cell line H1 and put into ATOs. Same as the T-iPSC studies, the introduction of a TCR induced allelic exclusion and generated mature T cells that are CD3⁺ TCR $\alpha\beta$ ⁺ CD8 $\alpha\beta$ CD4⁻. The NY-ESO1 TCR⁺ T cells presented antigen specific cytotoxicity both *in vivo* and *in vitro* [50].

1.7 *In vitro* generation of CAR-T cell from PSC

Similar to its effect in T cell differentiation from HSPCs, CAR tonic signaling may disturb essential checkpoints during T cell differentiation or even during hematopoietic specification from PSC. So far only one group published successful generation of spontaneously positively selected CD8 $\alpha\beta$ CAR-T cells using the PSC-ATO system while previous attempts mostly ended up with unconventional lymphocytes containing some innate characteristics.

As one of the earliest studies exploring the potential of producing universal, off-the-shelf, CAR-T cell products from human PSCs, Themeli et al. showed in proof of concept of generating CD19-targeting effector lymphocytes from T-iPSCs [57]. Using an EB-based differentiation protocol, they isolated hematopoietic precursor-enriched day 10 EB cells and transferred them onto OP9-DL1 feeder cells in the presence of the cytokines SCF, FLT3L, and IL-7. The culture yielded CD7⁺ CD3⁺ TCR $\alpha\beta$ ⁺ lymphoid cells, although the expression of conventional $\alpha\beta$ T cell markers CD4 or CD8 β were undetected, and a small fraction of the cells presented CD8 $\alpha\alpha$ or CD56⁺ NK-like phenotypes. Immunophenotypic and transcriptional analysis indicated that these cells were more closely related to $\gamma\delta$ T cells rather than to $\alpha\beta$ T lineage. These cells expressed pronounced levels of $\gamma\delta$ T cell signatures including FASLG, TYROBP, CCL20, TNFSF11 (RANKL), CXCR6, RORC, PLZF, CD161, and high expressions of cytotoxic genes *TNFSF10* (*TRAIL*), *GPLY*, *GZMB*, *FASL*, *LTA*. Post expansion, these cells upregulated natural cytotoxicity receptors such as NKp44, NKp46 and NKG2D, polarized toward a type 1 phenotype. Nonetheless, *in vitro* and *in vivo* evaluation of the anti-tumor potential of these cells demonstrated antigen-specific cytotoxicity against CD19⁺ tumors, leading to partial cure in their *in vivo* i.p. RAJI tumor model.

Of note, in this culture system, even without the CAR transgene, the non-transduced T-iPSC derived lymphocytes still displayed $\gamma\delta$ -like phenotype including low CD5 expression, lack of expression of CD4 and CD8 β , and aberrant expression of CD56 and PLZF, suggesting that the $\gamma\delta$ -T cell like phenotype was not solely induced by the constitutive expression of the CAR, but at least partially by the system that lacked essential components to support conventional T cell development [57]. This could include the lack of a 3D architecture that is known to be indispensable for thymic T cell development, the lack of some soluble factors such as ascorbic acid, or the instability of the OP9 media that contains high serum. As such it is difficult to isolate the specific effect of CAR signaling on lymphoid development in this model.

The Kaneko group published a related study reporting the processing of iPSC-derived anti-glypican-3 CAR-expressing NK/ILCs. Using a 3-step standard protocol very similar to T cell differentiation, they showed reproducible production and expansion of NK/ILC-like CAR expressing cells with CD45+, CD7+, CD3-, CD5-, CD8 α -, CD8 β -, CD4- phenotypes. These cells expressed a panel of NK receptors NKG2A, NKG2D, NKRP1, NKp30, NKp44 and DNAM1 and demonstrated both antigen-specific and NK-mediated tumor suppression capacities both *in vitro* and *in vivo*. The CAR used in this paper was a third-generation anti-GPC3-CAR 28bbz, containing the CD8 α transmembrane domain and signaling domains from CD28, 4-1BB and CD3z [58]. Comparing this with their previous work [56] we could see that the NK/ILC phenotypes in these two papers were similar and may not be completely due to the expression of the class II TCR or the constitutive signaling from the CAR, but rather the properties of the differentiation method.

Using a modified PSC-ATO system, Wang and colleagues reported generation of functional CD19-targeting CAR-T cells from T cell derived iPSCs (T-iPSCs) [59]. Their T-iPSC-derived CAR-T cells demonstrated conventional $\alpha\beta$ T cell phenotypes with expression of T lineage

markers CD3, CD5, CD7, TCR $\alpha\beta$, and CD8 $\alpha\beta$ while lacking expression of innate/NK like markers NKG2A, NKP46, CD16, CD19. These iPSC CAR-T cells had an overall similar transcriptional profile compared to conventional CAR-T cells generated from primary PBMCs, with a lower activation status at steady state.

The CD19-targeting iPSC CAR-T cells had comparable *in vitro* killing capacity to PBMC-derived conventional CAR-T cells. In xenograft mouse model using Nalm6 intraperitoneal (i.p.) for modeling *in vivo* anti-tumor response, they showed that in combination with human IL-15 secreting nurse cells (NS0-hIL15), the iPSC CAR-T cells had improved anti-tumor efficacy and prolonged mouse survival. In a more aggressive intravenous (i.v.) Nalm6 model, treatment of T-iPSC CAR-T cells + NS0-hIL15 demonstrated better tumor control, despite being unable to eradicate the tumor. When compared with PBMC derived conventional CAR-T cells, T-iPSC CAR-T cells demonstrated similar anti-tumor efficacy and enhanced survival when combined with NS0-hIL15.

However, although the T-iPSCs expressed high levels of the CAR transgene, the CAR expression in the differentiated T cells was much lower compared to conventional CAR-T cells transduced with the same construct. The authors described this as a result of the hypermethylation status of the CpG-enriched EF1a promoter during downstream T cell differentiation, which led to silence of the CAR transgene in mature T cells [59]. Although it didn't seem to affect the anti-tumor capacity of the CD19 CAR T cells tested in this paper, it is known that certain scFvs require high cell surface expression to be effective in treating cancer. Therefore, the effect of CAR signaling in T cell differentiation using this method needs to be further investigated using PSC differentiation-resistant promoters for wider application.

1.8 Human innate lymphoid cell subsets

In addition to T cells, the use of alternative lymphoid cells for cancer immunotherapy is being investigated and evaluated, including NK cells, unconventional T cells, such as invariant natural killer T (iNKT), gamma delta T ($\gamma\delta$ T), mucosal-associated invariant T (MAIT) cells and other innate immune cells. Human innate lymphoid cells (ILC) are a recently identified family of largely tissue resident innate lymphoid cells. ILCs lack expression of somatically rearranged antigen receptors recognizing specific antigens like B cells and T cells but they can rapidly respond to environmental cytokine stimuli and play important roles in host defense and tissue homeostasis [60]. Interestingly, ILCs mirror the adaptive T lymphocytes in terms of their master transcriptional factor expression and cytokine secretion profiles. While natural killer (NK) cells, which are considered as part of the group 1 ILCs, resemble cytotoxic CD8 T cells, the helper ILC cells phenocopy the CD4 T helper cell family. ILC1s express T-bet and secrete type 1 cytokines including $\text{IFN}\gamma$ upon infection by intracellular pathogens like Th1 cells. Similar to Th2 cells, ILC2s express high level of GATA3 and produce type 2 cytokines IL-5 and IL-13 in response to epithelial-derived alarmins, including IL-25, IL-33, and thymic stromal lymphopoietin (TSLP). And ILC3s have high expression of $\text{ROR}\gamma\text{t}$ and secrete IL-17 and IL-22 upon activation by extracellular microorganisms, mirroring the Th17 cells. More recently, an additional subset of ILCs producing IL-10 -- ILCregs, represent the innate counterpart of regulatory T cells (Tregs) [61].

Identifying ILCs as single subset lineage can sometimes be challenging. In fact, similar to their CD4 T helper cell counterparts, ILCs are functionally plastic and can be polarized to have similar phenotypes to other subsets upon stimulation with appropriate cytokines through epigenetic regulation [62]. The pro-inflammatory cytokine IL-12 has been shown to induce upregulation of T-bet and IL-12 receptor in both ILC3s and ILC2s and convert them into a ILC1-like state with

the capability to secrete IFN- γ [63-68]. Studies have also suggested other types of plasticity, including IL-23 mediated conversion of ILC1s to ILC3s and Notch induced ILC2 to ILC3 conversion [69]. Thus, it can sometimes be difficult to distinguish ILC subset simply by looking at surface markers and cytokine secretion, especially under infection or inflammation conditions.

1.9 ILC development

Murine ILC differentiation has been widely studied and it has become clear that most ILCs develop in the bone marrow from the common lymphoid progenitor (CLP) and the more committed α -lymphoid precursors (α -LP), early innate lymphoid progenitors (EILP), common helper ILC progenitors (CHILP) and ILC precursors (ILCP). Using transgenic mouse models, a complex network of transcription factors has been shown to control ILC differentiation and maturation, including *Id2*, *Nfil3*, *Zbtb16*, *Tcf7*, *Bcl11b*, *Rora*, *Gata3*, *Ets1*, and *Tox* [70-72].

Human ILC development hasn't been studied as detailed but increasing evidence is suggesting a similar developmental hierarchy. Likewise, CD34⁺CD38⁻CD45RA⁺CD90⁻ CLPs that can give rise to B, T, and NK cells have been identified in the bone marrow [73]. A circulating Lin⁻ CD127⁺ CD117⁺ ILC precursor (ILCP) was found to have the potential to differentiate into both NK and helper ILC subsets and ILCPs with similar properties were also found in fetal liver, cord blood, tonsil, and lung [74]. Separately, Freud et. al. identified the presence of CD34⁺ CD45RA⁺ CD117⁺ IL-1R1⁺ integrin β 7⁺ human common ILC progenitors (CILCP) in secondary lymphoid tissues (tonsil and spleen) but absence in BM or peripheral blood. More committed downstream subset specific ILC precursors have been identified in different tissues, including Lin⁻ CD34⁺ CD45RA⁺ CD10⁺ CD7⁺ CD127⁻ NK precursors (NKP) from fetal liver, fetal BM, cord blood and adult tonsils [75], and CD34⁺ CD45RA⁺ CD117⁺ α 4 β 7⁺ ROR γ t⁺ CD7⁻ CD127⁻ ILC3

precursors (ILC3P) from tonsil and intestinal lamina propria but not from BM or peripheral blood [76]. These studies indicate a working model of human ILC development in which circulating ILCPs sense cytokine stimuli from inflamed tissues and migrate from the peripheral into tissues where they expand and differentiate into appropriate mature ILC subsets and become tissue resident since then [70].

1.10 ILC2s in the thymus

Although it is largely acknowledged that most ILCs develop in the bone marrow, increasing evidence has shown the potential of ILC development in the thymus, especially ILC2s. ILCs shape pre-natal development of secondary lymphoid organs including lymph nodes and thymus. A subset of group 3 ILCs, lymphoid tissue inducer (LTi) cells [77], were discovered long before the other ILCs for their role in facilitating the development and maturation of functional thymic epithelial cells. After birth, however, ILC3s drop in number while ILC2s emerge and become the predominant ILC subtype in the thymus [78]. Although majority of ILCs are found in mucosal tissues, presence of ILC2-like cells was found both in adult and embryonic thymi [78-81]. The importance of thymic ILC2s in adults was unclear until recently, Cosway et al. reported that the type 2 cytokine IL-5 provided by thymic ILC2s are required for the recruitment of eosinophils that play indispensable roles in thymic regeneration upon irradiation induced damage [82].

Among all the different ILC subsets, ILC2s are the closest related to T cells. ILC2s share many developmental features with T cells including a requirement for Notch and IL-7 receptor signaling. In 2013, Gentek et.al. first reported presence of ILC2s in the human thymus with IL7Ra+ Lin- CRTH2+ CD161+ cKit+ phenotype. Using OP9-DLL1 coculture system, they demonstrated co-development of T lineage cells and ILC2 cells from CD34+CD1a- thymic progenitors. Ectopic

expression of intracellular domain of NOTCH1 (NICD1) in thymic progenitors led to differentiation of ILC2 and this ILC2 induction was promoted by Notch in a signal strength dependent manner at the expense of T cell potential [80]. Later in 2018, cross-titration of Notch and IL-7 in murine fetal liver CLP/ stroma coculture elegantly demonstrated the differential requirements of Notch and IL-7 in T versus ILC2 development that conventional T cells develop upon durable, strong Notch activation with low concentration of IL-7, while ILC2s preferentially develop under shortly pulsed, intermediate Notch signaling with high IL-7 concentration [83].

ILC2s also share a lot in common with T cell development in terms of transcriptional regulation. ILC2 development requires coordinated activity of different transcription factors, including GATA3, TCF1, BCL11B, RORA, ETS1, PLZF, and ID2 [84-90]. Among these, it has been well established that GATA3, BCL11B, and TCF1 are indispensable for T cell development [91]. However, it seems conflicting that during T cell commitment, BCL11B inhibits ID2 and NFIL3 which are required for ILC development but BCL11B itself is critical for ILC2 development, and ILC2 indeed co-express BCL11B and ID2. This was explained partially by BCL11B utilizing different regions across the genome in cell type-specific patterns and regulating different target gene sets in different cell types [92]. With the help of a multi-TF-driven reporter polychromILC mouse model combined with multiplexed sequencing techniques, Ferreira et.al. demonstrated that ILC2s and T cells develop from a common progenitor within the murine embryonic thymus and proposed a new transcriptional circuit where for thymic T cell commitment, Notch turns on BCL11B that represses NFIL3 and ID2, reinforcing T cell development by E proteins; for ILC2, however, expression of RORA in ILC2p cells override repression of NFIL3 and ID2 induced by BCL11B, enabling a balanced co-expression of BCL11B and ID2 to direct ILC2 development. The differential outcomes of T versus ILC2 development from the same

progenitor in the same tissue likely results from the heterogeneous thymic microenvironments, details of which requires more investigation [81].

Initially ILCs were considered to develop and function in a RAG-independent way separate from the T cell lineage from studies using *Rag*^{-/-} and nude mice [93]. Recently, however, multiple groups have provided evidence of non-productive TCR gene rearrangement in both bone marrow ILC progenitors and tissue resident mature ILCs [94, 95]. Differential expressions of TCR constant region transcripts were detected in all three subsets of ILCs. Specifically, ILC2 showed abundant rearrangement at their TCR γ loci in a pattern similar to mature V γ 2+ $\gamma\delta$ T cells and their V γ 2-J γ 1 rearrangements were found to be mostly out-of-frame, indicating the possibility of thymic ILCs being a product of abortive T cell development that failed to form functional TCR γ/δ loci [94].

1.11 *In vitro* generation of ILC2s

In vitro differentiation of ILCs from hematopoietic stem and progenitors has been modeled since the discovery of ILCs as well as in the subsequent studies elucidating ILC progenitors and their differentiation potential. The OP9 and/or OP9-DL1/4 monolayer coculture system was often used in combination with different cytokine conditions to achieve development of different ILC subsets from different progenitor and precursor populations [74, 96-102], however a standardized protocol that enables development of all ILC subsets with comprehensive validation was lacking. Recently, Hernández et. al. reported an *in vitro* platform that reliably differentiates ILC lineages using cord blood or bone marrow derived CD34⁺ CD45RA⁺ HPCs. This paper illustrated that differentiation into different ILC subsets indeed requires distinct signals and ILC2s can be generated when cocultured with OP9-DL1 without addition of IL-15 and this condition also allows

co-development of T cell precursors [103]. Besides NK cells, generation of helper ILCs from PSCs, however, has not been reported so far to our knowledge.

1.12 Role of ILC2 in cancer

ILC2s can be found in various human tissues, including adult blood, bone marrow, tonsils, spleen, lymph nodes, skin, adenoids, and adipose tissues [104]. ILC2s were first discovered to be involved in host protection or pathogenesis in the mucosal tissues during infection and inflammation as well as the tissue repair after damage. The presence of ILC2s in the tumor microenvironment was initially associated with dampened tumor control and poor prognosis [105]. High IL-13 production was indeed associated with poor survival in acute myeloid leukemia, prostate cancer, and bladder cancer [106-108]. More recently, surprisingly, independent studies have reported the conflicting role of ILC2s in facilitating tumor killing in metastatic melanoma, colorectal cancer, melanoma, and pancreatic cancer [109-111]. ILC2s were shown to activate tumor-infiltrating dendritic cells and CD8⁺ T cells, and IL-33 and anti-PD-1 enhanced this protective response [110]. In a separate report, IL-5 and GM-CSF produced by ILC2s were found to recruit eosinophils to improve anti-tumor response [109]. With these seemingly conflicting reports it is apparent that more detailed investigations are needed to distinguish the differential roles which different subsets of ILC2s play in different tumors under different conditions, but it could be promising to attempt to target ILC2s in the tumor microenvironment to enhance their anti-tumor effect or even to develop engineered ILC2s as cell-based immunotherapies to facilitate CD8 T cell mediated tumor killing.

CHAPTER 2: Strength of CAR Signaling Determines T versus ILC2 Lineage

Differentiation from Pluripotent Stem Cells

2.1 Introduction

Autologous CAR-T cells have shown promise in the treatment of advanced malignancies, and *in vitro* generation of allogeneic CAR-T cells from CAR-engineered “master” pluripotent stem cell (PSC) lines has the potential to expand patient access to CAR-T cell therapies [20, 32]. In contrast to peripheral blood T cells, however, constitutive expression of CARs in both PSCs and primary hematopoietic stem/progenitor cells (HSPCs) may perturb critical stages of early T cell differentiation due to either tonic or antigen-specific signaling during development, and indeed the first demonstration of T cell differentiation from CAR-transduced PSCs reported cells with an innate phenotype and function, reminiscent of $\gamma\delta$ or NK-like cells [57]. Complicating this picture is the wide range of tonic and antigen-induced signaling strengths achievable through modifications to structural or signaling element of the CAR [21, 26, 27, 30, 112], rendering studies on the impact of CARs on T cell differentiation specific not only to the *in vitro* T cell differentiation platform used but also the integrated signaling properties of the CAR used for each study.

We recently developed the artificial thymic organoid (ATO) system, a 3D culture method that supports mature, effector T cell differentiation from PSCs and human hematopoietic stem/progenitor cells *in vitro* [40, 47, 50]. We used this platform to interrogate the effect of constitutive expression of different CD19-targeted CARs on lymphoid development from PSCs. We report here the unexpected finding that certain CD19-targeted CARs led to a diversion of T lineage commitment to that of the closely related ILC2 lineage, resulting in a near complete loss of T cell output but generation of functionally mature CAR-ILC2s.

ILC2s are a helper-type innate lymphoid cell (ILC) lineage characterized by a predominantly type 2 cytokine response to epithelial-derived alarmins, including IL-25, IL-33, and thymic stromal lymphopoietin (TSLP) [60, 113]. Despite not subject to RAG-mediated $\alpha\beta$ TCR rearrangement during development, ILC2s share many developmental features with T cells including a requirement for Notch and IL-7 receptor signaling, and potential for intrathymic differentiation from common T/ILC2-primed lymphoid progenitors [80, 81, 83]. Despite these similarities, microenvironmental determinants governing T versus ILC2 commitment from lymphoid progenitors remains poorly understood. In contrast to microenvironmental cues, transcriptional regulation of ILC2 development has been characterized in some detail in mice, with ILC2 development sharing expression of key transcription factors with early T cell development, including BCL11B, TCF7, and GATA3 [85-90, 114], superimposed on which is ID2-mediated inhibition of E-protein activity essential for suppressing T-lineage potential [115].

We used the unexpected finding of CAR-mediated T-to-ILC2 lineage diversion in ATOs to identify the timing and potential mechanisms of CAR-mediated ILC2 differentiation and to identify strategies for both mitigating the CAR-imposed block in T differentiation or, conversely, directing ILC2 commitment from PSCs. We propose these findings as a starting point for investigating physiological control of this important but poorly understood branchpoint in human lymphocyte development, and as a framework for understanding the principles of CAR-T cell differentiation from PSCs.

2.2 Materials and Methods

2.2.1 Experimental models and subject details

2.2.1.1 Cell lines

The MS5-hDLL4 cell line was generated in our lab as previously described [50]. The MS5-hDLL4-CD19 cell line was generated by further transduction with a lentiviral vector encoding truncated human CD19 and purified in bulk by FACS using an anti-CD19 antibody. CAR target cells RAJI-ffLuc-eGFP and RAJI-ffLuc-eGFP-CD19^{KO} cells were gifted by Yvonne Chen (UCLA). Nalm6 cells were purchased from ATCC and for live imaging in Incucyte assays were transduced with a lentiviral vector encoding a nuclear-localized mKate2 fluorescent protein [116].

2.2.1.2 Human pluripotent cell lines

The human embryonic stem cell (hESC) lines H1 [117](WiCell, Madison, WI) and ESI-017[118] (ESI BIO, Alameda, CA) were maintained and expanded on Matrigel Growth Factor Reduced (GFR) Basement Membrane Matrix (BD Biosciences, Cat. 356231) in mTeSR Plus medium (Stem Cell Technologies, Cat. 100-0267). All H1-CAR lines were generated by transduction of H1 hESCs with pCCL-UBC lentiviral vectors encoding different CARs with 2A-linked eGFP. Transduced hESC lines were sorted by FACS according to eGFP expression and expanded for use in some cases used to derive clonal lines. Clonal lines were generated by plating sorted H1-CAR hESCs at limiting dilution density on 10 cm Matrigel-coated plates until single colonies were visible and transferred with a pipet to 24-well plates for expansion and validation. Vector copy number (VCN) quantification on certain lines was performed by droplet digital PCR.

2.2.2 Methods details

2.2.2.1 Generation and isolation of human embryonic mesodermal progenitors (hEMPs)

Mesoderm commitment was induced as previously described [50, 119, 120] with certain optimizations. Briefly, hESC cells were maintained on Matrigel-coated 6-well plates in mTeSR plus complete medium. At day (D) -18, mesoderm induction was initiated in X-VIVO 15 medium (Lonza, Cat. 04-418Q) supplemented with rhActivin A (10 ng/ml) (R&D Systems, Cat. 338-AC-010), rhBMP4 (10 ng/ml) (R&D Systems, Cat. 314-BP-010), rhVEGF (10 ng/ml) (R&D Systems, Cat. 298-VS-005), rhFGF (10 ng/ml) (R&D Systems, Cat. 233-FB-025), and ROCK inhibitor Y-27632 dihydrochloride (10 μ M) (Tocris, Cat. 1254). hESCs were plated on Matrigel coated 6-well plates at 3×10^6 cells per well in 3ml. Medium was then changed daily with X-VIVO 15 supplemented with rhBMP4 (10 ng/ml), rhVEGF (10 ng/ml), and rhFGF (10 ng/ml). At D-14, cells were washed with PBS and incubated with Accutase (Innovative Cell Technologies, Cat. AT-104) (1 mL per well, for 10 min at 37°C). Cells were harvested and hEMPs isolated by depletion of CD326+ cells by magnetic cell sorting (MACS) using CD326 (EpCAM) MicroBeads (Miltenyi, Cat. 130-061-101).

2.2.2.2 Pluripotent stem cell-derived embryonic mesoderm organoids (EMO) and reaggregated artificial thymic organoid (ATO) cultures

The sequential generation of hemato-endothelial cells in EMOs and then lymphoid cells in ATOs is depicted in Fig 1C. First, EMOs were established by aggregating hEMPs with MS5-hDLL4 cells by centrifugation. MS5-hDLL4 cells were harvested by trypsinization and resuspended in hematopoietic induction medium composed of EGM2 (Lonza Ref CC-4176) supplemented with ROCK inhibitor Y-27632 dihydrochloride (10 μ M) and TGF β RI inhibitor SB-

431542 (10 μ M) (Tocris Bioscience, Cat. 1614). At D-14, 5×10^5 MS5-hDLL4 cells were combined with 5×10^4 purified hEMP per EMO in 1.5 mL Eppendorf tubes and centrifuged at 300 g for 5 min at 4°C in a swinging bucket centrifuge. Supernatants were carefully removed, and the cell pellet was resuspended by brief vortexing and resuspended in hematopoietic induction medium at a volume of 6 μ l per EMO. 6 μ l of cells were plated as EMO on a 0.4 μ m Millicell transwell inserts (EMD Millipore, Billerica, MA; Cat. PICM0RG50) (3 EMOs per insert were plated) and placed in 6-well plates containing 1 mL of hematopoietic induction medium per well. Medium was changed completely every 2-3 days for 7 days. At D-7, medium was changed to EGM2 + 10 μ M SB-431542 with the hematopoietic cytokines 5 ng/ml rhTPO (R&D Systems, Cat. 288-TP), 5 ng/ml rhFLT3L (R&D Systems, Cat. 308-FK-025), and 50 ng/ml rhSCF (R&D Systems, Cat. 300-07). This medium was changed every 2-3 days for an additional 7 days.

At D0, EMOs were harvested into single cell suspensions in MACS buffer (PBS/0.5% bovine serum albumin/2mM EDTA) by mechanical dissociation for reaggregation into ATOs. Reaggregation served dual purposes of removing adherent, non-hematopoietic elements, resulting in more consistent lymphoid differentiation, and permitting stage-specific manipulation of certain conditions at EMO or ATO stages, as described below. Briefly, EMOs were washed off culture inserts by pipetting and gently dissociated with the help of a syringe tip before passaging through a 50 μ m nylon strainer. Live, round, hematopoietic EMO cells were counted with trypan blue and $1-5 \times 10^3$ live cells were reaggregated with 2.5×10^5 fresh MS5-hDLL4 cells per ATO. Lymphoid induction medium “RB27” (composed of RPMI 1640 (Corning, Manassas, VA), 4% B27 supplement (ThermoFisher Scientific, Grand Island, NY), 30 μ M L-ascorbic acid 2-phosphate sesquimagnesium salt hydrate (Sigma-Aldrich, St. Louis, MO) reconstituted in PBS, 1% penicillin/streptomycin (Gemini Bio-Products, West Sacramento, CA), and 1% GlutaMAX

(ThermoFisher Scientific, Grand Island, NY)) was supplemented with 10 ng/ml rhSCF, 5 ng/ml rhFLT3L, and 5 ng/ml rhIL-7 (R&D Systems, Cat. 207-IL-25). Medium was changed completely every 3-4 days for 5-8 weeks.

For downstream analysis, ATOs were harvested at the indicated timepoints by adding MACS buffer (PBS/0.5% bovine serum album/2mM EDTA) to each well and briefly disaggregating the ATO by pipetting with a 1 mL ‘‘P1000’’ pipet, followed by passage through a 50 μ m nylon strainer. Cells were then analyzed by FACS or, for functional assays, debris and apoptotic cells were removed by MACS using the Dead Cell Removal Kit (Miltenyi, Auburn CA, Cat. 130-090-101) prior to use.

2.2.2.3 Lentiviral vectors and transduction

All CD19-targeted CARs used the scFv derived from FMC63 [121]. Long or short IgG4 spacer/hinge domains were as previously described [24] followed by a human CD28 or CD8 α transmembrane domain, a CD28 or 4-1BB costimulatory domain, and CD3 ζ intracellular signaling domain, as previously described [122, 123]. The codon optimized CAR coding sequences were cloned into the second generation pCCL lentiviral vector downstream of a ubiquitin C (UBC) promoter (gift of Donald Kohn, UCLA). A furin cleavage site, spacer, and 2A-linked eGFP fluorescent protein coding sequence was added downstream of CD3 ζ .

Packaging and concentration of lentivirus particles was performed as previously described [40]. Briefly, 293T cells (ATCC) were co-transfected with lentiviral vector plasmid, pCMV- Δ R8.9, and pCAGGS-VSVG using TransIT-293 (Mirus Bio, Madison, WI, Cat. MIR 2700) for 17 hours followed by treatment with 10 mM sodium butyrate for 8 hours, followed by generation of cell supernatants in serum-free UltraCulture for 48 hours. Supernatants were concentrated by

ultrafiltration using Amicon Ultra-15 100 KDa filters (EMD Millipore, Billerica, MA, Cat. UFC910024) at 4000 g for 40 minutes at °4C and stored as aliquots at -80C.

2.2.2.4 Flow Cytometry

For phenotypic analysis, all surface flow cytometry stains were performed in PBS/0.5% BSA/2 mM EDTA for 20-30 min on ice. TruStain FcX (Biolegend, San Diego, CA) was added to all samples prior to antibody staining. DAPI was added to all samples prior to analysis for viability staining.

For intracellular transcription factor profiling, cells were stained for surface markers and Zombie Aqua Fixable Viability dye (Biolegend, San Diego, CA) prior to fixation and permeabilization with True Nuclear Transcription Factor Staining kit (Biolegend, Cat. 424401) and intracellular stained with antibodies against GATA3, Eomes, Tbet, and ROR γ t.

Analysis was performed on an LSRII Fortessa, and FACS sorting on FACSARIA or FACSARIA-H instruments (BD Biosciences, San Jose, CA) at the UCLA Broad Stem Cell Research Center Flow Cytometry Core. For all analyses, viable cells were gated based on the viability dye, and single cells were gated based on FSC-H, FSC-W, SSC-H, and SSC-W parameters. Anti-human antibody clones used for surface and intracellular staining were obtained from Biolegend (San Diego, CA): CD107a (H4A3), CD117 (104D2), CD127 (A019D5), CD16 (3G8), CD161 (HP-3G10), CD19 (H1B19), CD2 (RPA-2.10), CD22 (HIB22), CD200R (OX-108), CD235a (HI264), CD25 (BC96), CD294 (BM16), CD3 (UCHT1), CD34 (581), CD4 (RPA-T4), CD43 (CD43-10G7), CD45 (HI30), CD5 (UCHT2), CD56 (HCD56), CD7 (CD7-6B7), CD8 α (SK1), CD94 (DX22), GM-CSF (BVD2-21C11), ICOS (C398.4A), interferon g (4S.B3), IL-13 (JES10-5A2), IL-2 (MQ1-17H12), IL-4 (MP4-25D2), IL-5 (JES1-39D10), NKG2D (1D11),

NKp44 (P44-8), NKp46 (9E2), PD-1 (EH12.2H7), Tbet (4B10), TCR $\alpha\beta$ (IP26), TNF α (Mab11), Invitrogen: Eomes (Clone WD1928), ROR γ t (Clone AFKJS-9), and BD Biosciences (San Jose, CA): GATA3 (Clone L50-823). Anti-mouse CD29 (clone HMb1-1) was obtained from Biolegend. Flow cytometry data were analyzed with FlowJo software (Tree Star Inc.). A list of antibodies used is included in the key resources table.

2.2.2.5 In vitro proliferation assays

H1-CAR ILC2s were isolated from week 5-9 ATOs as described above. For proliferation assays, up to 1×10^5 cells were plated in 200 μ l AIM V (ThermoFisher Scientific, Cat. 12055091), 5% human AB serum (Gemini Bio, Cat. 100-512) with 20 ng/mL rhIL-2 (Peprotech) and 20 ng/mL rhIL-7 (Peprotech) plus indicated cytokines at 20 ng/mL (Peprotech) in the absence or presence of irradiated Nalm6 cells in a 3:1 effector to target (E:T) ratio. Fresh cytokines were replenished at day 3 via half-media change, and cells were replated into larger wells when confluent, approximately every 2-3 days. Irradiated Nalm6 cells were added again on day 7 of expansion. Cells were counted twice a week on a hemocytometer.

H1-CAR T cells were expanded at 5×10^5 cells/mL in AIM V (ThermoFisher Scientific, Cat. 12055091) supplemented with 5% human AB serum (Gemini Bio, Cat. 100-512), 5 ng/ml rhIL-7 (R&D), and 100 IU/ml rhIL-2 (Miltenyi Biotec, Cat. 130-097-748) with irradiated Nalm6 cells added at a 3:1 E:T ratio for 5 days prior to functional assays.

2.2.2.6 Intracellular cytokine assays

For intracellular cytokine detection, ILC2 or T cells were stimulated with PMA/ionomycin/protein transport inhibitor cocktail or control protein transport inhibitor cocktail

(eBioscience, Cat 00-4975-93, Cat 00-4980-03, San Diego, CA) for 6 hours prior to fixation and staining. APC-labeled CD107a antibody (Biolegend, clone H4A3) was added to wells at a 1:100 dilution for the final 2 hours of culture. Cells were washed and stained for surface markers and Zombie Aqua Fixable Viability dye (Biolegend, Cat. 423101) prior to fixation and permeabilization with an intracellular staining buffer kit (eBioscience, Cat. 88-8824-00) and intracellular staining with antibodies against corresponding cytokines. For antigen-specific CAR-T cytokine assays, T cells were expanded for 5 days with irradiated Nalm6 cells as above and 1×10^5 CAR-T cells were co-cultured with RAJI or RAJI-CD19^{KO} cells at a 1:1 ratio for 6 hours with addition of APC anti-CD107a for the final 2 hours and stained as above.

2.2.2.7 In vitro ILC2 plasticity assay

Week 6 H1-CAR ILC2 were purified from mechanically dissociated ATOs using the Dead Cell Removal Kit (Miltenyi, Auburn CA), followed by staining with PE-anti-CD8 and anti-PE MicroBeads (Miltenyi, Auburn CA) to deplete any CD8⁺ T and NK/ILC1 cells. 1.5×10^5 ILC2-enriched cells were plated in 96-well U-bottom plates as per proliferation assays above. For type 1 polarization, 20 ng/mL rhIL-12 (Peprotech) was added in addition to rhIL-7 and rhIL-2 as described above. For type 2 polarization, rhIL-25, rhIL-33, and rhTSLP were added in addition to rhIL-7 and rhIL-2 at 20 ng/ml each. On day 5, protein transport inhibitor cocktail (eBioscience, San Diego, CA) was added to each well and incubated for 6 hours. Cells were washed and stained for surface markers and Zombie Aqua (Biolegend, San Diego, CA) prior to fixation and permeabilization with an intracellular staining buffer kit (eBioscience, San Diego, CA) and intracellular staining with antibodies against IFN γ , TNF α , IL-5, and IL-13 (Biolegend, San Diego, CA).

2.2.2.8 In vitro cytotoxicity assays

1.5x10⁴ RAJI cells transduced with nuclear-localized mKate2 as described above were plated in 100 μ L RPMI 1640 with 10% FBS on black-walled tissue culture treated flat-bottom 96-well plates (Corning, Cat. 3904) pre-coated with 50 μ L/well poly-L-lysine (Sigma, Cat.P4832-50mL) for 1 h at room temperature followed by 3 washes with 200 μ L PBS, followed by drying at room temperature for 2 h. Cells were incubated for 30 to 60 min to settle and adhere. CAR-T cells isolated from H1-CAR ATOs and expanded as above were added at a 1:1 E:T ratio in 100 μ L RPMI 1640 with 10% FBS supplemented with 2X rhIL-7 (R&D) and rhIL-2 (Miltenyi) for a final concentration of 5 ng/mL and 100 IU/mL, respectively. Control T cells from H1 ATOs were isolated from ATOs and used as CAR-negative controls. Triplicate wells were set up for each condition, and live cell imaging was performed for 5 days on an Incucyte Zoom instrument. Red fluorescence was evaluated at each timepoint using the manufacturer's software.

2.2.2.9 Bulk RNA sequencing

H1 ATO mature CD8SP T cells were FACS sorted as DAPI-CD3+TCR $\alpha\beta$ +CD4-CD8 $\alpha\beta$ +CD45RA+ and H1-CAR-DN cells, containing ILC2s, as DAPI-eGFP+CD3-TCR $\alpha\beta$ -CD8 α -CD4- from week 6 ATOs. Biological triplicate samples were sorted from three independent experiments using a FACSAria II flow cytometer. Total RNA was isolated from 3-5x10⁴ cells using the RNeasy Micro kit (QIAGEN) and 1.5 ng of total RNA was input to generate sequencing libraries with SMARTer Stranded Total RNA-Seq (Pico) Kit (Clontech, Cat. 635005). Paired end 150 bp sequencing was performed on an Illumina HiSeq 3000.

2.2.2.10 Bulk RNA sequencing data processing

Raw sequence files were obtained, and quality checked using Illumina's proprietary software. The STAR ultrafast universal RNA-seq aligner v2.5.2b [124] was used to generate the genome index and perform paired-end alignments. Reads were aligned to a genome index that includes both the genome sequence (GRCh38 primary assembly) and the exon/intron structure of known gene models (Gencode v26 basic genome annotation). Alignment files were used to generate strand-specific, gene-level count summaries with STAR's built-in gene counter. Only protein-coding, long-noncoding, anti-sense and T-cell receptor genes in the Gencode v26 annotation were considered (98% of total counts on average). Independent filtering was applied as follows: genes with less than one count per sample on average, count outliers or low mappability were filtered out for downstream analysis [9, 125]. Counts were normalized per-sample in units of FPKMs after correcting for gene mappable length and sample total counts. Differential expression analysis was performed with DESeq2 [125]. Pairwise differential expression was performed to classify genes as differentially expressed between any two cell types (Wald test adjusted p-value $< 1e-10$, fold change > 2).

2.2.2.11 Single cell RNA sequencing

Day 0, 4, and 7 ATOs were harvested into single cell suspensions in MACS buffer (PBS/0.5% bovine serum albumin/2mM EDTA) by mechanical dissociation. Live cells were first enriched with the Dead Cell Removal Kit (Miltenyi Biotec, Cat 130-019-101). Cells were then stained and FACS-sorted as DAPI- mouse CD29- (Biolegend, San Diego, CA) to deplete any residual dead cells and MS5 stromal cells, respectively. Sorted cells were delivered to the UCLA TCGB (Technology Center for Genomics and Bioinformatics) Core for single cell 3' RNA

sequencing using the 10X Genomics Chromium™ Controller Single Cell Sequencing System (10X Genomics), following the manufacturer’s instructions and the TCGB Core’s standard protocol. Cells were loaded in the Chromium™ Controller for partitioning single cells into nanoliter-scale Gel Bead-In-Emulsions (GEMs) aiming for a recovery of up to 10,000 cells. Single Cell 3’ reagent kit was used for reverse transcription, cDNA amplification and library construction of gene expression libraries (10x Genomics) according to the manufacturer’s instructions. Libraries were sequenced on a NovaSeq 6000 S4 Flow cell (CeGaT GmbH T€ubingen).

2.2.2.12 Single cell RNA sequencing data processing

Single-cell RNA analysis (including quality control, data normalization, dimension reduction, cluster detection, differential expression testing) were performed using Seurat 4.0 package [126] in R following standard workflow.

Transcriptome data were mapped to the GRCh38 reference genome assembly with Cell Ranger (10X Genomics) and subjected to Seurat for pre-processing and normalization using SCTransform. Cell cycle scores, percent of mitochondrial genes, and percent of ribosomal genes were assigned and regressed out during scaling. Normalized data were integrated based on identification of ‘anchors’ between pairs of datasets with reciprocal PCA. Then PCA was performed, and significant PCs were selected based on the elbow of standard deviations of PCs. The first 20 PCs were used for calculation of UMAP (Uniform Manifold Approximation and Projection) and the neighborhood graph for clustering. The FindAllMarkers function was used to find specific genes for each cluster, which uses the Wilcoxon rank-sum test. Cell types were annotated based on the marker genes compared to canonical markers.

Clusters expressing *CD7* and/or *IL7R* were defined as lymphoid cells and selected for further analysis. Lymphoid cells were then subjected for reclustering. To better appreciate the heterogeneity within these cells, PCA was recalculated in the lymphoid subset and PC of 20 was used for UMAP projection and clustering again. Differential gene expression analyses were performed with the FindMarkers function using the Wilcoxon test with a log fold-change threshold of 0.25 and a minimum expression frequency of 0.1. Pathway analysis was performed using the Single Cell Pathway Analysis (SCPA) package in R [127]. Wikipathways were used as input gene sets using the msigdb package.

2.2.2.13 Gene set enrichment analysis (GSEA)

T and ILC2 gene signatures were defined based on single cell RNA-sequencing transcriptomes of human fetal hematopoietic cells. Raw transcript counts were obtained from GEO (GEO: GSE163587, [128]) and further processed using Seurat 4 in R. Single-cell data analysis (including quality control, data normalization, dimension reduction, clusters detection) were performed as described in Liu et al., 2021. T and ILC2 lineage specific clusters were identified based on highly expressed specific markers in each cluster. Signature genes were defined by all the upregulated differentially expressed genes. Gene Set Enrichment Analysis (GSEA) [129] was performed by the GSEA software based on human T and ILC2 gene signatures between H1 SP8 T cells and H1-CAR DN ILC2 enriched cells.

2.2.2.14 Quantification and statistical analysis

Data are presented as mean \pm standard deviation (s.d.) or mean \pm standard error of the mean (SEM) as indicated. Statistical tests used are stated in each figure legend, adjusted p value

significance was classified as such: * $p < 0.05$; ** $p < 0.01$; *** $p < 0.001$; when tested. Statistical analyses were performed using GraphPad Prism software.

2.2.2.15 Data and code availability

The GEO accession number for the bulk and single cell RNA-seq data reported in this paper is (pending submission). This paper does not report original code. All code for data processing has been previously published.

2.3 Results

2.3.1 CAR-induced inhibition of T cell differentiation from PSCs

We applied the artificial thymic organoid (ATO) differentiation system to study the effects of CAR expression during T cell development from human pluripotent stem cells (PSCs). Using a lentiviral vector expression system previously validated for TCR expression in PSC ATOs [50], we transduced the H1 embryonic stem cell (ESC) line [117] with a 2nd generation CD19-targeted CAR containing an FMC63 scFv, IgG4 CH2/CH3 long spacer and hinge, CD28 transmembrane (TM), CD28 costimulatory, and CD3 ζ signaling domains [121, 130, 131] (Fig 1A) 2A-linked to eGFP to generate a stable, clonal CAR-expressing PSC line (H1-CAR). Surface CAR expression was readily detectable on this line using an anti-idiotypic antibody (Fig 1B).

Lymphocyte differentiation followed a three-phase protocol as previously described [50], comprising feeder-free generation of embryonic-like mesoderm progenitors (EMP) followed by aggregation with the MS5-hDLL4 stromal cell line in 3D culture on permeable cell culture inserts to form embryonic mesoderm organoids (EMO), which support mesoderm differentiation (day (D-

14 to D-7) and hematopoietic specification (D-7 to D0). In a modification to the original protocol, non-adherent cells were isolated from EMOs on D0 and reaggregated at defined ratios with fresh MS5-hDLL4 cells to form ATOs, which supported T cell commitment and maturation (D0 to weeks 5-8) (Fig. 1C).

Analysis of ATO differentiation from H1 PSCs showed orderly T cell differentiation from T-lineage (CD7⁺ CD5⁺), CD4⁻ CD8⁻ double negative (DN) precursors to CD4⁺ CD8⁺ double positive (DP) precursors, CD3⁺ TCR $\alpha\beta$ ⁺ “late” DPs and, ultimately, CD3⁺ TCR $\alpha\beta$ ⁺ CD8⁺ CD4⁻ “single-positive” (CD8SP) mature T cells between weeks 3 and 6 (Fig. 2A). As previously reported, at week 6, CD3⁺ TCR $\alpha\beta$ ⁺ CD4⁺ CD8⁻ single-positive (CD4SP) T cells were a clear but minor population, as were CD3⁺ TCR $\alpha\beta$ ⁻ cells (previously shown to be enriched for $\gamma\delta$ T cells) [50]. In contrast, H1-CAR ATOs, while still producing CD7⁺ lymphoid precursors, exhibited a block in T-lineage differentiation, generating some early, transient DPs at week 3, but largely failing to develop CD3⁺TCR $\alpha\beta$ ⁺ T cells by week 6 (Fig 2B). Despite the lack of T cell generation in H1-CAR ATOs, cell numbers at week 6 were largely preserved (Fig 3A) and still comprised a majority of CD7⁺ lymphoid cells (Fig 2B), prompting us to look for evidence of ILC generation (Fig 3B).

2.3.2 CAR-induced ILC2-biased innate lymphoid differentiation from PSCs

In flow cytometry analysis of week 6 ATOs, T-lineage cells were defined as either CD4⁺ (which includes early ISP4 and DP precursors) or CD3⁺ (including late DP and SP T cells) (Fig. 4A). As the CD4⁻CD3⁻ population could theoretically contain DN T cell precursors, sorting this population from either H1 or H1-CAR ATOs at week 2 followed by re-aggregation in new ATOs did not lead to generation of DPs or CD3⁺ T cells, suggesting clearance of DN T-precursors by week 2 (Fig. 4B). Among the CD3⁻ CD4⁻ population in week 6 H1-CAR ATOs there was a modest

expansion of CD7⁺ NK/ILC1-like cells, accounting for <10% of CD45⁺ cells (Fig 5A), which heterogeneously expressed CD2, CD5, CD56, and CD8 α (Fig 4C). Based on these minimal surface markers, we designated this population “NK/ILC1” due to the inability to distinguish between these group 1 ILC populations based on surface markers alone [132-134]. Of the remaining cells, while we did not detect CD117⁺NKp44⁺ ILC3s, the majority unexpectedly showed an ILC2 phenotype, defined as CD7⁺CD200R⁺CD25^{hi} (Fig 3B).

When we compared multi-lymphoid differentiation in week 6 ATOs between H1-CAR with H1 quantitatively, we saw a significant increase in generation of ILC2 cells induced by the CAR expression, with a slight increase in NK/ILC1 (Fig 5A). Time course analysis of weekly ATO culture revealed that although there was a transient expansion of T cell precursors (defined as CD3⁺CD4⁺ which includes ISP4s and early DPs) in early culture, majority of the T precursors didn't mature into CD3⁺ T cells as the H1 control, while the ILC2 lineage cells occurred as early as week 1 and continuously grew in culture, eventually consisting about 80% of the total culture (Figs 5 B, C). We also determined that CAR-mediated T-to-ILC2 diversion was not specific to the H1 ESC line, as a second line, ESI-017 [118], revealed the same ILC2-bias in ATOs when transduced with the same CAR construct (Fig 5D).

2.3.3 CAR-ILC2 cells are type 2 cells by immunophenotype and transcriptional profiles

Further examination of this population revealed expression of other canonical ILC2 surface markers including c-Kit, CRTH2, CD161, and ICOS [135], and negativity for T markers including CD2, TCR $\gamma\delta$, CD27 and CD28, as well as being negative for a panel of NK markers CD56, CD94, CD16, NKp44, NKp46, NKG2D, and KIR2DL1. (Fig 6A). Bright expression of CD200R and CD25 was therefore used to reliably identify this ILC2-like population in subsequent

experiments. We confirmed the ILC2 identity of these cells by intracellular staining, which showed high protein expression of GATA3 and low levels of Eomes, T-bet and ROR γ t, excluding the presence of other ILC subtypes (Fig 6B).

To further characterize the ILC2 population, we performed bulk RNA sequencing of sorted DN cells from H1-CAR ATOs compared to CD8SP T cells from control H1 ATOs. This revealed in the H1-CAR DN population a strong ILC2 gene expression signature that included high expression of further ILC2-defining receptors including IL2RA, IL1RL1 (IL33R/ST2), IL17RB (IL25R); type 2 cytokines including CSF2 (GM-CSF), IL4, and IL13; and the ILC2-associated transcription factors ZBTB16, GATA3 and TCF7 (Figs 7A, 8). Interestingly, while the canonical ILC gene ID2 was expressed at similar levels between the ILC2-like and CD8SP T cells, expression of its functional homolog, ID3, was specifically increased in the ILC2-like cells (Fig 8). Gene set enrichment analysis [129] using gene signatures from an independent study of human fetal ILC2s and T cells [128] showed that the H1-CAR DN transcriptome correlated positively with the ILC2 gene signature and negatively with the T cell signature, whereas the opposite was true of H1 ATO-derived CD8SP T cells (Fig 7B).

2.3.4 CAR-ILC2 are type 2 cells subject to functional plasticity

We next confirmed the H1-CAR ILC2-like cells were functional ILC2s. Freshly isolated CAR-ILC2s from ATOs robustly produced type 2 cytokines IL-4, IL-13, and GM-CSF in response to PMA/ionomycin, in addition to IL-2 and TNF α (Fig. 9A) which are also reportedly produced by ILC2s in mice and humans [136, 137]. Although type 2 cytokines IL-5 and IL-9 were found to be produced by ILC2s in some reports [60], we didn't see their expression in the freshly isolated

CAR-ILC2s, potentially indicating some tissue specific heterogeneity or a less mature phenotype of the CAR-ILC2s we generated (Fig. 9A).

Several studies have described type I helper plasticity of ILC2s in response to IL-12, resulting in type 1 “polarized” ILC2s capable of producing IFN γ [63-66]. We tested the type I plasticity potential of CAR-ILC2s by culturing them with either IL-12 or the combination of IL-25, IL-33, and TSLP followed by PMA/ionomycin stimulation. While some baseline IFN γ production was seen in IL-25/33/TSLP cultured cells, the majority produced IL-5 under these conditions, consistent with ILC2 type 2 function. Conversely, IL-12 not only increased the frequency of IFN γ -producing cells but also suppressed IL-5 producing cells, consistent with the type I plasticity ascribed to ILC2s (Figs 9B, C).

While primary ILC2s lack rearranged antigen receptors and physiologically respond to epithelial-derived alarmins including IL-25, IL-33, and TSLP, we found that CAR-ILC2s additionally expanded in response to CD19-positive Nalm-6 cells in the presence of IL-7 and IL-2, which was modestly increased by addition of IL-25, IL-33, and TSLP (Fig. 9D), indicating novel antigen-specific functionality through the CAR.

2.3.5 scRNA-seq revealed multilineage hematopoiesis in early ATOs

We next sought to understand the transcriptional events leading to ILC2 differentiation in CAR-ATOs. We first analyzed global hematopoietic differentiation in H1 and H1-CAR ATOs by flow cytometry and single cell RNA sequencing (scRNA-seq) at ATO Day 0, Day 4, and Day7 timepoints (Fig 10A). Flow cytometry at these timepoints showed no obvious differences in hematopoietic differentiation based on expression of CD43 and CD45 (Fig 10B). Based on the expression of CD235a for erythroid differentiation and CD7 for lymphoid differentiation on Day

7, both H1 and H1-CAR culture had predominant erythroid development as well as emergence of lymphoid lineages.

scRNA-seq at the same timepoints revealed multilineage hematopoietic development based on canonical, lineage-defining genes (Fig 11). Gene expression clusters were annotated representing erythroid (exemplified by expression of *HBZ*, *HBA1*, *HBG1*, *GYP A*, *KLF1*), megakaryocyte (*PPBP*, *PF4*, *GP1BB*, *ITGA2B*, *GP9*), myeloid, and lymphoid development. Myeloid lineages included monocyte (*FCER1G*, *SOD2*, *CTSD*, *CD68*, *CTSS*), neutrophil (*DEFA3*, *MPO*, *AZU1*, *PRTN3*, *LYZ*), and eosinophil (*PRG2*, *EPX*, *PRG3*, *IL5RA*, *IL1RL1*) clusters, as well as a surprisingly prominent mast cell (*TPSB2*, *HPGD*, *TPSAB1*, *CPA3*, *GATA2*) cluster (Figs 11B, C). The lymphoid cluster expressed *IL7R*, *CD7*, *CD3D*, *CD3G*, and *CD247*, with a B cell signature notably absent. Also absent was a clear signature of hematopoietic stem/progenitor cells, suggesting that multipotent progenitor cells may have emerged and differentiated within the preceding EMO stage prior to ATO Day 0. Aside from a slightly higher lymphoid-to-erythroid ratio in H1 versus H1-CAR ATOs mostly coming from Day 7 (Figs 12B, 13B), also seen by flow cytometry (Fig 10C), no major CAR-associated differences in multilineage cluster dynamics were appreciated (Figs 12, 13).

2.3.6 scRNA-seq revealed multi-lymphoid differentiation in early ATOs

As a multipotent progenitor stage was not identified, we focused our attention on the lymphoid cluster characterized by expression of *IL7R* and *CD7*. To validate that our scRNA-seq analysis was representing early lymphoid progenitors/precursors rather than mature cells, we determined by flow cytometry that mature ILC2s co-expressing CD200R and CD25 were rare, representing no more than 1% of H1 or H1-CAR ATOs at Day 7 (Fig 14A). Within the CD7+

population by flow, immature single-positive CD4⁺ (ISP4) and some CD3-negative early DP T cell precursors were seen at D7, however the frequency of DPs was markedly lower in H1-CAR compared to H1 ATOs, consistent with an already evident block in T cell differentiation (Fig 14B).

By scRNAseq, reclustering the lymphoid clusters from concatenated Day 0, Day 4, and Day 7 samples revealed multilymphoid development (Figs 15A, B, C). There was global lymphoid expression of *IL7R*, *CD7* and, surprisingly, the TCR components *CD3D*, *CD3E*, *CD3G* and *CD247* (Figs 15C, D). A major continent contained the three main ATO lymphoid lineages: T, ILC2, and NK/ILC1. The T lineage cluster was characterized by expression of *RAG1*, *PTCRA*, and *CD8B*, whereas the ILC2 precursor cluster was negative for these genes but expressed *GATA3*, *PTGDR2* (encoding CRTH2) and *KLRB1*. The NK/ILC1 precursor cluster expressed canonical genes including *GZMB*, *TBX21*, *NKG7*, and high *ID2* (Figs 15B, C, 18A).

Outside of these three main clusters, a small ILC3-lineage cluster expressed high *ID2*, *RORC*, *KIT*, and *IL1R1* (Figs 15B, C, 18A). A *KLF1* and *GYP A*-positive erythroid-like cluster that co-expressed low levels of *IL7R*, *CD7*, and the *CD3* genes was of unclear significance (Figs 15B, C). Finally, a small cluster containing a low frequency of cells expressing *IL7R*, *CD7* and *CD3D* as well as *CD34* was the sole lymphoid-like cluster detected at Day 0 and was not detectable by Day 4 (Figs 15C, 17). This cluster also contained cells expressing the embryonic hematopoietic progenitor-associated genes *SPI1*, *SPINK2*, and *RUNX1* (Fig 15C), however a larger proportion of this cluster expressed myeloid genes including MPO, LYZ, and AZU1 (data not shown), making the ultimate identity of this putative progenitor cluster unclear.

2.3.7 CAR activation in early lymphoid progenitors precedes ILC2-biased differentiation

While the NK/ILC1 lineage cluster was represented at a similar frequency between H1 and H1-CAR groups, the ILC2 and T lineage clusters showed a clear inverse relationship between the H1 and H1-CAR groups (Figs 16, 17). Interestingly, the T lineage cluster emerged at very low frequency on day 4 and didn't expand until day 7 while the ILC2 precursor cluster had an early occurrence on day 4 and persisted on day 7 (Fig 17B), suggesting that the ILC2 lineage might appear earlier than T lineage during development.

Focusing specifically on transcription factors expressed within the T, ILC2, and NK/ILC1 clusters, all three were noted to share expressions of *RUNX3* and *ETS1*, the latter slightly higher in the NK/ILC1 cluster. The NK/ILC1 cluster showed high levels of *TBX21* and *ID2*. The T and ILC2 clusters shared expression of *TCF7* and *BCL11B*, whereas high levels of *GATA3* and *ID3* distinguished ILC2 from T lineages (Fig 18A). *ID2* has been shown to enforce both NK and ILC2 lineage commitment in mice through suppression of E-protein activity required for T cell lineage progression [138]. Consistent with this, *ID2* was expressed in both NK/ILC1 and ILC2 precursor clusters. Surprisingly *ID2* expression was much lower in the ILC2 cluster than NK/ILC1; conversely, its functional homolog *ID3* was highly expressed in the ILC2 precursor cluster (Fig 18B) and, intriguingly, also in our earlier bulk RNA-seq of mature CAR-ILC2s (Fig 8). We also noted expression of certain genes associated with the NK/ILC1 lineage in the ILC2 cluster including *ZBTB16* (encoding PLZF), *ZNF683* (encoding HOBIT), *GNLY*, *NKG7*, and *FCER1G* (Fig 18A), although these were at much lower levels than in the NK/ILC1 cluster.

Having identified putative ILC2 precursors enriched in the H1-CAR ATOs, we performed pathway analysis on genes differentially expressed between ILC2 and T precursor clusters. This revealed an unexpected enrichment in the direction of the ILC2 cluster of genes associated with

TCR signaling and T cell activation (Fig 19A). Gene sets associated with STAT3 and type 2 cytokine receptor signaling, including IL-4, IL-5, and IL-9, were also enriched, however the redundancy of genes activated by these programs and CAR-mediated CD28/CD3 ζ signaling is unclear. Actin cytoskeleton remodeling pathways were also activated, raising the possibility of CAR-derived CD28 signaling which has been shown to mediate TCR-independent cytoskeletal remodeling in T cells [139]. We hypothesized that the signature of TCR activation represented CAR activation in ILC2 precursors. Indeed, the critical CD3 ζ signal transduction molecules *LCK*, *ZAP70*, and *LAT* were expressed across all lymphoid clusters, theoretically supporting CAR activation even in these early precursors (Fig 19B). Upregulation of the TCR activation marker CD69 specifically within the ILC2-lineage cluster provided further indirect support of CAR activation within ILC2 precursors (Fig 19B). As expected, genes downregulated in the ILC2 cluster were enriched in pathways associated with conventional T cell development including Notch, AHR, and TSLP signaling pathways (Fig 19C).

2.3.8 Tuning CAR expression level controls T versus ILC2 lineage output

Given the possibility of constitutive CAR signaling driving T to ILC2 diversion in ATOs, we reasoned that modulating CAR signaling strength might offer specific control over T versus ILC2 lineage output. First, we excluded the possibility of antigen-dependent CAR signaling in ATOs, as CD19 expression was not detected in ATOs by either flow cytometry or RNA-seq (Fig 20), consistent with the absence of B cell lineage clusters by scRNA-seq. We next tested approaches to modulate tonic CAR signaling in ATOs.

Reports have shown lentiviral vector copy number (VCN)-dependent effects on CAR expression and thus functional outcomes in mature T cells [21, 140, 141]. We therefore tested the

effect of lowering CAR VCN on T versus ILC2 output in PSC ATOs. Using the same CD19-CD28 ζ CAR vector used in the previous experiments, we derived two additional H1-CAR lines with progressively lower CAR expression (designated H1-CAR-med and H1-CAR-low, respectively, with the original line designated H1-CAR-high for these experiments). We saw a close correlation between VCN and surface CAR expression in these lines (Figs 21A, B). Upon differentiation in ATOs, hematopoietic progeny cells maintained differential CAR surface expression (Fig 22C). We observed a dose-dependent positive correlation between CAR expression level and ILC2 output, with H1-CAR-high ATOs showing high ILC2 output and a near complete block in T cell differentiation, while H1-CAR-low ATOs showed low ILC2 generation and restoration of normal T cell differentiation, including maturation to CD3⁺ TCR $\alpha\beta$ ⁺ CD8SP T cells (Figs. 22A, B). H1-CAR-med ATOs showed intermediate output that was still heavily ILC2-biased.

2.3.9 Tuning CAR expression level affects CAR activation potential

We next tested whether phenotypically normal CD8SP T cells from H1-CAR-med and H1-CAR-low were functional through the CAR. While the small number of CD3⁺ CAR-T cells generated in H1-CAR-med ATOs underwent CD19-dependent activation as seen by downregulation of surface CAR and upregulation of CD25, CAR-T cells from H1-CAR-low ATOs showed diminished antigen-dependent activation, indicating that the threshold of tonic signaling below which normal T cell differentiation occurred was also suboptimal for antigen-dependent T cell activation through the CAR (Fig 23).

2.3.10 Antigen-dependent CAR activation during early ATO diverts T to ILC2 lineage

We used the low CAR expression of the H1-CAR-low PSC line to test the hypothesis that strong CAR signaling inhibits T cell differentiation and drives ILC2 output in ATOs. We tested whether by presentation of CD19 by ATO stromal cells in H1-CAR-low ATOs could recapitulate the phenotype of H1-CAR-med and H1-CAR-high ATOs. We generated a CD19-expressing ATO stromal line (MS5-hDLL4-CD19) and tested substitution with this line at either the EMO stage (Day -14 to Day 0), ATO stage (Day 0 onward), or both stages in H1-CAR-low ATOs (Figs 24, 25). We observed no effect on T cell development when CD19 was presented during the EMO stage only, however provision of CD19 at either the ATO stage or both EMO and ATO stages recapitulated robust ILC2 output and a near complete block in T cell differentiation, together with a modest increase in NK/ILC1 (Figs 24, 25). These findings were consistent with a role for CAR signaling in T-to-ILC2 diversion, and with our earlier scRNA-seq finding that CAR-mediated T/ILC2 lineage bifurcation occurred between ATO Day 0 to Day 7, rather than during earlier multilineage hematopoietic differentiation in EMOs.

2.3.11 CAR costimulatory domain substitution permits CAR-T cell development

Structural elements of the CAR have also been shown to influence both tonic and antigen-dependent CAR signaling, with modifications to the scFv, linker, hinge, transmembrane, and signaling domains all having been shown to affect signaling strength and downstream T cell function [21, 26-28, 142-144]. We tested the effect on T versus ILC2 differentiation of structural variations that potentially lower CAR tonic signaling. First, as the CD19 CAR used in the previous experiments used a long, non-mutated IgG4 hinge/ spacer with known potential for antigen-independent ligation by Fc receptors [24, 25, 142], we generated a H1-CAR line using an IgG4

short hinge (SH) in which the CH2-CH3 spacer containing the Fc binding site was deleted, but otherwise identical to the original CAR, containing a CD28 transmembrane (TM) and CD28 costim and CD3 ζ signaling domains (H1-CARSH.28TM.28 ζ) (Fig 26). Deletion of the IgG4 CH2-CH3 spacer had no effect on ILC2-biased differentiation in ATOs (Fig. 27).

CD19 CARs that use 4-1BB signaling domains have been shown to have lower overall signaling strengths compared to CD28 signaling domain CARs [21, 29, 30]. Furthermore, the transmembrane (TM) domain of CD28 itself, used in our original CAR construct, has also been implicated in enhanced CAR signaling strength [26-28]. We changed these two elements by generating H1 lines using CD19 short hinge CARs containing either CD8 α TM and 4-1BB signaling domains (H1-CARSH.8aTM.BB ζ), or CD28 TM and 4-1BB signaling domains (H1-CARSH.28TM.BB ζ) (Fig 26). We expressed high levels of these CARs to control for expression level. Both 4-1BB CARs were well expressed on the surface of the transduced H1 PSCs as well as the differentiated lymphocytes from ATOs at comparable levels to the previous CAR constructs (Fig 28A). Surprisingly, ATOs made with either 4-1BB CAR construct showed a complete restoration of CD3+TCR $\alpha\beta$ + CD8SP T cell differentiation with little to no ILC2 or NK/ILC1 generation (Figs 27, 28B). CAR-T cells expressed the conventional CD8 $\alpha\beta$ heterodimer and retained high expression of eGFP and surface CAR staining (Fig 28A). These data revealed that a) the CD28 transmembrane domain alone was insufficient to mediate T-to-ILC2 diversion, and b) that tonic signaling levels of 4-1BB as opposed to CD28 signaling domain CARs were constrained enough to support T cell over ILC2 development.

2.3.12 4-1BB costimulatory domain substitution permits functional CAR-T cell development

Functional testing of CD8SP CAR-T cells from 4-1BB CAR ATOs showed appropriate polyfunctional production of IFN γ , TNF α , and IL-2, as well as constitutive granzyme B expression upon maximal stimulation with PMA/ionomycin (Fig 29A). Consistent with high surface CAR expression, signaling through the CAR was intact, as CAR-T cells underwent antigen-specific cytokine release of IFN γ and TNF α , and CD107a-labeled degranulation in response to CD19-positive but not CD19KO RAJI cells (Fig 29B). Furthermore, 4-1BB CD8SP CAR-T cells but not CD8SP T cells from non-transduced H1 ATOs exhibited robust cytotoxicity against RAJI cells in Incucyte assays (Fig 29C).

2.3.13 CAR activation via 4-1BB during early ATO diverts T to ILC2 lineage

Having verified normal T cell differentiation in 4-1BB CAR ATOs, we tested whether the preservation of T cell differentiation was due to the inability of 4-1BB CARs to signal during lymphoid development, for example due to developmental lack of one or more 4-1BB signal transduction components in lymphoid precursors. To test this possibility, we again used stromal cell-presented CD19 beginning at Day 0 in 4-1BB CAR ATOs. Indeed, provision of CD19 at the ATO stage resulted in a complete block in T cell development and an expansion of ILC2 in both CD8 α TM) and CD28 TM (Fig 30) 4-1BB CAR PSC lines. An expanded population of presumed NK/ILC1-like cells (which heterogeneously expressed CD56 and CD8 $\alpha\alpha$) was also seen, similar to the observation in H1-CAR-low ATOs aggregated with CD19-expressing stromal cells (Fig 25). Taken together, these data suggested that a) 4-1BB CARs retained functionality at lymphoid progenitor/precursor stages, and b) agonist CAR signaling during early lymphoid development in ATOs can rationally direct T versus ILC2 lineage output.

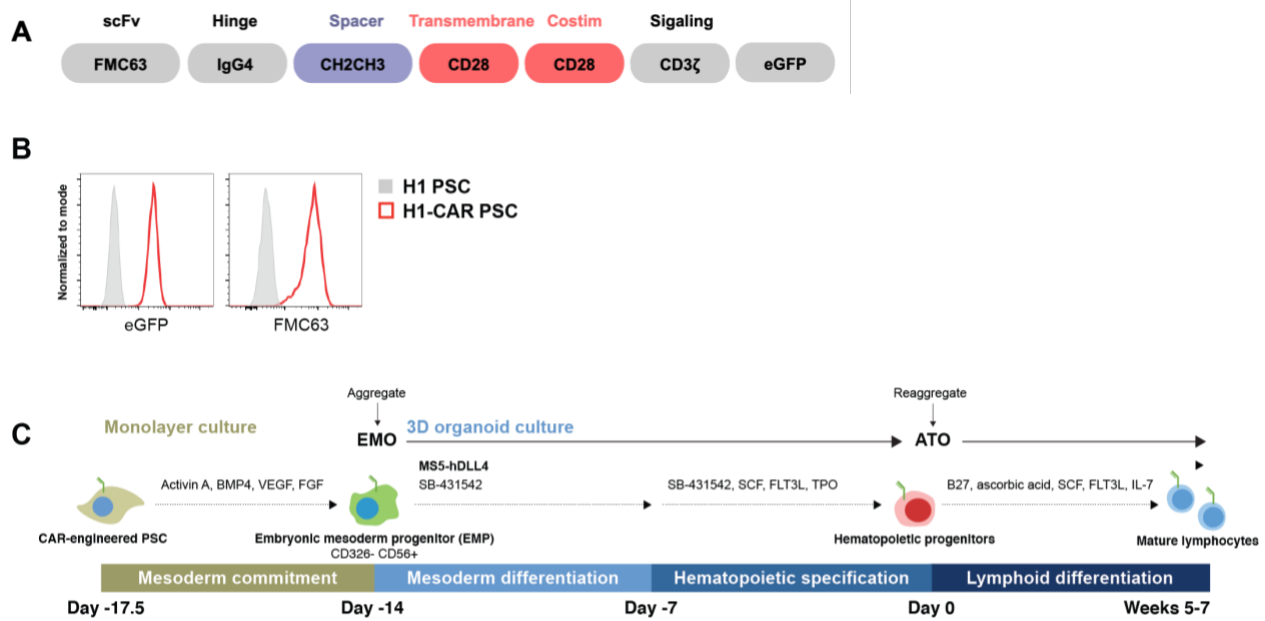


Figure 1. Generation of H1-CD19-CAR PSC and ATO differentiation scheme.

A) Structure of the CD19-targeting CAR. Second generation CAR consisting of a CD19-targeting scFv FMC63, long IgG4 hinge spacer, CD28 transmembrane domain, CD28 costimulatory domain and CD3z signaling domain. **B)** Flow cytometry analysis of GFP and surface expression of the CD19-targeting scFv aFMC63 of H1-CAR PSCs (red solid line) compared to non-transduced H1 PSCs (grey shaded). **C)** Schematic of the PSC-EMO-ATO differentiation protocol starting from human pluripotent stem cells. After 3.5 days of mesoderm induction, human embryonic mesoderm progenitors (hEMPs) are isolated and aggregated with MS5-DLL4 for 2 weeks in mesoderm differentiation and hematopoietic induction conditions (in EMO). EMO cells are then isolated and suspension cells are reaggregated with fresh MS5-DLL4 cells for 5-8 weeks for lymphoid differentiation (in ATO).

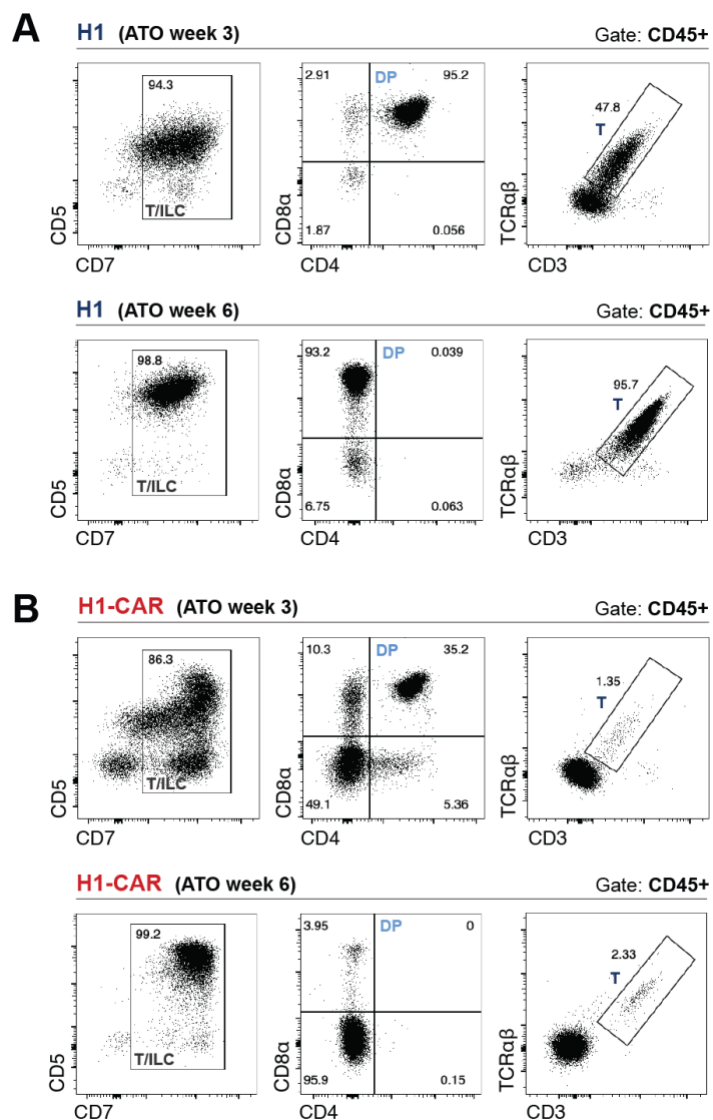


Figure 2. CAR-induced inhibition of T cell differentiation from PSCs.

A) Representative flow cytometry analysis of T cell differentiation of week 3 and week 6 ATO cultures starting from non-transduced H1 control, gated on DAPI- CD45+ cells (n=4). **B)** Representative flow cytometry analysis of T cell differentiation of week 3 and week 6 ATO cultures starting from H1-CAR, gated on DAPI- CD45+ cells (n=4).

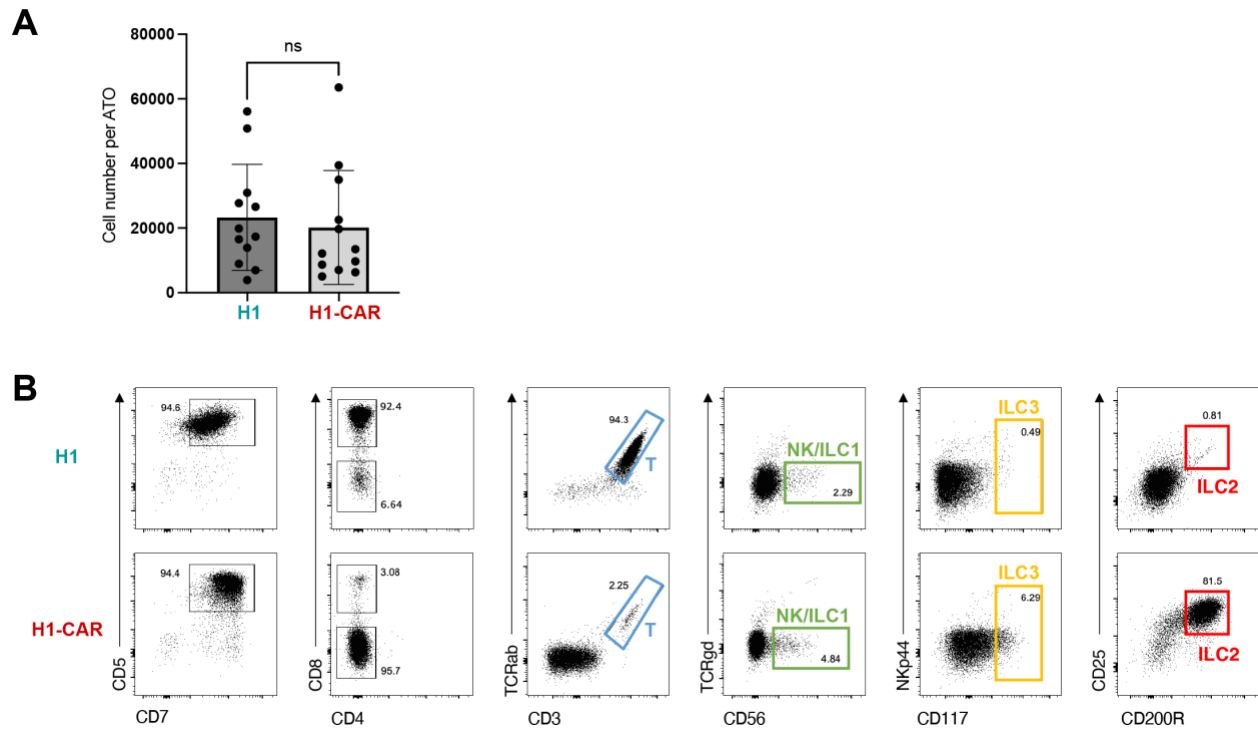


Figure 3. CAR-induced innate lymphoid differentiation from PSCs.

A) Number of CD7+ lymphoid cells generated per ATO at week 6 (mean \pm SD, n=12). **B)** Representative flow cytometry analysis of ILC subset differentiation of week 7 ATO cultures starting from H1-CAR, gated on DAPI- CD45+ cells.

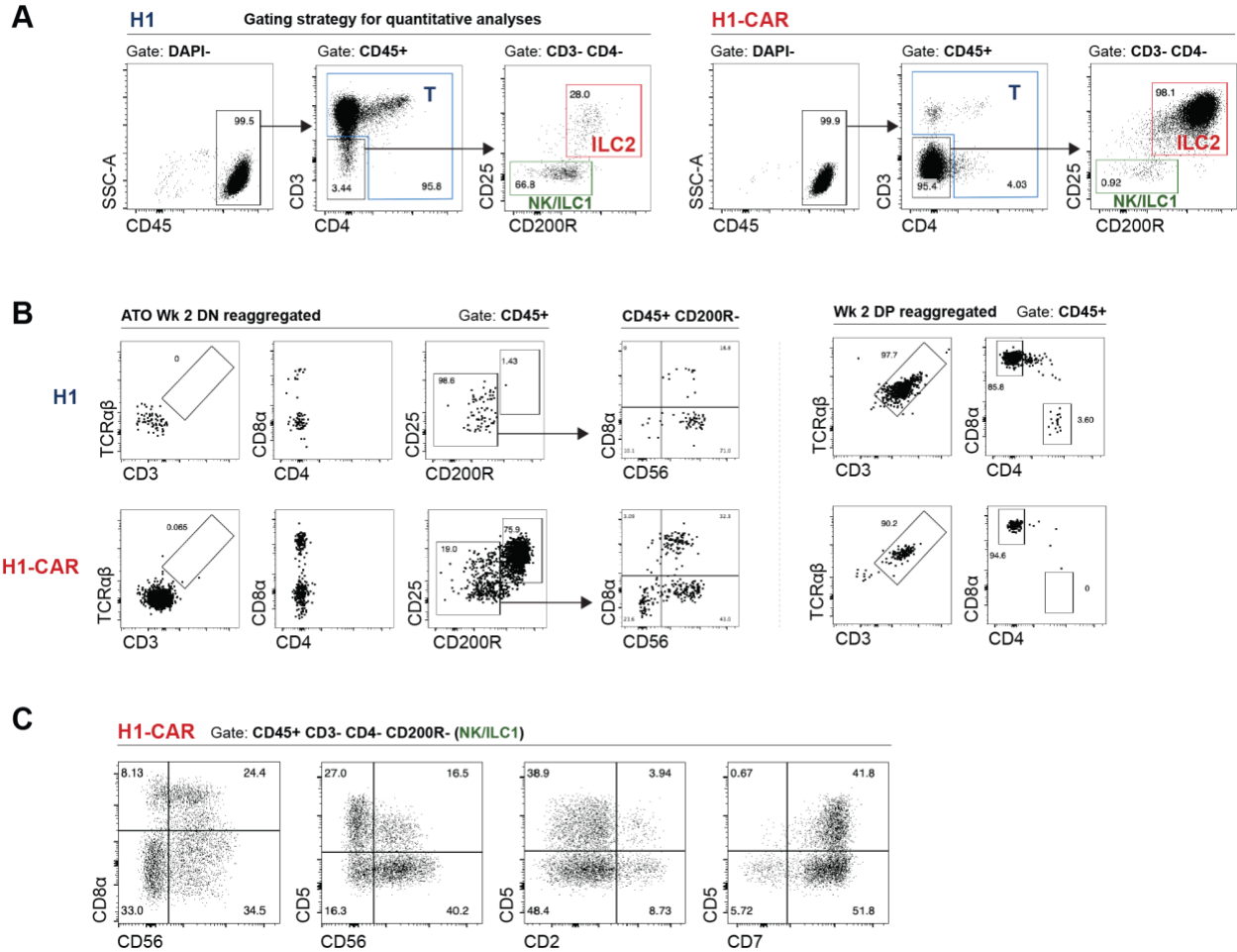


Figure 4. Gating strategy for lymphoid differentiation in the ATOs.

A) Gating strategy of T, ILC2, and NK/ILC1 cells in ATOs. **B)** Flow cytometry analysis of T, ILC2, and NK/ILC1 differentiation of week 6 ATO cultures. DP (CD4+CD8+) or DN (CD4-CD8-) cells were FACS purified from week 2 ATOs, reaggregated with fresh MS5-hDLL4 stroma and cultured for another 4 weeks (6 weeks total), gated on DAPI- CD45+ cells. **C)** Representative flow cytometry analysis showing heterogeneous expression of CD8a, CD56, CD2, CD7 and CD5 of CD3-CD4-CD200R- NK/ILC1 cells.

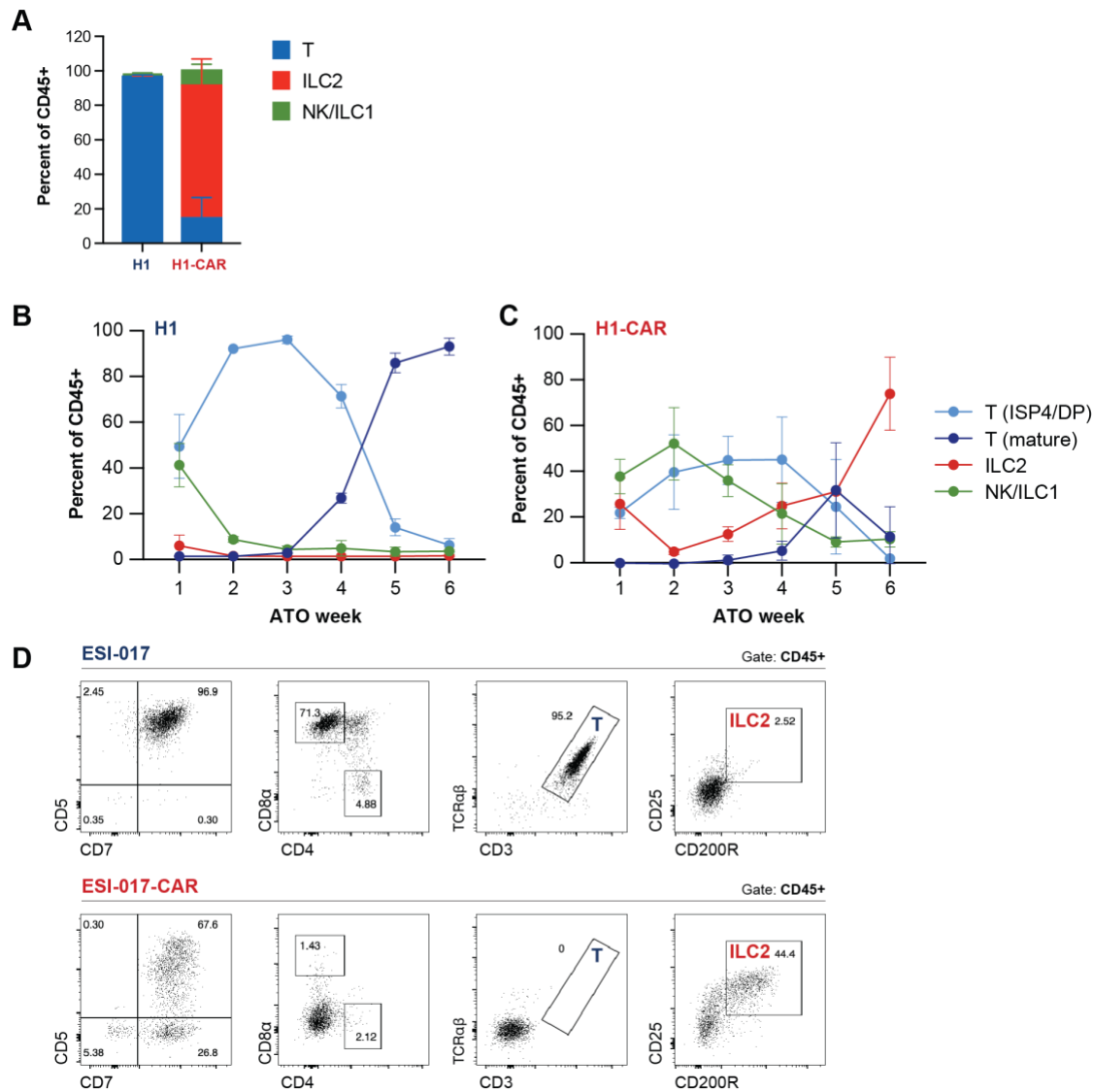


Figure 5. CAR-induced ILC2 differentiation from PSCs.

A) Frequencies of different lymphocyte populations (gated on CD45+ cells, gating strategy in Fig 4A) (mean \pm SD, technical triplicates, representative of $n = 9$ independent experiments). **B) C)** Frequencies of different lymphoid cell populations generated from H1 and CAR ATO cultures at the indicated time points (gating strategy in Fig 4A, T mature defined as CD3+, T precursors as CD3-CD4+) (mean \pm SD, $n=3$). **D)** Representative flow cytometry analysis of ILC differentiation of week 6 ATO cultures using a different PSC line expressing the same CD19-targeting CAR, ESI-017-CAR compared to its non-transduced control, gated on DAPI- CD45+ cells.

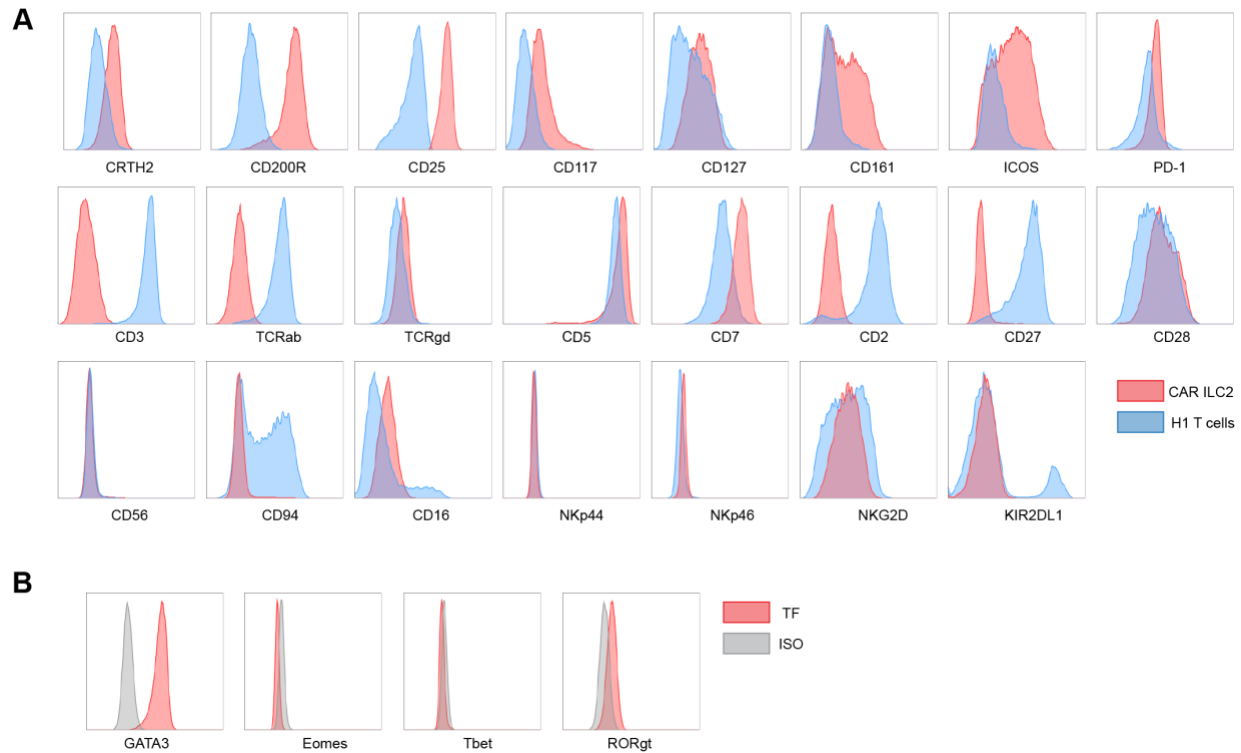


Figure 6. Immunophenotypes and transcription factor expression of CAR induced ILC2s.

A) Flow cytometry analysis of a panel of ILC2, T, and NK markers of week 7 H1-CAR ATO derived ILC2s (red shaded) compared to conventional T cells generated from H1 culture (blue shaded). **B)** Representative intracellular flow cytometry analysis of transcription factor expression (red shaded) gated on CD45⁺CD25⁺ population from week 7 H1-CAR ATO (n=2). Isotype staining controls are shown in shaded gray for each plot.

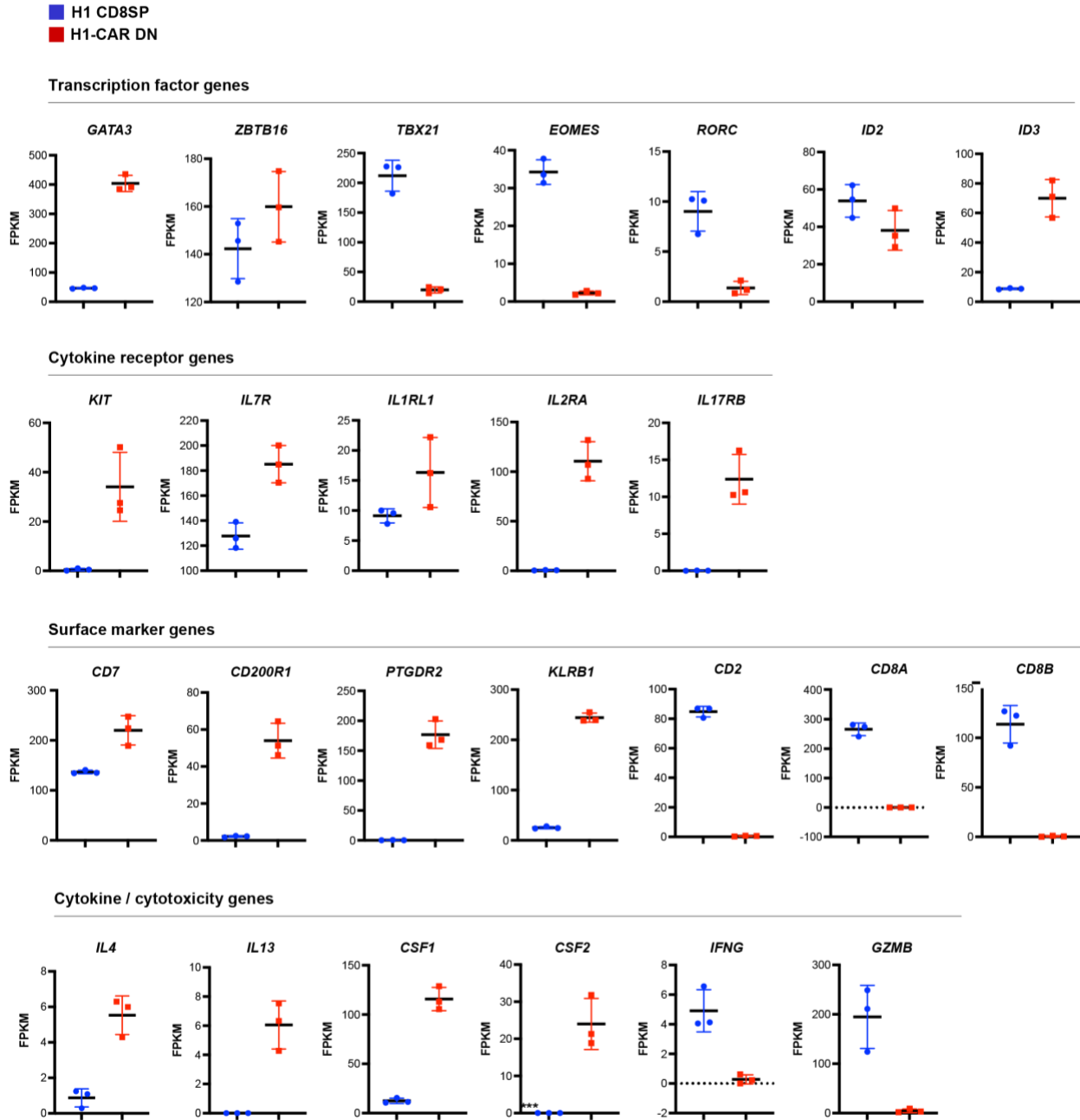


Figure 8. Selected gene expressions of CAR induced ILC2s.

FPKM of selected genes from RNA-seq profiling of CD8 T cells from non-transduced H1 culture and CD8-CD4- DN cells from H1-CAR culture. n = 3 biological replicates.

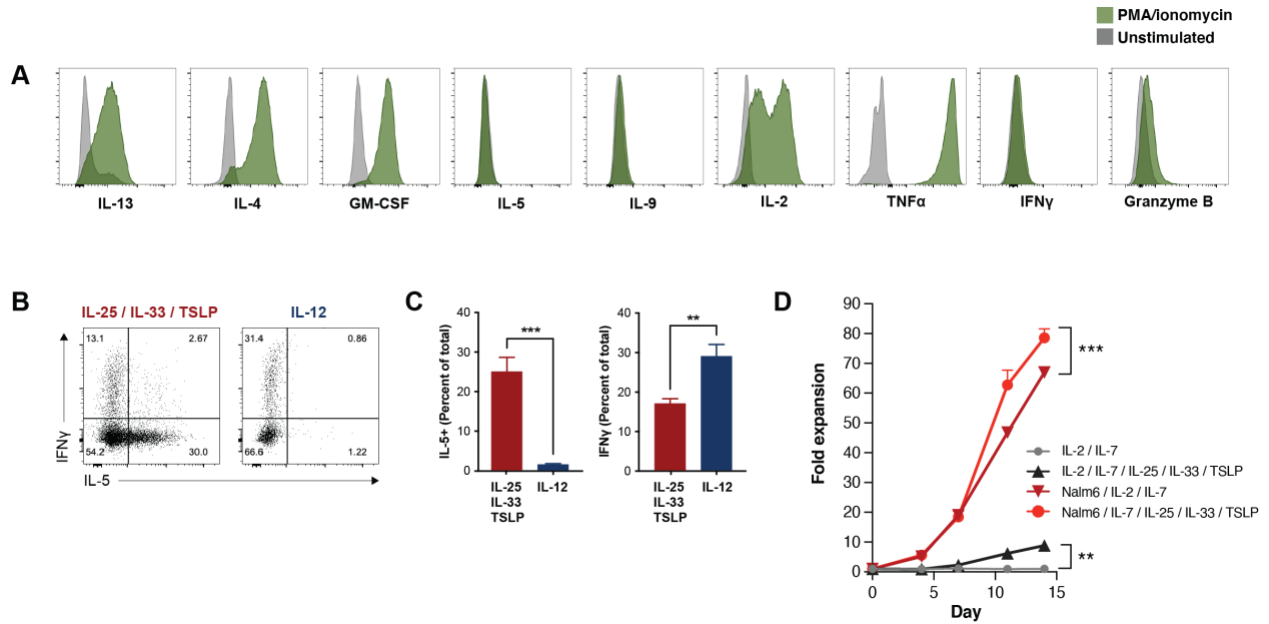


Figure 9. CAR-ILC2 are type 2 cells subject to functional plasticity.

A) Representative cytokine production of H1-CAR ATO derived ILC2s measured by intracellular flow cytometry after 6 hours of phorbol 12-myristate 13-acetate (PMA)/Iono stimulation (at least 2 independent experiments). **B)** Representative expression of IFN γ and IL-5 from CD19CAR ATO derived ILC2s stimulated with IL-12 or IL-25, IL-33, TSLP for 5 days by intracellular flow cytometry, PMA/Iono added during the last 6 hours of stimulation. **C)** Frequencies of IFN γ + and IL-5+ populations shown in B) (mean \pm SD, technical triplicates, representative of n = 2 independent experiments). **D)** Expansion of CD19CAR ATO derived ILC2 after stimulations with or without irradiated CD19+ Nalm6 cells in the presence of IL-2, IL-7, IL-25, IL-33, and TSLP for 14 days. Fresh cytokines were added every 3-4 days and irradiated Nalm6 cells were added at day 0 and day7. Fold expansions are shown (mean \pm SD, technical triplicates, representative of n = 2 independent experiments).

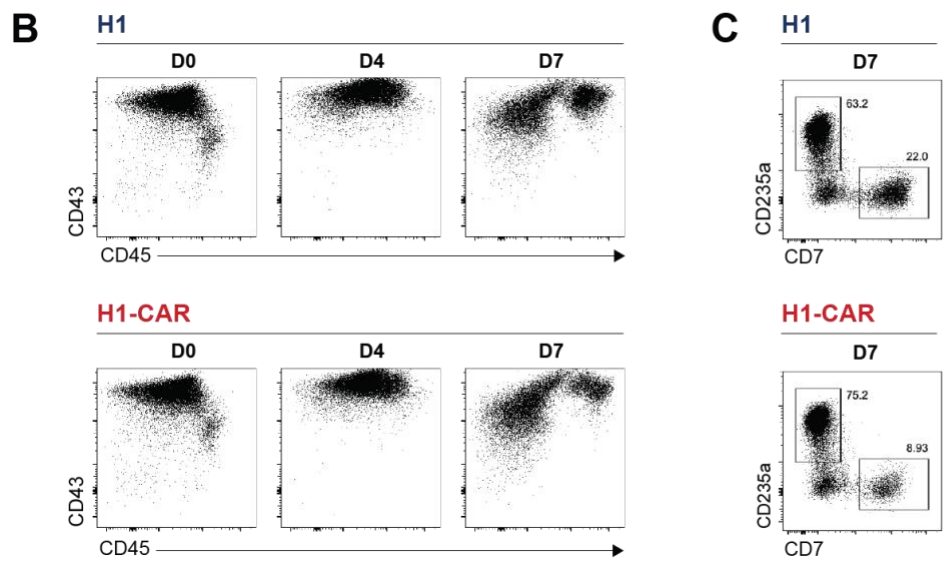
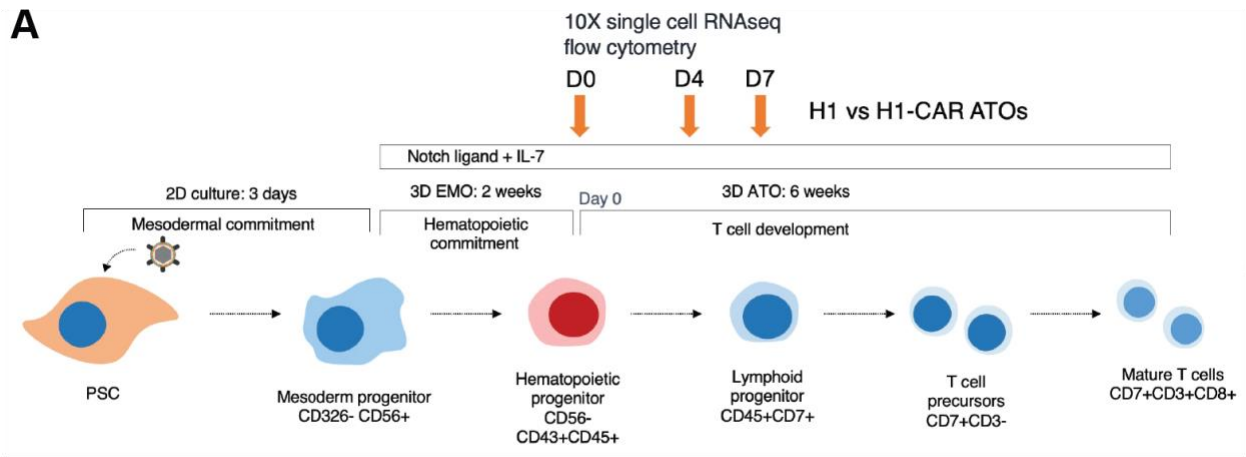


Figure 10. CAR had little effect on hematopoietic differentiation in early ATOs.

A) Schematic of the experimental design of scRNA-seq at different timepoints. **B)** Representative flow cytometry analysis of hematopoietic differentiation looking at expression of CD43 and CD45 of day 0 (the end of the EMO culture), day 4, and day 7 ATO cultures starting from non-transduced H1 control compared to H1-CAR, gated on DAPI- mCD29- cells (n=2). **C)** Representative flow cytometry analysis of erythroid and lymphoid differentiation looking at expression of CD235a and CD7 of day 7 ATO cultures starting from non-transduced H1 control compared to H1-CAR, gated on DAPI- mCD29- cells (n=2).

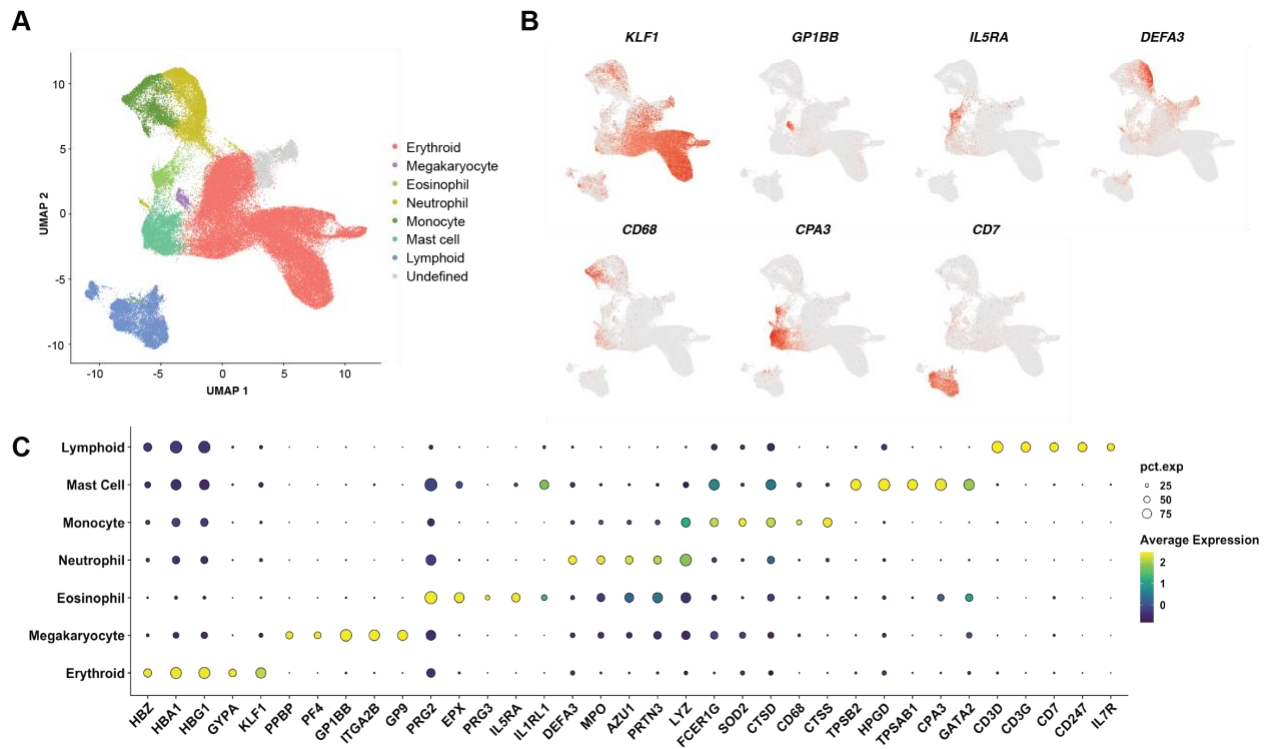


Figure 11. scRNA-seq revealed multilineage hematopoiesis in early ATOs.

A) UMAP dimensionality reduction projection of cell clusters on the scRNA-seq data of cells isolated from non-transduced H1 and H1-CAR ATO cultures at day 0, 4, and 7. Colors present different clusters identified. **B)** Feature plots showing signature gene expression of each cluster in **A)**. **C)** Dotplot showing expression of lineage defining genes of each cluster in **A)**.

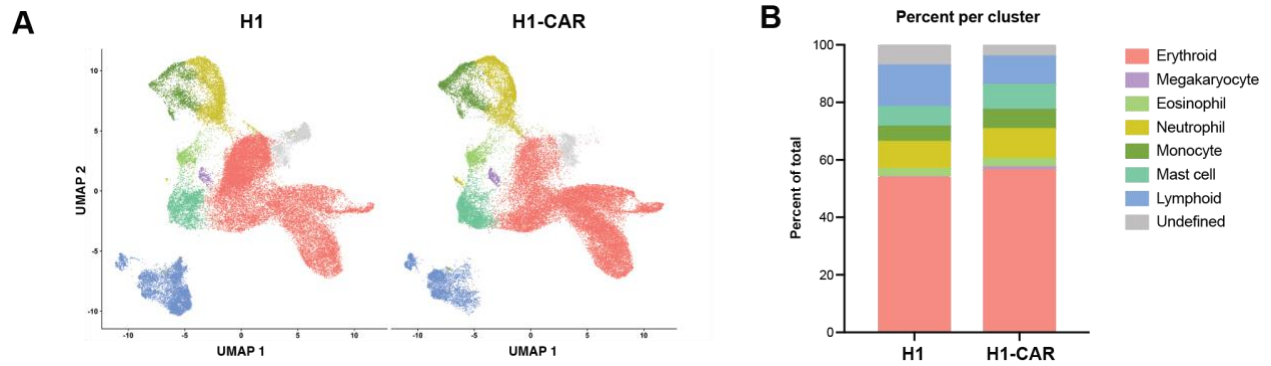


Figure 12. scRNA-seq comparing early ATO multilineage hematopoiesis in H1 and H1-CAR.

A) UMAP dimensionality reduction projection of cell clusters on the scRNA-seq data of cells isolated from non-transduced H1 and H1-CAR ATO cultures at day 0, 4, and 7, respectively, all 3 timepoints combined. Colors present different clusters identified. **B)** Frequencies of each cluster in H1 and H1-CAR samples shown in A).

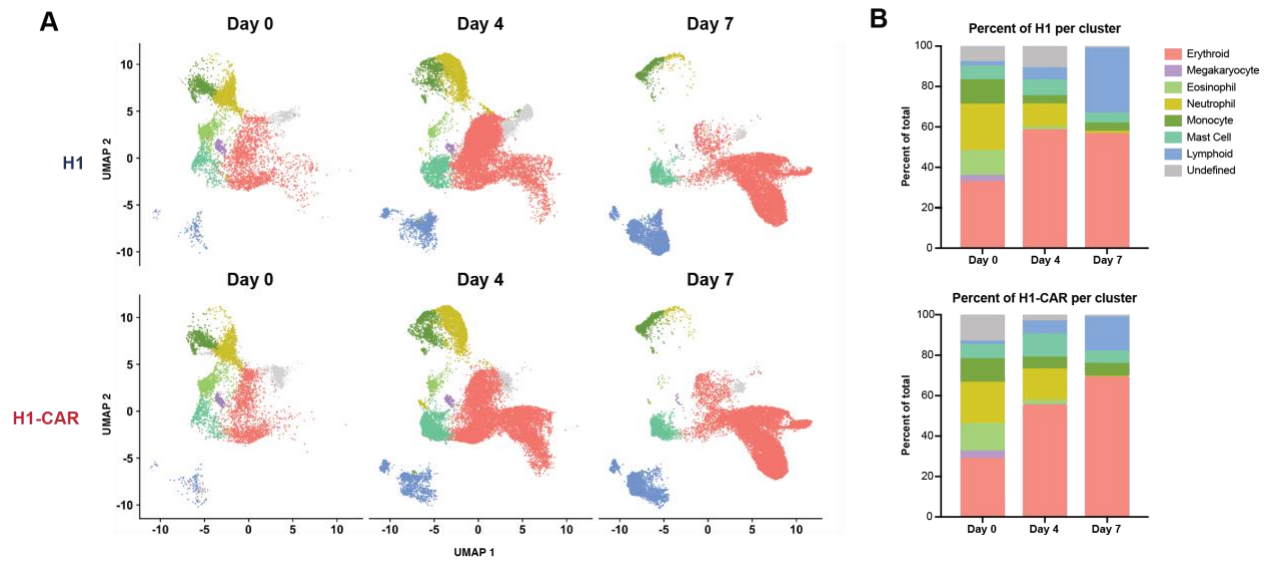


Figure 13. scRNA-seq comparing early ATO multilineage hematopoiesis in H1 and H1-CAR at different time points.

A) UMAP dimensionality reduction projection of cell clusters on the scRNA-seq data of cells isolated from non-transduced H1 and H1-CAR ATO cultures at day 0, 4, and 7, respectively. Colors present different clusters identified. **B)** Frequencies of each cluster in H1 and H1-CAR at each timepoint shown in A).

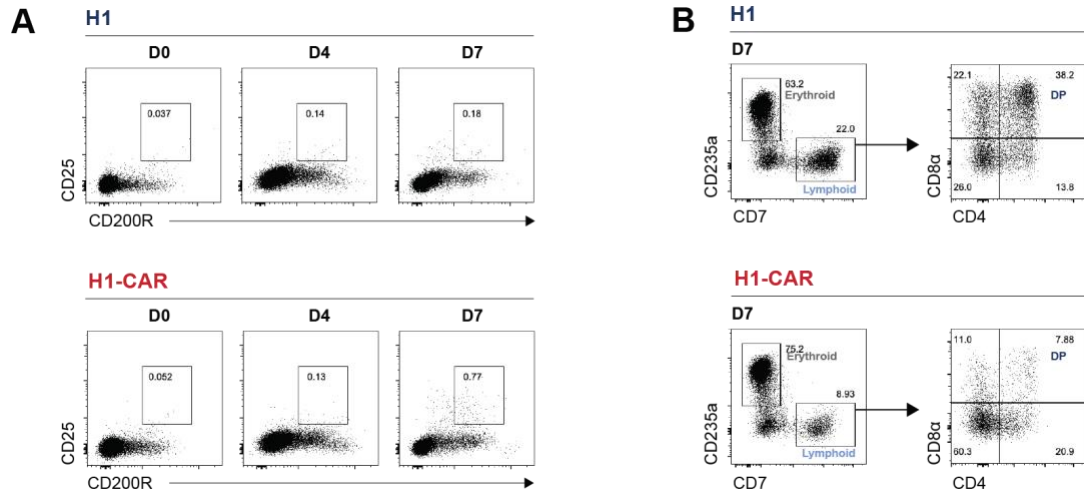


Figure 14. Immunophenotyping early lymphoid differentiation in ATOs.

A) Representative flow cytometry analysis of ILC2 differentiation looking at expression of CD25 and CD200R of day 0, day 4, and day 7 ATO cultures of H1 and H1-CAR, gated on DAPI- mCD29⁻ cells (n=2). **B)** Representative flow cytometry analysis of T and ILC2 development of day 7 ATO cultures of H1 and H1-CAR, gated on DAPI- mCD29⁻ cells then followed by gating on CD7⁺ as depicted (n=2).

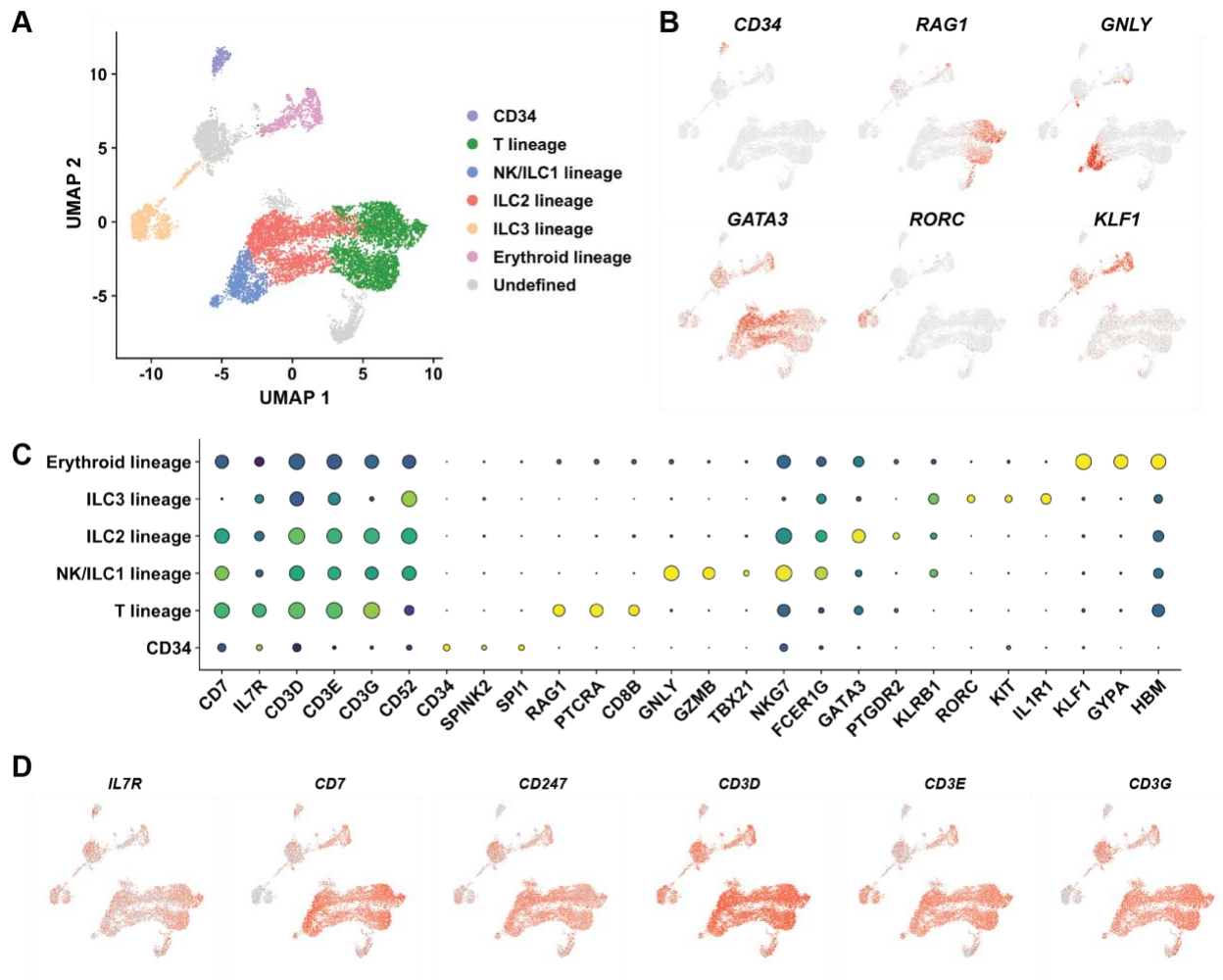


Figure 15. scRNA-seq revealed multilymphoid differentiation in early ATOs.

A) UMAP of the scRNA-seq data in Fig 11 A), subgating on CD7+ lymphoid cells only. Colors present different clusters identified. **B)** Feature plots showing signature gene expression of each cluster in A). **C)** Dotplot showing expression of general lymphoid markers and lineage defining genes of each cluster in A). **D)** Feature plots showing signature gene expression of pan-lymphoid markers *IL7R*, *CD7* and CD3 chains *CD247*, *CD3D*, *CD3E*, and *CD3G*.

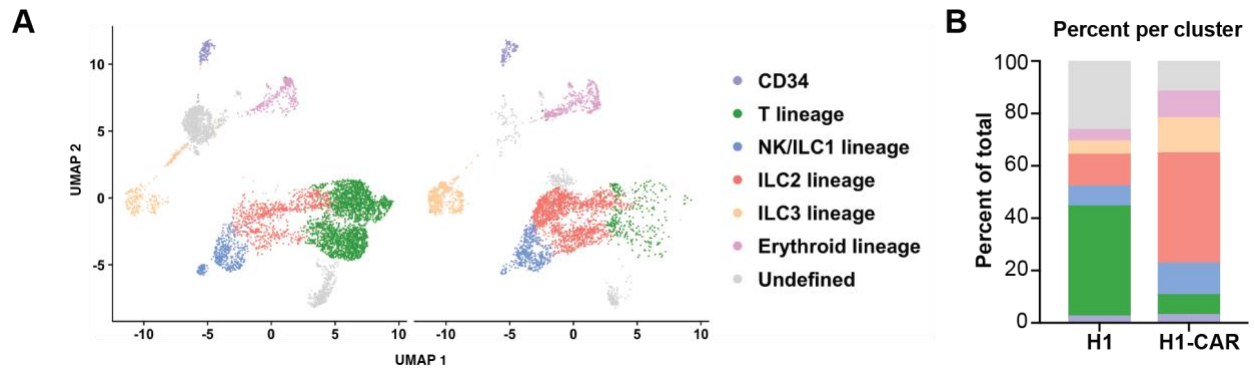


Figure 16. scRNA-seq comparing early ATO multilymphoid differentiation in H1 and H1-CAR.

A) UMAP dimensionality reduction projection of cell clusters on the scRNA-seq data of lymphoid subsets from H1 and H1-CAR ATO cultures at day 0, 4, and 7, respectively, all 3 timepoints combined. Colors present different clusters identified. **B)** Frequencies of each cluster in H1 and H1-CAR samples shown in A).

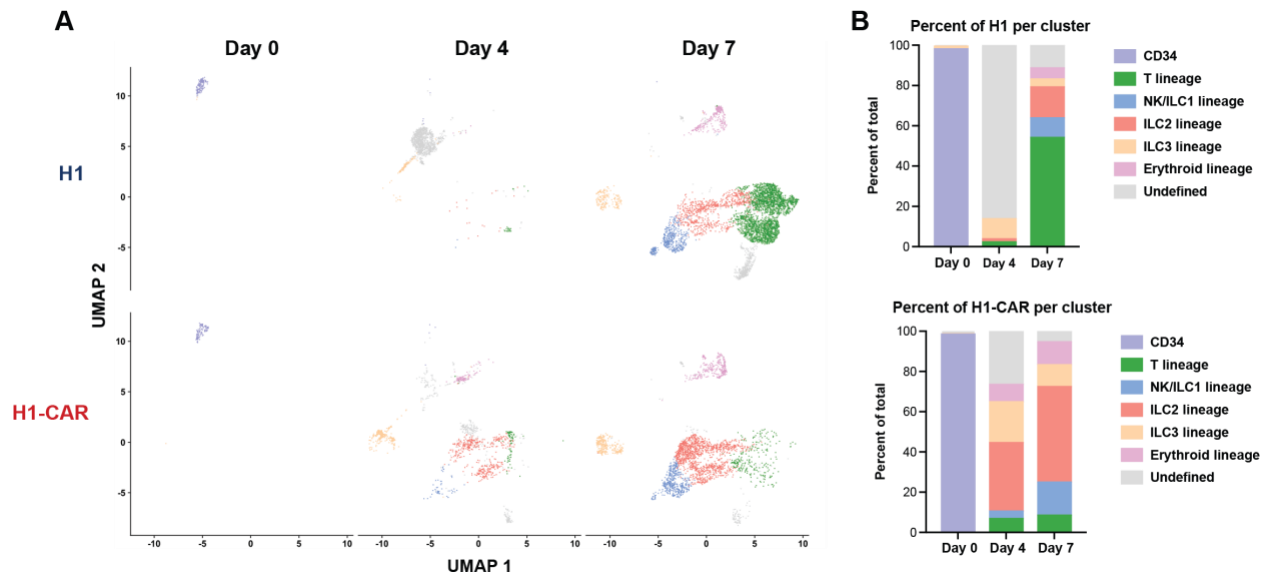


Figure 17. scRNA-seq comparing early ATO multilymphoid differentiation in H1 and H1-CAR at different time points.

A) UMAP dimensionality reduction projection of cell clusters on the scRNA-seq data of lymphoid subsets from H1 and H1-CAR ATO cultures at day 0, 4, and 7, respectively. Colors present different clusters identified. **B)** Frequencies of each cluster in H1 and H1-CAR samples at each timepoint shown in A).

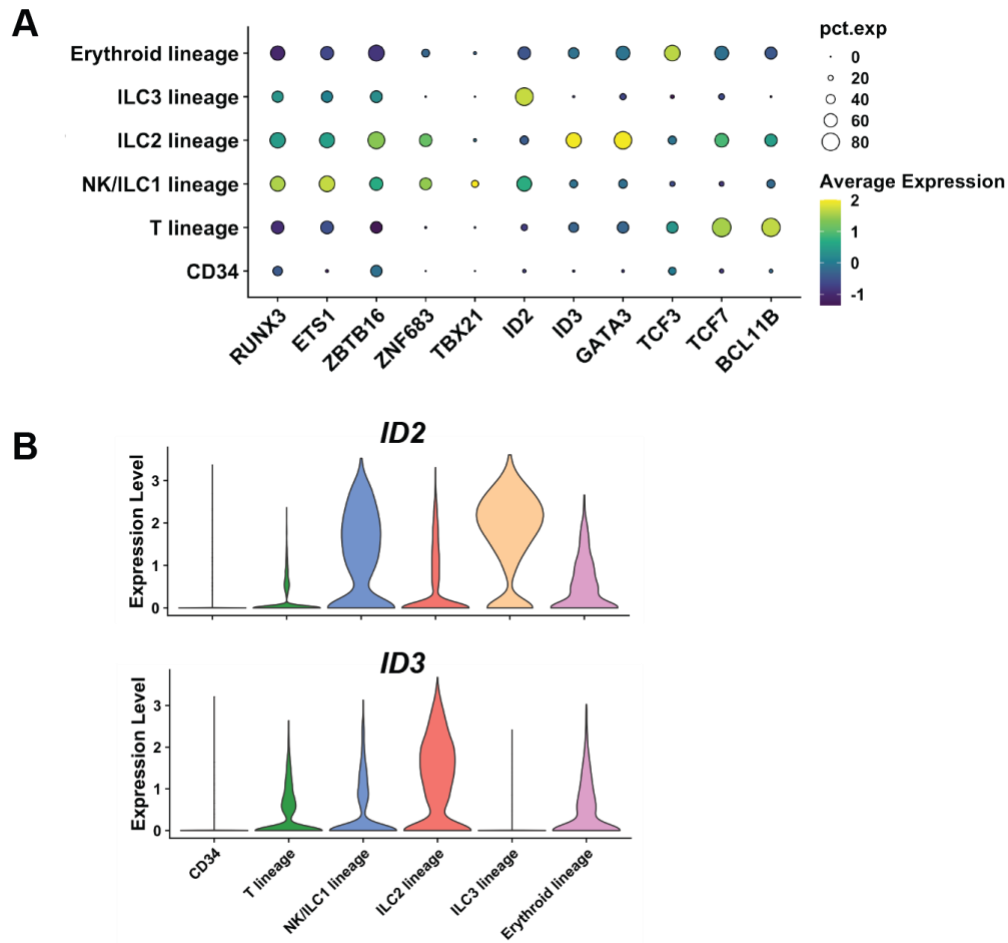


Figure 18. Transcription factor patterns of the early lymphoid cells in ATOs.

A) Dotplot showing expression of selected transcription factors of each cluster in 15A). **B)** Violin plot showing expression of *ID2* and *ID3* in each cluster.

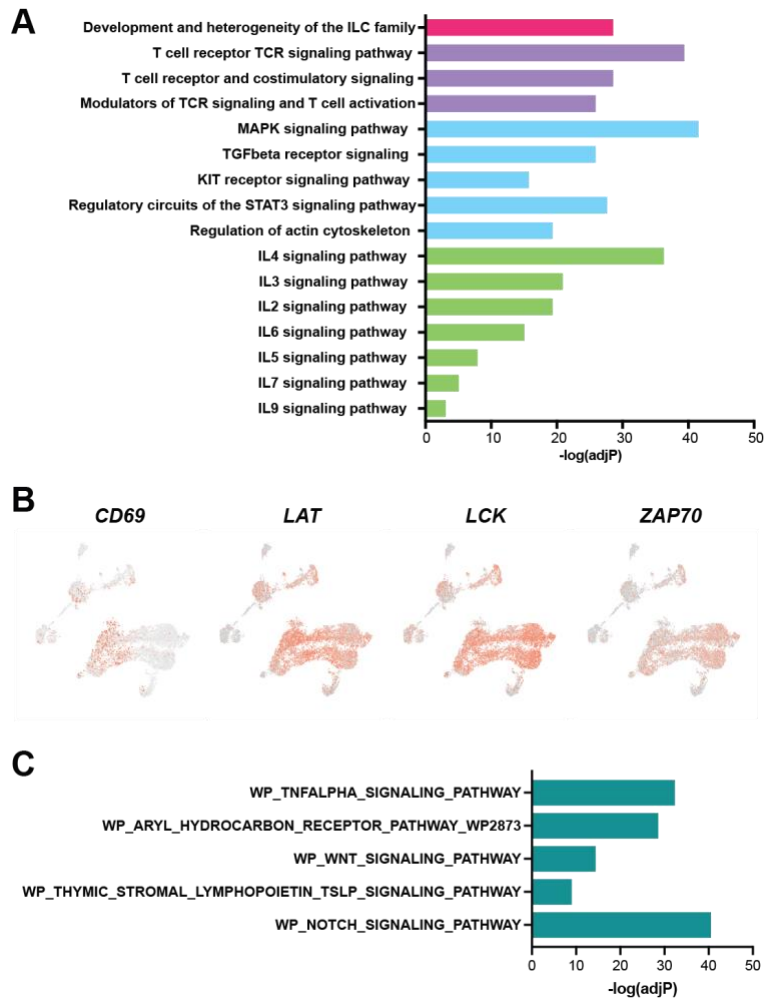


Figure 19. Gene set enrichment analysis comparing ILC2 versus T lineage.

A) Gene set enrichment analysis of Wikipathway gene sets in ILC2 lineage versus T lineage clusters identified in Fig 15A). Selected pathways positively enriched in the ILC2 lineage cluster are shown. **B)** Feature plots showing gene expression of CD69, and genes encoding TCR signal transduction molecules *LAT*, *LCK*, and *ZAP70* (all samples combined). **C)** Gene set enrichment analysis for genes significantly downregulated in H1-CAR cluster compared to H1 cluster in Fig 15A). Wikipathways considered.

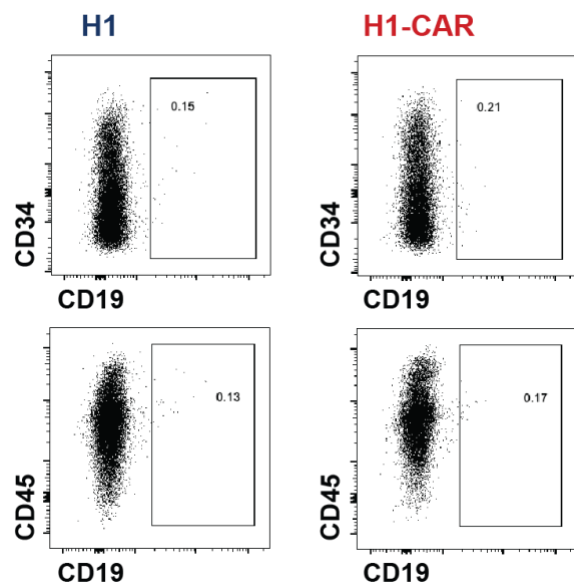


Figure 20. CAR induced ILC2 development in the ATO is antigen independent.

Representative flow cytometry analysis showing lack of CD19 expression in day 0 ATO cultures of H1 and H1-CAR, gated on DAPI- mCD29- cells.

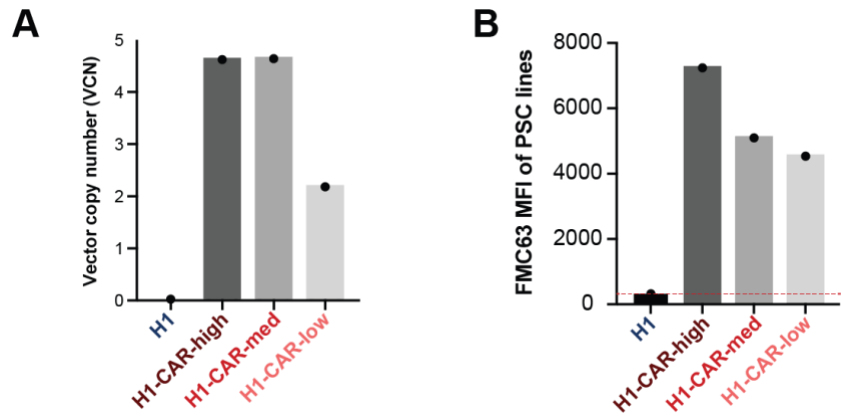


Figure 21. Generation of H1-CAR PSC lines with lower CAR surface expression levels.

A) Vector copy number (VCN) of H1 PSCs expressing high, medium, and low levels of CAR. **B)** Mean fluorescence intensity (MFI) of surface CAR expression using an antibody specific for the FMC63 scFv. CAR expression is shown for stable H1 PSC lines expressing different CAR levels.

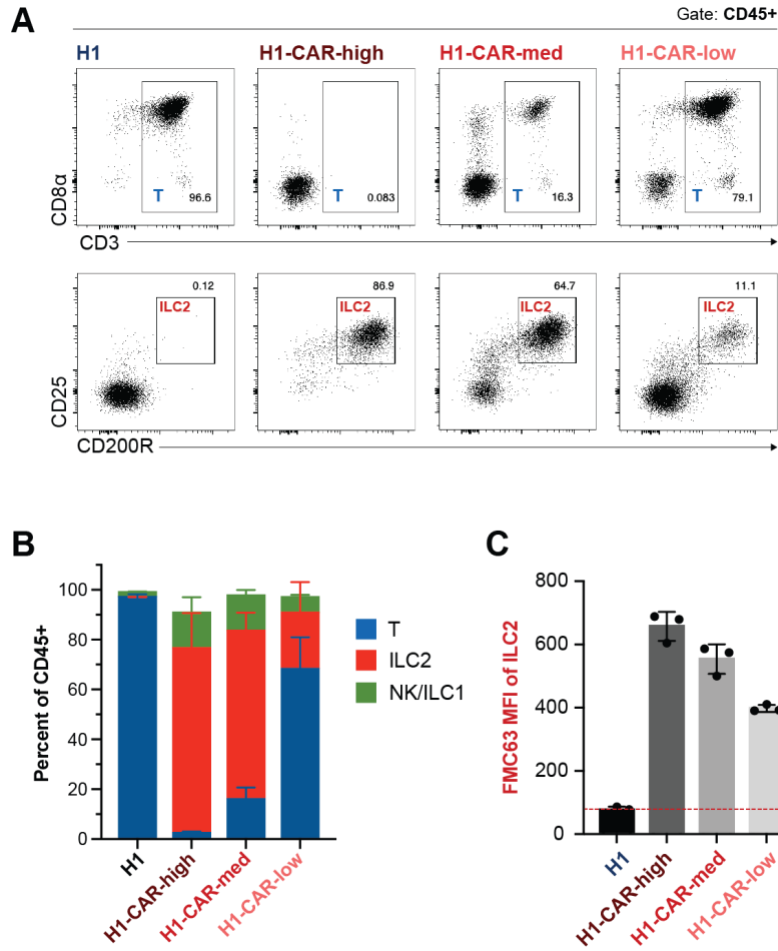


Figure 22. Tuning CAR expression level controls T versus ILC2 lineage.

A) Representative flow cytometry analysis of T cell and ILC2 differentiation in week 6 ATO cultures starting from H1 or H1-CAR PSCs with different levels of CAR expression, as shown in Fig 21B). Gated on total CD45+ cells. **B)** Frequencies of lymphocyte subsets as shown in A) (mean \pm SD of technical triplicates, representative of n=3 independent experiments). **C)** Mean fluorescence intensity (MFI) of surface CAR expression of ILC2s generated in week 6 ATOs using an antibody specific for the FMC63 scFv.

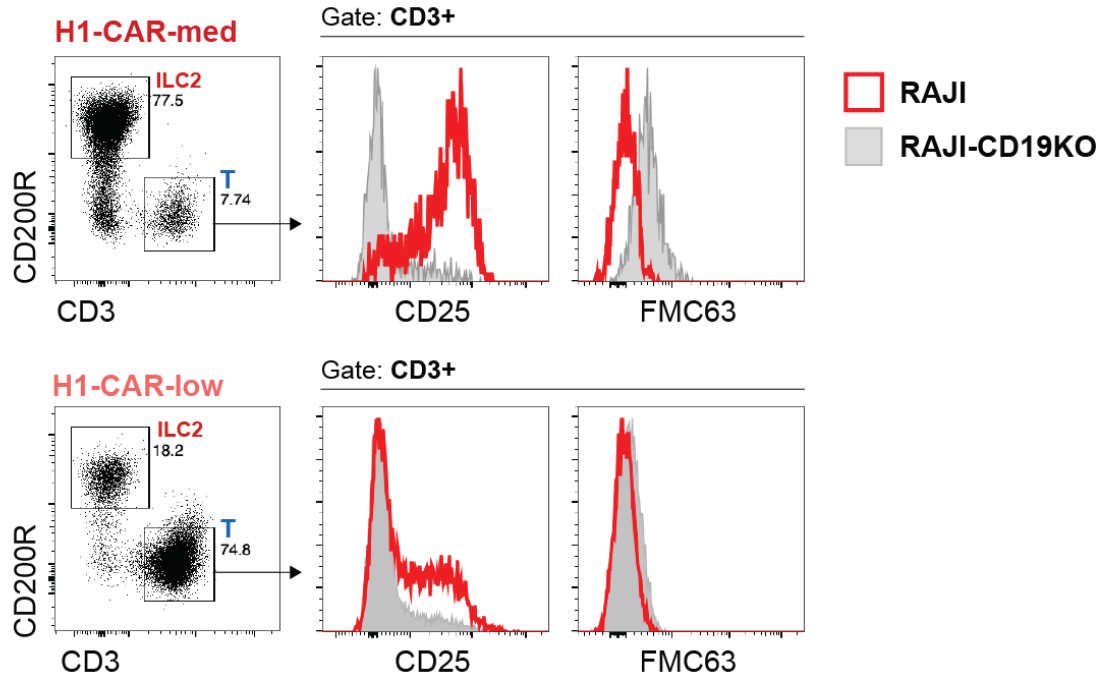


Figure 23. Tuning CAR expression level affects CAR activation potential.

Flow cytometry analysis of CAR-T cell activation shown by upregulation of CD25 and downregulation of surface CAR (FMC63) on CD3+ gated T cells. Cells were isolated from week 6 H1-CAR-med and H1-CAR-low ATOs and stimulated with CD19+ RAJI (red solid line) or RAJI-CD19 knockout (CD19KO) (grey shaded) cells for 24 hours.

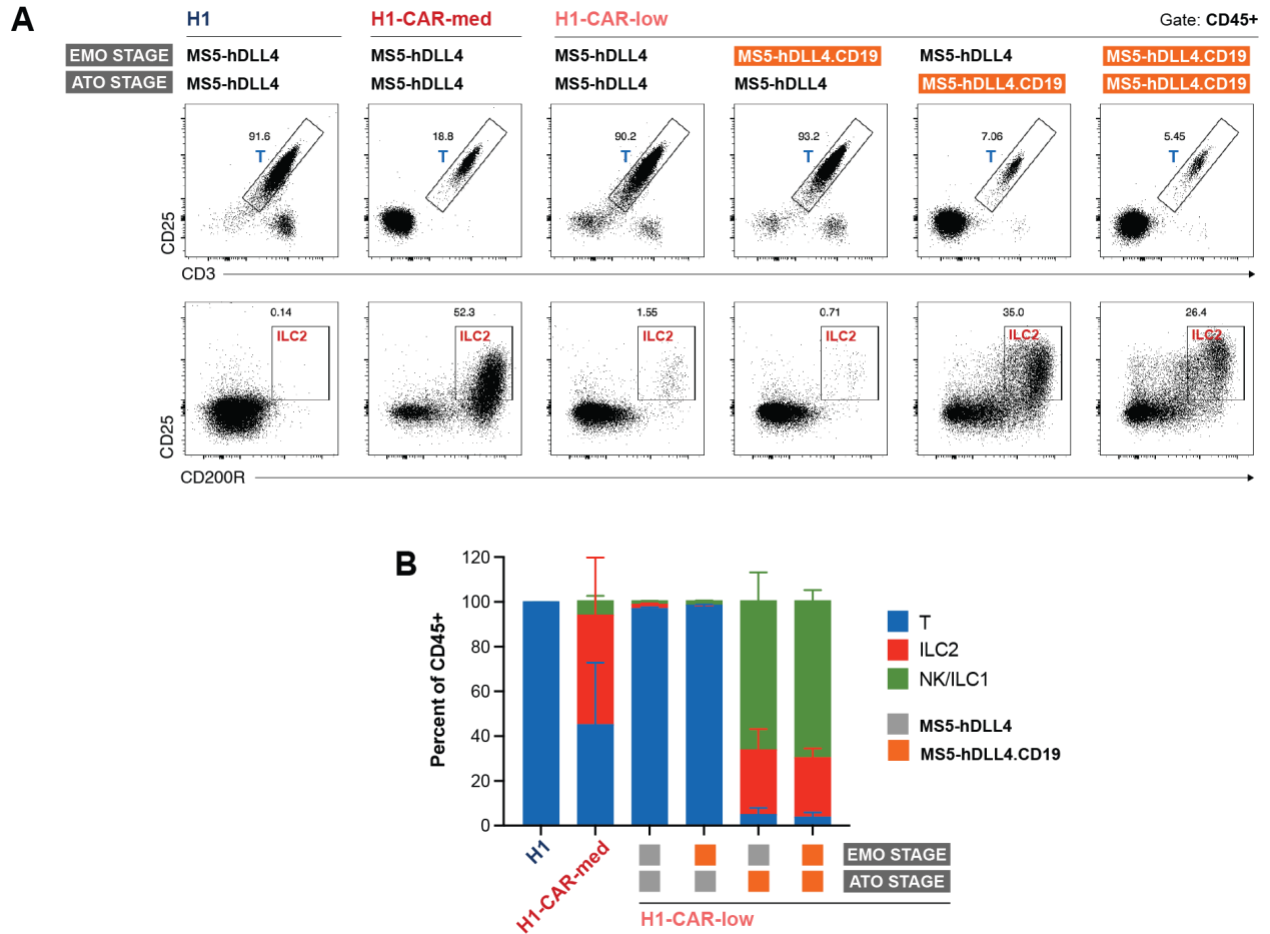


Figure 24. Antigen-dependent CAR activation during development diverts T to ILC2 lineage.

A) Representative flow cytometry analysis of T cell and ILC differentiation in week 6 ATO cultures starting from H1-CAR-low PSCs. Either normal (MS5-hDLL4) or CD19-expressing (MS5-hDLL4.CD19) stromal cell lines were used during EMO and/or ATO stages, as shown. H1 (T cell-biased) and H1-CAR-med (ILC2-biased) ATOs are shown as controls. **B)** Frequencies of lymphocyte subsets shown in F) (mean \pm SD of technical triplicates, representative of n=2 independent experiments).

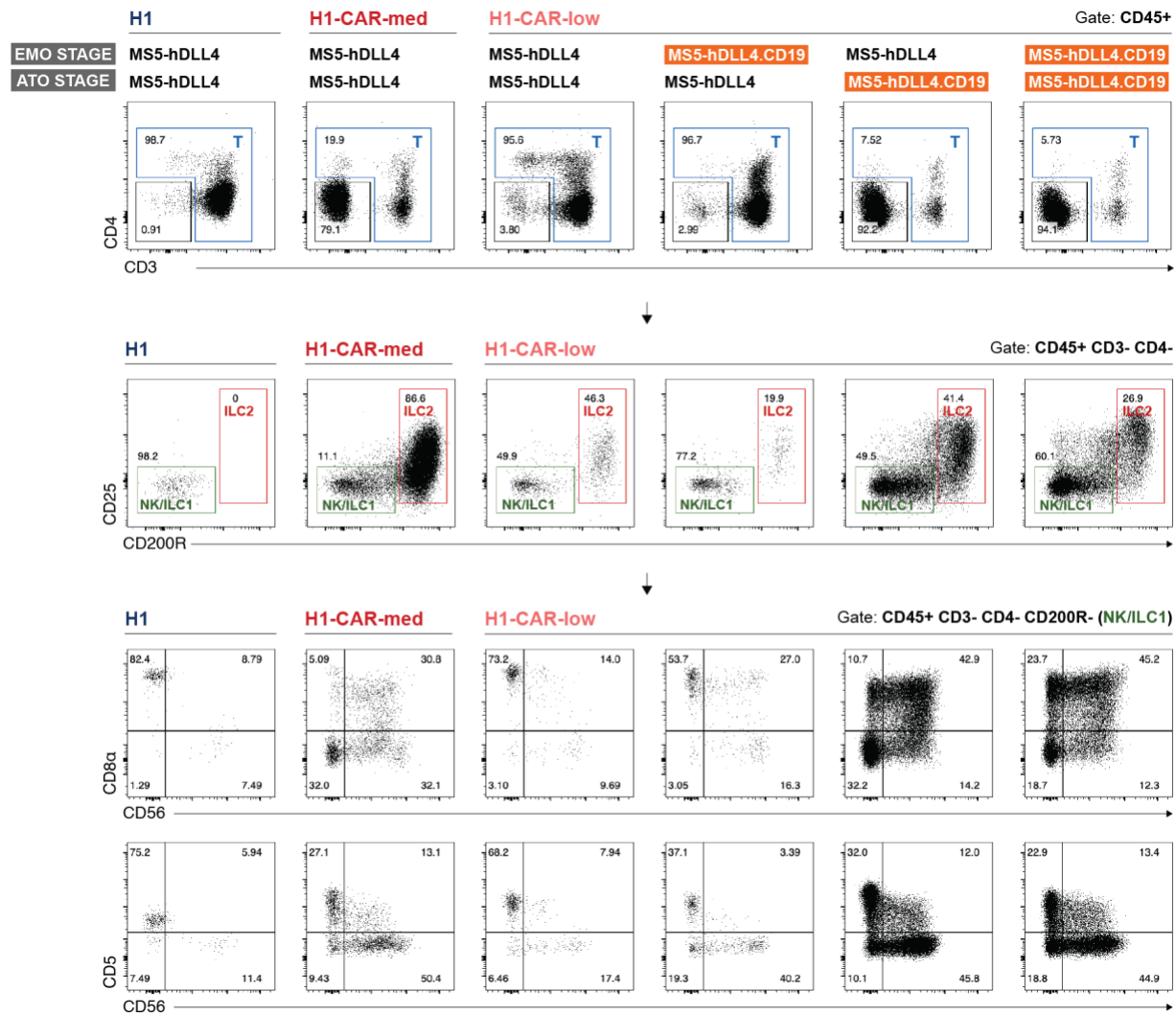


Figure 25. Antigen-dependent CAR activation during development diverts T to innate lineages.

Representative flow cytometry analysis of T and ILC differentiation in week 6 H1-CAR-low ATOs using with different stromal lines during EMO and/or ATO stages, as shown in Fig. 24. H1 (T-lineage biased) and H1-CAR-med (ILC2-lineage biased) ATOs are shown as controls. The gating strategy shown in Fig. 4A is used showing T, ILC2, and NK/ILC1 gates. Heterogenous expression of CD56, CD8 α , and CD5 is shown within the NK/ILC1 gate for each population.

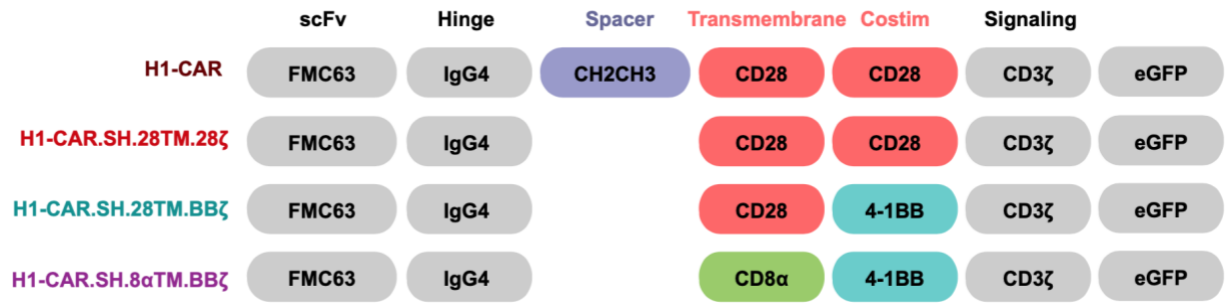


Figure 26. Generation of H1-CAR PSC lines with different CAR architectures.

Schematic of the structures of CD19-targeted (FMC63) CARs with variations in spacer, transmembrane, and costimulatory domains used for generation of alternative CAR-transduced H1 PSC lines used in the following experiments. H1-CAR shows the original CAR used in the preceding experiments.

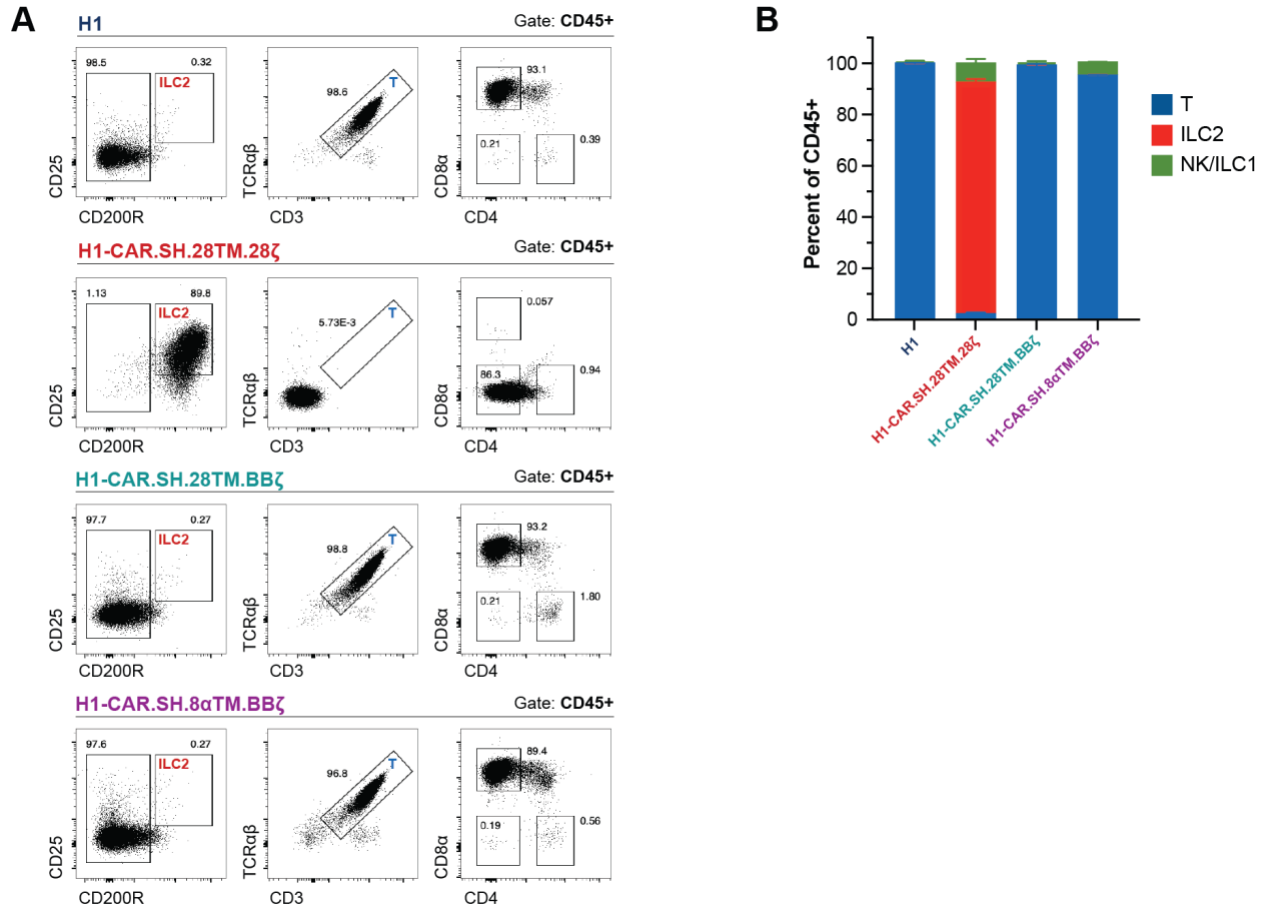


Figure 27. CAR costimulatory domain substitution permits CAR-T cell development.

A) Representative flow cytometry analysis of T and ILC differentiation of week 6 ATO cultures starting from H1 or H1-CAR lines expressing the different CAR architectures shown in A). Gated on total CD45+ cells. **B)** Frequencies of lymphocyte subsets shown in B) (mean \pm SD of technical triplicates, representative of n=2 independent experiments).

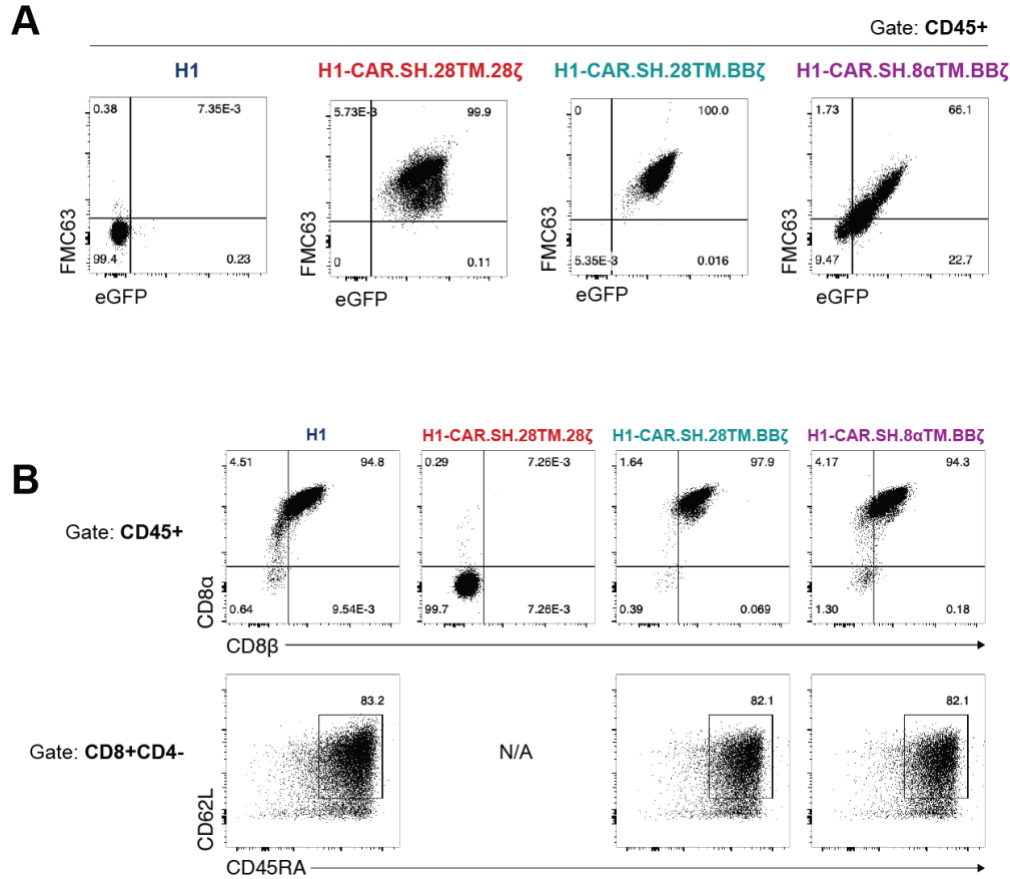


Figure 28. CAR costimulatory domain substitution generates mature naïve CAR-T cell with similar level of surface CAR expression.

A) Representative flow cytometry analysis of week 6 ATO cultures starting from H1 or H1-CAR lines expressing different CAR architectures, as shown in Figure 26 A), showing eGFP and surface CAR (FMC63) expression, gated on total CD45⁺ cells. **B)** Representative flow cytometry analysis of T cell phenotype in H1 or H1-CAR ATOs expressing different CAR architectures, as shown in Fig. 27A. CD8 α and CD8 β coexpression is shown (gated on total CD45⁺), and CD62L and CD45RA coexpression is shown on T cells (gated on CD45⁺CD3⁺CD8 α ⁺CD4⁺).

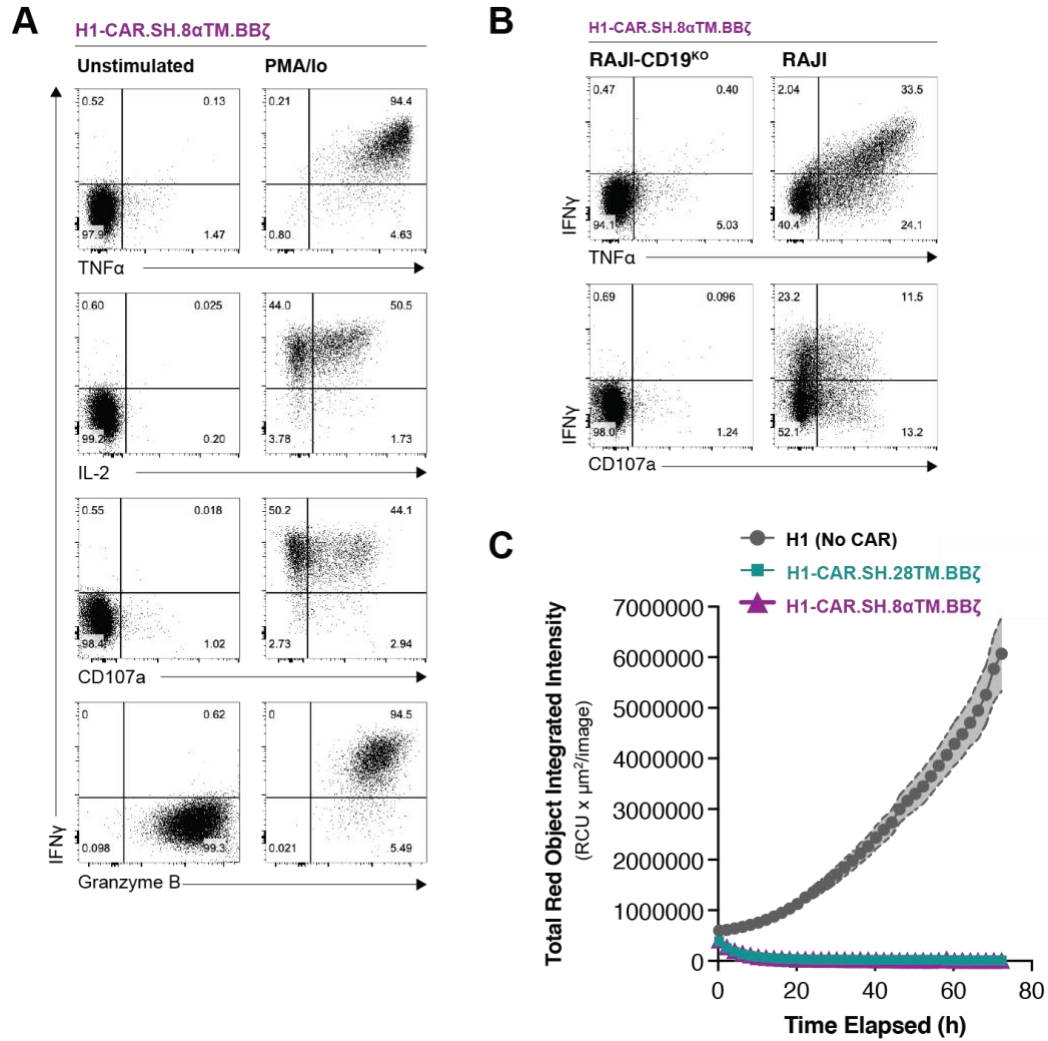


Figure 29. ATO derived 4-1BB CAR-T cells have antigen-specific cytokine response and *in vitro* tumor killing capacity.

A) Cytokine production and CD107a membrane mobilization of CAR-T cells from H1-CAR.SH.8TM.BBz ATOs treated with no stimulation or maximal stimulation with PMA/ionomycin for 6h. **B)** Cytokine production and CD107a membrane mobilization of CAR-T cells isolated from H1- CAR.SH.8TM.BBz ATOs in response to RAJI-CD19KO or CD19+ RAJI cells. **C)** Incucyte cytotoxicity curves measuring growth of mKate+ (red fluorescent) RAJI cells cocultured with T cells isolated from H1, H1-CAR.SH.28TM.BBz, and H1-CAR.SH.8TM.BBz ATOs at an effector to target ratio of 1:1 for 72 hours.

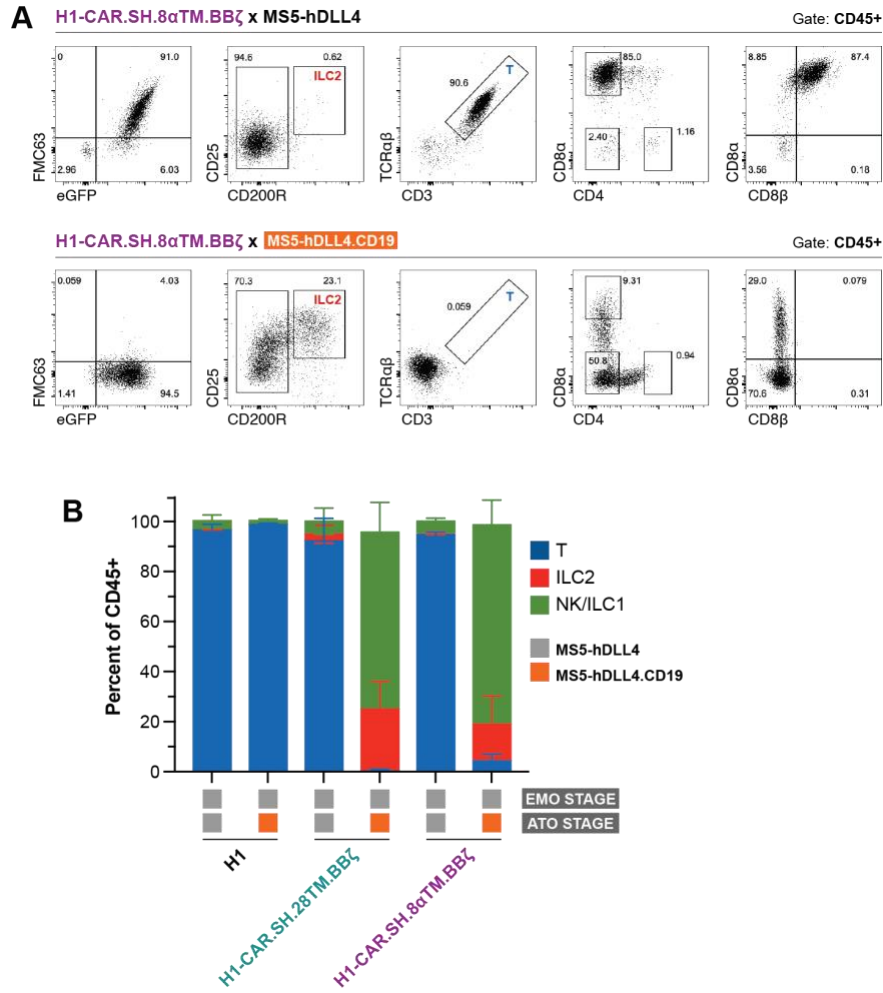


Figure 30. Early CAR activation in ATOs inhibits CAR-T cell development.

A) Representative flow cytometry analysis of T and ILC differentiation in week 6 H1-CAR.SH.8TM.BB ζ ATO cultures using either normal (MS5-hDLL4) or CD19-expressing (MS5-hDLL4.CD19) stromal cell lines at the ATO stage. Gated on total CD45+ cells. **B)** Frequencies of lymphocyte subsets shown in F) and including data for H1 control ATOs and H1-CAR.SH.28TM.BB ζ ATOs (mean \pm SD of technical triplicates).

CHAPTER 3: Concluding Remarks

3.1 Conclusions

Our data reveal an unexpected effect of constitutively expressed CD19 CARs by lentiviral transduction in spontaneously diverting T cell differentiation from human PSCs to the closely related ILC2 lineage in ATOs. We conclude that integrated CAR tonic signaling strength determines T versus ILC2-biased differentiation based on our observations that: a) CAR signaling in ATOs is antigen-independent due to the absence of the cognate antigen CD19 in the system; b) ILC2-biased differentiation was seen with high but not low expression levels of CD28 ζ CARs, and c) CD19 CARs containing the 4-1BB signaling domain, which have lower tonic signaling properties, preserved T cell differentiation.

This mechanistic conclusion was indirectly supported by evidence from single cell RNA sequencing analysis we performed at the earliest stages of lymphoid development in ATOs, which identified a cell cluster enriched in H1-CAR ATOs representing either lineage-primed or lineage-committed ILC2 precursors that expressed a gene signature of T cell activation, including expression of *CD69*. Indeed, triggering antigen-dependent CAR activation in low tonic signaling conditions during this developmental window was sufficient to mimic high tonic signaling CAR conditions and recapitulate T to ILC2 (and, to a lesser extent, NK/ILC1) lineage diversion.

In summary, our data provide a framework for understanding and applying CAR technology to T cell differentiation from PSCs, and illuminates the potential to rationally control lymphoid lineage fate decisions for developmental modeling and future therapeutic applications.

3.2 Discussion

Our findings point to the importance of tuning CAR tonic signaling for the generation of conventional CAR-T cells from PSCs using constitutively expressed lentiviral vectors. This would be especially true in situations in which the cognate antigen is inevitably present during T cell differentiation. One caveat of our study is the use of a single scFv targeting a single antigen which, while allowing us to test the effect of varying surface CAR expression level and other CAR components, limits extrapolation of our specific modifications to other CARs. However, the principle of CAR interference with T cell development as the integration of CAR structure plus cellular variables such as CAR expression level, developmental capacity of the CAR to signal, and the platform used for T cell differentiation suggests that empirical optimization of every CAR will be required to achieve conventional T cell differentiation from PSCs. Moreover, our findings highlight the pitfalls of constitutive CAR expression and point to a need for exploring synthetic approaches such as stage-specific or logic-gated CAR expression to circumvent the effect of CARs on T cell development.

The general finding of CAR-associated innate cell diversion was previously observed by the Sadelain group who using OP9-DL1 co-cultures described innate-like lymphoid differentiation from a T cell-derived induced pluripotent stem cell (iPSC) line transduced with a second generation CD19-targeted CD28 ζ CAR. In contrast to our findings, CAR lymphoid cells produced in this model were NK/ $\gamma\delta$ -like, characterized by diminished or absent expression of CD2, CD5, CD4 and CD8 β , high expressions of *TBX21* and *PLZF*, expression of CD8 $\alpha\alpha$ and CD56, and upregulation of NKp44, NKG2D, and NKp46 following activation [57]. Interestingly, the authors showed that this innate phenotype was not CAR-specific, as non-transduced T-iPSC cells in their model displayed the same phenotype, with low to negative expression of CD5, CD4 and CD8 β ,

and aberrant expression of CD56 and PLZF, in agreement with a contemporary group working with unmodified T-iPSCs [145], suggesting that differentiation conditions used at that time were not optimal for conventional (i.e. at minimum CD8 $\alpha\beta$ +) T cell differentiation. As such it is difficult to speculate on the specific effect of CAR signaling on lymphoid development in that model.

One possible reason for the general innate/NK-like bias observed in OP9-based systems versus the ATO may be lower levels or duration of DLL/Notch interactions in monolayer co-cultures compared to in tightly organized ATOs, given the requirement for high Notch signaling in both conventional T and ILC2 differentiation in mice and humans [54, 80, 81, 83]. Indeed, working with a T-iPSC OP9-based differentiation model, the Kawamoto group showed that while OP9-DL1 differentiation cultures were dominated by innate/NK-like cells, a minor population of conventional-type DP cells existed which upon TCR agonist engagement adopted a CD8 $\alpha\beta$ + mature phenotype, suggesting the potential for at least a subset of PSC-derived cells in monolayer systems to achieve a conventional T cell differentiation path [54]. The Kaneko group has also demonstrated the ability of CD3 stimulation and cytokine support during development to support or expand CD8 $\alpha\beta$ + T cells in OP9-based PSC cultures [146, 147], however differentiation of CAR-T cells using these refined monolayer approaches has not been reported to our knowledge.

More recently, a study using the ATO system and T-iPSCs lentivirally transduced with second generation CD19-targeted CD28 ζ or 4-1BB ζ CARs showed normal generation of polyfunctional CD8 $\alpha\beta$ + CAR-T cells that were cytotoxic both *in vitro* and *in vivo* against CD19-positive tumor cell lines [59]. In contrast to our findings, conventional $\alpha\beta$ T cell phenotypes were reported and ILC2 differentiation was not observed. While the study did not identify CARs that blocked T cell differentiation, the authors noted that despite the high level of CAR transgene expressed in the T-iPSC line, methylation of the transgenic EF-1a promoter during T cell

differentiation in ATOs led to diminished CAR expression during differentiation, a point contrast to our CAR vectors which used the *UBC* promoter and retained expression levels relatively well. CAR promoter methylation may therefore have fortuitously resulted in integrated signaling levels permissive of both T cell development and antigen-specific CAR-T cell responses in this situation.

Our findings also shed light on human T versus ILC2 lineage commitment, the timing and cues of which have yet to be fully elucidated. As a model of T and ILC2 development, modularity of the PSC ATO system and the ability to engineer the stromal cell component allowed us to show in this system that the T versus ILC2 lineage bifurcation occurs during the first 7 days of lymphoid differentiation in ATOs, and in fact likely between Day 0 and Day 4 when distinct T and ILC2 precursor clusters have already emerged. While we cannot infer from these developmental snapshots whether the CAR is delivering a supportive or instructive signal to promote ILC2 development, the reciprocal relationship with T cell differentiation strongly suggests a lineage-diverting mechanism, however this remains to be proven.

Indeed, common thymic progenitors have been identified that can give rise to both T cells and ILC2 [80, 81, 96, 138, 148], reinforcing the close relationship between these lineages and suggesting the existence of lineage-differentiating microenvironmental cues which have yet to be identified. Although non-physiologic, CAR signaling in our model provides a starting point for identifying molecular events in human T versus ILC2 lineage bifurcation to be further validated in primary models. For example, in addition to the signature of TCR/CAR activation discussed above, scRNA-seq of H1-CAR ATOs pointed to activation of IL-4 signaling in ILC2 precursors, a pathway previously implicated in ID2-mediated commitment of the ILC2 lineage in mice [138]. Whether this readout is confounded by transcriptional outputs from CAR signaling remains to be

determined, however we consider it highly likely that CAR signaling in our model is mimicking a physiologic cytokine signal required for ILC2 commitment *in vivo*.

Another interesting observation from our scRNA-seq data is the prominent CAR-specific upregulation of *ID3* in both H1-CAR ILC2-primed precursors and mature CAR-ILC2 cells, and its reciprocal pattern of expression with *ID2* in ILC2 and NK/ILC1 precursors. This contrasts with mouse ILC2 development in which *ID2* plays a central role [137, 149], and suggests a similarity between PSC-derived CAR-ILC2 and human neonatal circulating ILC2s which presumably develop during fetal life and have been characterized by a higher *ID3:ID2* ratio than adult ILC2s [150]. Thus, an intriguing possibility is that the ability of CARs to divert T cell differentiation to ILC2 from PSCs is a characteristic of fetal-like lymphopoiesis, as we have shown for certain aspects of PSC-derived CD8 T cell development in ATOs [50]. Supporting this hypothesis is the observation that CD19 CAR-transduced postnatal cord blood (CB) CD34+ HSPCs preferentially generated NK-like cells *in vitro* [46], a finding we have independently verified in the CB ATO system with the same CD19 CAR used in the present study (unpublished data). However, in contrast to PSC ATOs, the generation of low numbers of CD19-positive cells in CB ATOs may confound comparison of CD19 CAR signaling dynamics between PSC and CB systems.

3.3 Future studies

As discussed in 3.2, constitutive CAR expression using lentiviral based vectors can be problematic due to the high variability between different CARs, and this can lead to unpredictable and sometimes unfavorable outcomes during differentiation. Therefore, alternative genetic engineering strategies are needed, for example, expressing the CAR at later developmental stages using lineage specific promoters to avoid aberrant early activation during development. The timely

regulated expression will diminish the effect of CAR tonic signaling in differentiation and potentially serve as a universally applicable approach for any CAR, given that an ideal locus for CAR insertion exists. Promising candidate loci should meet the following requirements: a) it switches on strictly at a late developmental stage such as post selection mature SP8; b) it stays on further on to ensure constitutive expression of the CAR during expansion, activation, and tumor clearance; c) the promoter needs to be strong enough to drive sufficient CAR surface expression to be functional in antigen recognition and activation; d) CAR expression at that locus doesn't have disadvantages in cell survival, proliferation or cell fitness. This can also be combined with additional genetic manipulations in PSCs to enhance CAR T cell efficacy and *in vivo* persistency to make better effector cell products for cancer immunotherapies.

Although studies investigating roles of tumor infiltrating ILC2s are rather limited and sometimes conflicting in different models and different type of tumors, evidence of ILC2s facilitating tumor control is growing, therefore it is promising to target ILC2s in the tumor microenvironment in certain tumors to enhance tumor control [109-111]. It would also be interesting to generate engineered ILC2s alongside with T cells as cell-based immunotherapy. The CAR-ILCs could home to the tumor and synergize with CAR-T cells to improve tumor killing by direct activation of CD8⁺ T cells, or through recruiting and activating other immune cells in the tumor microenvironment such as dendritic cells, eosinophils, or NK cells.

A remaining question is the molecular mechanism of the CAR induced ILC2 diversion. We know from this study that the T versus ILC2 bifurcation happens during the first week of lymphoid differentiation in ATO, but the identity of the progenitor and precursor cell population responding to the CAR activation remains unclear, and the molecular events and signaling pathways downstream of TCR/CAR activation are yet to be identified. The scRNA-seq data

revealed activation of various cytokine signaling pathways in ILC2 precursors, including IL-4 signaling which is previously implicated in ID2-mediated commitment of the ILC2 lineage in mice [138], and TGF- β receptor signaling which is required for bone marrow ILC2p generation and upregulation of ST2 therefore indispensable for ILC2 development [96, 151]. We hypothesize that CAR activation in the ATOs may be mimicking physiological cytokine signals and playing a role in the T and ILC2 bifurcation in ATOs. Pharmacological manipulation could be used to test this. For example, supplying IL-4 or TGF- β during early development in non-transduced H1 ATOs could lead to increased development of ILC2s, and on the contrary, inhibition of IL-4 or TGF- β signaling in H1-CAR ATOs may potentially attenuate ILC2 predominance and result in normal T cell differentiation.

Although not physiologic, we here provide an *in vitro* model recapitulating human ILC2 development from PSCs for interrogating molecular changes during this process. While majority of the studies on ILC development utilize various transgenic mouse models, it is not always translatable to human. It is sometimes not feasible to obtain human equivalent materials so the use of PSCs as the starting culture gives an alternative opportunity. For example, we demonstrated that both the CAR induced ILC2 precursors and mature ILC2 cells showed upregulation of *ID3* while the NK/ILC1 population had high level of *ID2*. This stands in contrast to mouse ILC2 development where *ID2* is indispensable and is highly expressed in ILC2 progenitors and precursors [137, 149, 152, 153]. It has been reported that human cord blood ILC2s express higher *ID3* than *ID2* [150], so our finding here could suggest a novel role of *ID3* in human ILC2 differentiation, specifically human fetal-like lymphopoiesis. This can be tested by genetic inhibition of *ID3* in CAR expressing PSCs and see if it allows normal CAR T cell development or

by overexpression of *ID3* in wildtype PSCs to see if it drives ILC2 development in the ATOs. The same strategy can be applied to study other transcription factors as well.

REFERENCES

1. Kohn, L.A., et al., *Lymphoid priming in human bone marrow begins before expression of CD10 with upregulation of L-selectin*. Nat Immunol, 2012. **13**(10): p. 963-71.
2. Galy, A., et al., *Human T, B, natural killer, and dendritic cells arise from a common bone marrow progenitor cell subset*. Immunity, 1995. **3**(4): p. 459-73.
3. Le, J., et al., *Single-Cell RNA-Seq Mapping of Human Thymopoiesis Reveals Lineage Specification Trajectories and a Commitment Spectrum in T Cell Development*. Immunity, 2020. **52**(6): p. 1105-1118.e9.
4. Lavaert, M., et al., *Integrated scRNA-Seq Identifies Human Postnatal Thymus Seeding Progenitors and Regulatory Dynamics of Differentiating Immature Thymocytes*. Immunity, 2020. **52**(6): p. 1088-1104.e6.
5. Koch, U., et al., *Delta-like 4 is the essential, nonredundant ligand for Notch1 during thymic T cell lineage commitment*. J Exp Med, 2008. **205**(11): p. 2515-23.
6. Shah, D.K. and J.C. Zúñiga-Pflücker, *An overview of the intrathymic intricacies of T cell development*. J Immunol, 2014. **192**(9): p. 4017-23.
7. Taghon, T., E. Waegemans, and I. Van de Walle, *Notch signaling during human T cell development*. Curr Top Microbiol Immunol, 2012. **360**: p. 75-97.
8. Hao, Q.L., et al., *Human intrathymic lineage commitment is marked by differential CD7 expression: identification of CD7- lympho-myeloid thymic progenitors*. Blood, 2008. **111**(3): p. 1318-26.

9. Casero, D., et al., *Long non-coding RNA profiling of human lymphoid progenitor cells reveals transcriptional divergence of B cell and T cell lineages*. Nat Immunol, 2015. **16**(12): p. 1282-91.
10. Carpenter, A.C. and R. Bosselut, *Decision checkpoints in the thymus*. Nat Immunol, 2010. **11**(8): p. 666-73.
11. Biro, J., et al., *Regulation of T cell receptor (TCR) beta gene expression by CD3 complex signaling in immature thymocytes: implications for TCRbeta allelic exclusion*. Proc Natl Acad Sci U S A, 1999. **96**(7): p. 3882-7.
12. Klein, L., et al., *Positive and negative selection of the T cell repertoire: what thymocytes see (and don't see)*. Nat Rev Immunol, 2014. **14**(6): p. 377-91.
13. Moran, A.E. and K.A. Hogquist, *T-cell receptor affinity in thymic development*. Immunology, 2012. **135**(4): p. 261-7.
14. Perry, J.S.A., et al., *Distinct contributions of Aire and antigen-presenting-cell subsets to the generation of self-tolerance in the thymus*. Immunity, 2014. **41**(3): p. 414-426.
15. Verdegaal, E.M., et al., *Neoantigen landscape dynamics during human melanoma-T cell interactions*. Nature, 2016. **536**(7614): p. 91-5.
16. Rosenberg, S.A., et al., *Use of tumor-infiltrating lymphocytes and interleukin-2 in the immunotherapy of patients with metastatic melanoma. A preliminary report*. N Engl J Med, 1988. **319**(25): p. 1676-80.
17. June, C.H., S.R. Riddell, and T.N. Schumacher, *Adoptive cellular therapy: a race to the finish line*. Sci Transl Med, 2015. **7**(280): p. 280ps7.

18. Morgan, R.A., et al., *Cancer regression in patients after transfer of genetically engineered lymphocytes*. Science, 2006. **314**(5796): p. 126-9.
19. Kochenderfer, J.N., et al., *Eradication of B-lineage cells and regression of lymphoma in a patient treated with autologous T cells genetically engineered to recognize CD19*. Blood, 2010. **116**(20): p. 4099-102.
20. June, C.H., et al., *CAR T cell immunotherapy for human cancer*. Science, 2018. **359**(6382): p. 1361-1365.
21. Long, A.H., et al., *4-1BB costimulation ameliorates T cell exhaustion induced by tonic signaling of chimeric antigen receptors*. Nat Med, 2015. **21**(6): p. 581-90.
22. Frigault, M.J., et al., *Identification of chimeric antigen receptors that mediate constitutive or inducible proliferation of T cells*. Cancer Immunol Res, 2015. **3**(4): p. 356-67.
23. Watanabe, N., et al., *Fine-tuning the CAR spacer improves T-cell potency*. OncoImmunology, 2016. **5**(12): p. e1253656.
24. Hudecek, M., et al., *The nonsignaling extracellular spacer domain of chimeric antigen receptors is decisive for in vivo antitumor activity*. Cancer Immunol Res, 2015. **3**(2): p. 125-35.
25. Jonnalagadda, M., et al., *Chimeric antigen receptors with mutated IgG4 Fc spacer avoid fc receptor binding and improve T cell persistence and antitumor efficacy*. Mol Ther, 2015. **23**(4): p. 757-68.
26. Alabanza, L., et al., *Function of Novel Anti-CD19 Chimeric Antigen Receptors with Human Variable Regions Is Affected by Hinge and Transmembrane Domains*. Mol Ther, 2017. **25**(11): p. 2452-2465.

27. Majzner, R.G., et al., *Tuning the Antigen Density Requirement for CAR T-cell Activity*. *Cancer Discov*, 2020. **10**(5): p. 702-723.
28. Muller, Y.D., et al., *The CD28-Transmembrane Domain Mediates Chimeric Antigen Receptor Heterodimerization With CD28*. *Front Immunol*, 2021. **12**: p. 639818.
29. Kawalekar, O.U., et al., *Distinct Signaling of Coreceptors Regulates Specific Metabolism Pathways and Impacts Memory Development in CAR T Cells*. *Immunity*, 2016. **44**(3): p. 712.
30. Li, W., et al., *Redirecting T Cells to Glypican-3 with 4-1BB Zeta Chimeric Antigen Receptors Results in Th1 Polarization and Potent Antitumor Activity*. *Hum Gene Ther*, 2017. **28**(5): p. 437-448.
31. Feucht, J., et al., *Calibration of CAR activation potential directs alternative T cell fates and therapeutic potency*. *Nat Med*, 2019. **25**(1): p. 82-88.
32. Themeli, M., I. Rivière, and M. Sadelain, *New cell sources for T cell engineering and adoptive immunotherapy*. *Cell Stem Cell*, 2015. **16**(4): p. 357-66.
33. Plum, J., et al., *Human CD34+ fetal liver stem cells differentiate to T cells in a mouse thymic microenvironment*. *Blood*, 1994. **84**(5): p. 1587-93.
34. Anderson, G., et al., *MHC class II-positive epithelium and mesenchyme cells are both required for T-cell development in the thymus*. *Nature*, 1993. **362**(6415): p. 70-73.
35. Plum, J., et al., *Human T lymphopoiesis. In vitro and in vivo study models*. *Ann N Y Acad Sci*, 2000. **917**: p. 724-31.
36. Schmitt, T.M. and J.C. Zúñiga-Pflücker, *Induction of T cell development from hematopoietic progenitor cells by delta-like-1 in vitro*. *Immunity*, 2002. **17**(6): p. 749-56.

37. La Motte-Mohs, R.N., E. Herer, and J.C. Zúñiga-Pflücker, *Induction of T-cell development from human cord blood hematopoietic stem cells by Delta-like 1 in vitro*. *Blood*, 2005. **105**(4): p. 1431-9.
38. Trotman-Grant, A.C., et al., *DL4- μ beads induce T cell lineage differentiation from stem cells in a stromal cell-free system*. *Nature Communications*, 2021. **12**(1): p. 5023.
39. Reimann, C., et al., *Human T-lymphoid progenitors generated in a feeder-cell-free Delta-like-4 culture system promote T-cell reconstitution in NOD/SCID/ γ c(-/-) mice*. *Stem Cells*, 2012. **30**(8): p. 1771-80.
40. Seet, C.S., et al., *Generation of mature T cells from human hematopoietic stem and progenitor cells in artificial thymic organoids*. *Nat Methods*, 2017. **14**(5): p. 521-530.
41. Clay, T.M., et al., *Potential use of T cell receptor genes to modify hematopoietic stem cells for the gene therapy of cancer*. *Pathol Oncol Res*, 1999. **5**(1): p. 3-15.
42. Yang, L. and D. Baltimore, *Long-term in vivo provision of antigen-specific T cell immunity by programming hematopoietic stem cells*. *Proc Natl Acad Sci U S A*, 2005. **102**(12): p. 4518-23.
43. Malissen, M., et al., *Regulation of TCR α and β gene allelic exclusion during T-cell development*. *Immunology today*, 1992. **13**(8): p. 315-322.
44. Giannoni, F., et al., *Allelic exclusion and peripheral reconstitution by TCR transgenic T cells arising from transduced human hematopoietic stem/progenitor cells*. *Molecular Therapy*, 2013. **21**(5): p. 1044-1054.
45. Snauwaert, S., et al., *In vitro generation of mature, naive antigen-specific CD8+ T cells with a single T-cell receptor by agonist selection*. *Leukemia*, 2014. **28**(4): p. 830-841.

46. Maluski, M., et al., *Chimeric antigen receptor-induced BCL11B suppression propagates NK-like cell development*. J Clin Invest, 2019. **129**(12): p. 5108-5122.
47. Montel-Hagen, A. and G.M. Crooks, *From pluripotent stem cells to T cells*. Exp Hematol, 2019. **71**: p. 24-31.
48. Galic, Z., et al., *T lineage differentiation from human embryonic stem cells*. Proc Natl Acad Sci U S A, 2006. **103**(31): p. 11742-7.
49. Timmermans, F., et al., *Generation of T cells from human embryonic stem cell-derived hematopoietic zones*. J Immunol, 2009. **182**(11): p. 6879-88.
50. Montel-Hagen, A., et al., *Organoid-Induced Differentiation of Conventional T Cells from Human Pluripotent Stem Cells*. Cell Stem Cell, 2019. **24**(3): p. 376-389.e8.
51. Montel-Hagen, A., et al., *Generation of Artificial Thymic Organoids from Human and Murine Hematopoietic Stem and Progenitor Cells*. Curr Protoc, 2022. **2**(4): p. e403.
52. Rother, M.B., et al., *Decreased IL7Ra and TdT expression underlie the skewed immunoglobulin repertoire of human B-cell precursors from fetal origin*. Sci Rep, 2016. **6**: p. 33924.
53. Rechavi, E., et al., *Timely and spatially regulated maturation of B and T cell repertoire during human fetal development*. Sci Transl Med, 2015. **7**(276): p. 276ra25.
54. Maeda, T., et al., *Regeneration of CD8 $\alpha\beta$ T Cells from T-cell-Derived iPSC Imparts Potent Tumor Antigen-Specific Cytotoxicity*. Cancer Res, 2016. **76**(23): p. 6839-6850.
55. Vizcardo, R., et al., *Regeneration of Human Tumor Antigen-Specific T Cells from iPSCs Derived from Mature CD8 $^+$ T Cells*. Cell Stem Cell, 2013. **12**(1): p. 31-36.

56. Ueda, N., et al., *Generation of TCR-Expressing Innate Lymphoid-like Helper Cells that Induce Cytotoxic T Cell-Mediated Anti-leukemic Cell Response*. *Stem Cell Reports*, 2018. **10**(6): p. 1935-1946.
57. Themeli, M., et al., *Generation of tumor-targeted human T lymphocytes from induced pluripotent stem cells for cancer therapy*. *Nat Biotechnol*, 2013. **31**(10): p. 928-33.
58. Ueda, T., et al., *Non-clinical efficacy, safety and stable clinical cell processing of induced pluripotent stem cell-derived anti-glypican-3 chimeric antigen receptor-expressing natural killer/innate lymphoid cells*. *Cancer Sci*, 2020. **111**(5): p. 1478-1490.
59. Wang, Z., et al., *3D-organoid culture supports differentiation of human CAR(+) iPSCs into highly functional CAR T cells*. *Cell Stem Cell*, 2022.
60. Vivier, E., et al., *Innate Lymphoid Cells: 10 Years On*. *Cell*, 2018. **174**(5): p. 1054-1066.
61. Wang, S., et al., *Regulatory Innate Lymphoid Cells Control Innate Intestinal Inflammation*. *Cell*, 2017. **171**(1): p. 201-216.e18.
62. Colonna, M., *Innate Lymphoid Cells: Diversity, Plasticity, and Unique Functions in Immunity*. *Immunity*, 2018. **48**(6): p. 1104-1117.
63. Lim, A.I., et al., *IL-12 drives functional plasticity of human group 2 innate lymphoid cells*. *J Exp Med*, 2016. **213**(4): p. 569-83.
64. Ohne, Y., et al., *IL-1 is a critical regulator of group 2 innate lymphoid cell function and plasticity*. *Nat Immunol*, 2016. **17**(6): p. 646-55.
65. Bal, S.M., et al., *IL-1 β , IL-4 and IL-12 control the fate of group 2 innate lymphoid cells in human airway inflammation in the lungs*. *Nat Immunol*, 2016. **17**(6): p. 636-45.

66. Camelo, A., et al., *IL-33, IL-25, and TSLP induce a distinct phenotypic and activation profile in human type 2 innate lymphoid cells*. *Blood Adv*, 2017. **1**(10): p. 577-589.
67. Bernink, J.H., et al., *Interleukin-12 and -23 Control Plasticity of CD127(+) Group 1 and Group 3 Innate Lymphoid Cells in the Intestinal Lamina Propria*. *Immunity*, 2015. **43**(1): p. 146-60.
68. Cella, M., K. Otero, and M. Colonna, *Expansion of human NK-22 cells with IL-7, IL-2, and IL-1 β ; reveals intrinsic functional plasticity*. *Proceedings of the National Academy of Sciences*, 2010. **107**(24): p. 10961-10966.
69. Zhang, K., et al., *Cutting Edge: Notch Signaling Promotes the Plasticity of Group-2 Innate Lymphoid Cells*. *The Journal of Immunology*, 2017. **198**(5): p. 1798-1803.
70. Lim, A.I. and J.P. Di Santo, *ILC-poiesis: Ensuring tissue ILC differentiation at the right place and time*. *European Journal of Immunology*, 2019. **49**(1): p. 11-18.
71. Serafini, N., C.A.J. Vosshenrich, and J.P. Di Santo, *Transcriptional regulation of innate lymphoid cell fate*. *Nature Reviews Immunology*, 2015. **15**(7): p. 415-428.
72. Zook, E.C. and B.L. Kee, *Development of innate lymphoid cells*. *Nature Immunology*, 2016. **17**(7): p. 775-782.
73. Karamitros, D., et al., *Single-cell analysis reveals the continuum of human lympho-myeloid progenitor cells*. *Nat Immunol*, 2018. **19**(1): p. 85-97.
74. Lim, A.I., et al., *Systemic Human ILC Precursors Provide a Substrate for Tissue ILC Differentiation*. *Cell*, 2017. **168**(6): p. 1086-1100.e10.
75. Renoux, V.M., et al., *Identification of a Human Natural Killer Cell Lineage-Restricted Progenitor in Fetal and Adult Tissues*. *Immunity*, 2015. **43**(2): p. 394-407.

76. Montaldo, E., et al., *Human ROR γ t(+)CD34(+) cells are lineage-specified progenitors of group 3 ROR γ t(+) innate lymphoid cells*. *Immunity*, 2014. **41**(6): p. 988-1000.
77. Mebius, R.E., P. Rennert, and I.L. Weissman, *Developing lymph nodes collect CD4+CD3-LTbeta+ cells that can differentiate to APC, NK cells, and follicular cells but not T or B cells*. *Immunity*, 1997. **7**(4): p. 493-504.
78. Jones, R., et al., *Dynamic changes in intrathymic ILC populations during murine neonatal development*. *European Journal of Immunology*, 2018. **48**(9): p. 1481-1491.
79. Kernfeld, E.M., et al., *A Single-Cell Transcriptomic Atlas of Thymus Organogenesis Resolves Cell Types and Developmental Maturation*. *Immunity*, 2018. **48**(6): p. 1258-1270.e6.
80. Gentek, R., et al., *Modulation of Signal Strength Switches Notch from an Inducer of T Cells to an Inducer of ILC2*. *Front Immunol*, 2013. **4**: p. 334.
81. Ferreira, A.C.F., et al., *ROR α is a critical checkpoint for T cell and ILC2 commitment in the embryonic thymus*. *Nat Immunol*, 2021. **22**(2): p. 166-178.
82. Cosway, E.J., et al., *Eosinophils are an essential element of a type 2 immune axis that controls thymus regeneration*. *Science Immunology*, 2022. **7**(69): p. eabn3286.
83. Koga, S., et al., *Peripheral PDGFR α (+)gp38(+) mesenchymal cells support the differentiation of fetal liver-derived ILC2*. *J Exp Med*, 2018. **215**(6): p. 1609-1626.
84. Zook, E.C., et al., *The ETS1 transcription factor is required for the development and cytokine-induced expansion of ILC2*. *J Exp Med*, 2016. **213**(5): p. 687-96.
85. Yu, Y., et al., *The transcription factor Bcl11b is specifically expressed in group 2 innate lymphoid cells and is essential for their development*. *J Exp Med*, 2015. **212**(6): p. 865-74.

86. Califano, D., et al., *Transcription Factor Bcl11b Controls Identity and Function of Mature Type 2 Innate Lymphoid Cells*. *Immunity*, 2015. **43**(2): p. 354-68.
87. Klein Wolterink, R.G., et al., *Essential, dose-dependent role for the transcription factor Gata3 in the development of IL-5+ and IL-13+ type 2 innate lymphoid cells*. *Proc Natl Acad Sci U S A*, 2013. **110**(25): p. 10240-5.
88. Yagi, R., et al., *The transcription factor GATA3 is critical for the development of all IL-7Ra-expressing innate lymphoid cells*. *Immunity*, 2014. **40**(3): p. 378-88.
89. Hoyler, T., et al., *The transcription factor GATA-3 controls cell fate and maintenance of type 2 innate lymphoid cells*. *Immunity*, 2012. **37**(4): p. 634-48.
90. Walker, J.A., et al., *Bcl11b is essential for group 2 innate lymphoid cell development*. *J Exp Med*, 2015. **212**(6): p. 875-82.
91. Hosokawa, H. and E.V. Rothenberg, *Cytokines, Transcription Factors, and the Initiation of T-Cell Development*. *Cold Spring Harb Perspect Biol*, 2018. **10**(5).
92. Hosokawa, H., et al., *Cell type-specific actions of Bcl11b in early T-lineage and group 2 innate lymphoid cells*. *J Exp Med*, 2020. **217**(1).
93. Bando, J.K. and M. Colonna, *Innate lymphoid cell function in the context of adaptive immunity*. *Nat Immunol*, 2016. **17**(7): p. 783-9.
94. Shin, S.B., et al., *Abortive $\gamma\delta$ TCR rearrangements suggest ILC2s are derived from T-cell precursors*. *Blood Adv*, 2020. **4**(21): p. 5362-5372.
95. Harly, C., et al., *Development and differentiation of early innate lymphoid progenitors*. *J Exp Med*, 2018. **215**(1): p. 249-262.

96. Wong, S.H., et al., *Transcription factor ROR α is critical for nuocyte development*. Nat Immunol, 2012. **13**(3): p. 229-36.
97. Constantinides, M.G., et al., *A committed precursor to innate lymphoid cells*. Nature, 2014. **508**(7496): p. 397-401.
98. Klose, Christoph S.N., et al., *Differentiation of Type 1 ILCs from a Common Progenitor to All Helper-like Innate Lymphoid Cell Lineages*. Cell, 2014. **157**(2): p. 340-356.
99. Montaldo, E., et al., *Human ROR γ ⁺CD34⁺ Cells Are Lineage-Specified Progenitors of Group 3 ROR γ ⁺ Innate Lymphoid Cells*. Immunity, 2014. **41**(6): p. 988-1000.
100. Scoville, S.D., et al., *A Progenitor Cell Expressing Transcription Factor ROR γ ^t Generates All Human Innate Lymphoid Cell Subsets*. Immunity, 2016. **44**(5): p. 1140-50.
101. Chen, L., et al., *CD56 Expression Marks Human Group 2 Innate Lymphoid Cell Divergence from a Shared NK Cell and Group 3 Innate Lymphoid Cell Developmental Pathway*. Immunity, 2018. **49**(3): p. 464-476.e4.
102. Nagasawa, M., et al., *KLRG1 and NKp46 discriminate subpopulations of human CD117⁺CRTH2⁻ ILCs biased toward ILC2 or ILC3*. Journal of Experimental Medicine, 2019. **216**(8): p. 1762-1776.
103. Hernandez, D.C., et al., *An in vitro platform supports generation of human innate lymphoid cells from CD34(+) hematopoietic progenitors that recapitulate ex vivo identity*. Immunity, 2021. **54**(10): p. 2417-+.
104. Meininger, I., et al., *Tissue-Specific Features of Innate Lymphoid Cells*. Trends in Immunology, 2020. **41**(10): p. 902-917.

105. Jacquelot, N., et al., *Innate lymphoid cells and cancer*. Nature Immunology, 2022. **23**(3): p. 371-379.
106. Trabanelli, S., et al., *CD127+ innate lymphoid cells are dysregulated in treatment naïve acute myeloid leukemia patients at diagnosis*. Haematologica, 2015. **100**(7): p. e257-60.
107. Chevalier, M.F., et al., *ILC2-modulated T cell-to-MDSC balance is associated with bladder cancer recurrence*. J Clin Invest, 2017. **127**(8): p. 2916-2929.
108. Trabanelli, S., et al., *Tumour-derived PGD2 and NKp30-B7H6 engagement drives an immunosuppressive ILC2-MDSC axis*. Nat Commun, 2017. **8**(1): p. 593.
109. Jacquelot, N., et al., *Blockade of the co-inhibitory molecule PD-1 unleashes ILC2-dependent antitumor immunity in melanoma*. Nat Immunol, 2021. **22**(7): p. 851-864.
110. Moral, J.A., et al., *ILC2s amplify PD-1 blockade by activating tissue-specific cancer immunity*. Nature, 2020. **579**(7797): p. 130-135.
111. Kim, J., et al., *Intratumorally Establishing Type 2 Innate Lymphoid Cells Blocks Tumor Growth*. J Immunol, 2016. **196**(5): p. 2410-23.
112. Gomes-Silva, D., et al., *Tonic 4-1BB Costimulation in Chimeric Antigen Receptors Impedes T Cell Survival and Is Vector-Dependent*. Cell Rep, 2017. **21**(1): p. 17-26.
113. Artis, D. and H. Spits, *The biology of innate lymphoid cells*. Nature, 2015. **517**(7534): p. 293-301.
114. Yang, Q., et al., *T cell factor 1 is required for group 2 innate lymphoid cell generation*. Immunity, 2013. **38**(4): p. 694-704.

115. Morrow, M.A., et al., *Overexpression of the Helix-Loop-Helix protein Id2 blocks T cell development at multiple stages*. Mol Immunol, 1999. **36**(8): p. 491-503.
116. Lanigan, T.M., et al., *Real time visualization of cancer cell death, survival and proliferation using fluorochrome-transfected cells in an IncuCyte(®) imaging system*. J Biol Methods, 2020. **7**(2): p. e133.
117. Thomson, J.A., et al., *Embryonic stem cell lines derived from human blastocysts*. Science, 1998. **282**(5391): p. 1145-7.
118. Crook, J.M., et al., *The generation of six clinical-grade human embryonic stem cell lines*. Cell Stem Cell, 2007. **1**(5): p. 490-4.
119. Chin, C.J., et al., *Genetic Tagging During Human Mesoderm Differentiation Reveals Tripotent Lateral Plate Mesodermal Progenitors*. Stem Cells, 2016. **34**(5): p. 1239-50.
120. Evseenko, D., et al., *Mapping the first stages of mesoderm commitment during differentiation of human embryonic stem cells*. Proc Natl Acad Sci U S A, 2010. **107**(31): p. 13742-7.
121. Nicholson, I.C., et al., *Construction and characterisation of a functional CD19 specific single chain Fv fragment for immunotherapy of B lineage leukaemia and lymphoma*. Mol Immunol, 1997. **34**(16-17): p. 1157-65.
122. Imai, C., et al., *Chimeric receptors with 4-1BB signaling capacity provoke potent cytotoxicity against acute lymphoblastic leukemia*. Leukemia, 2004. **18**(4): p. 676-84.
123. Maher, J., et al., *Human T-lymphocyte cytotoxicity and proliferation directed by a single chimeric TCRzeta /CD28 receptor*. Nat Biotechnol, 2002. **20**(1): p. 70-5.

124. Dobin, A., et al., *STAR: ultrafast universal RNA-seq aligner*. *Bioinformatics*, 2013. **29**(1): p. 15-21.
125. Love, M.I., W. Huber, and S. Anders, *Moderated estimation of fold change and dispersion for RNA-seq data with DESeq2*. *Genome Biol*, 2014. **15**(12): p. 550.
126. Hao, Y., et al., *Integrated analysis of multimodal single-cell data*. *Cell*, 2021. **184**(13): p. 3573-3587.e29.
127. Bibby, J.A., et al., *Systematic Single Cell Pathway Analysis (SCPA) reveals novel pathways engaged during early T cell activation*. *bioRxiv*, 2022: p. 2022.02.07.478807.
128. Liu, C., et al., *Delineating spatiotemporal and hierarchical development of human fetal innate lymphoid cells*. *Cell Res*, 2021. **31**(10): p. 1106-1122.
129. Subramanian, A., et al., *Gene set enrichment analysis: a knowledge-based approach for interpreting genome-wide expression profiles*. *Proc Natl Acad Sci U S A*, 2005. **102**(43): p. 15545-50.
130. Kochenderfer, J.N., et al., *Construction and preclinical evaluation of an anti-CD19 chimeric antigen receptor*. *J Immunother*, 2009. **32**(7): p. 689-702.
131. Kowolik, C.M., et al., *CD28 costimulation provided through a CD19-specific chimeric antigen receptor enhances in vivo persistence and antitumor efficacy of adoptively transferred T cells*. *Cancer Res*, 2006. **66**(22): p. 10995-1004.
132. McFarland, A.P., et al., *Multi-tissue single-cell analysis deconstructs the complex programs of mouse natural killer and type 1 innate lymphoid cells in tissues and circulation*. *Immunity*, 2021. **54**(6): p. 1320-1337.e4.

133. Seillet, C., L. Brossay, and E. Vivier, *Natural killers or ILC1s? That is the question*. *Curr Opin Immunol*, 2021. **68**: p. 48-53.
134. Yudanin, N.A., et al., *Spatial and Temporal Mapping of Human Innate Lymphoid Cells Reveals Elements of Tissue Specificity*. *Immunity*, 2019. **50**(2): p. 505-519.e4.
135. Mjösberg, J.M., et al., *Human IL-25- and IL-33-responsive type 2 innate lymphoid cells are defined by expression of CRTH2 and CD161*. *Nat Immunol*, 2011. **12**(11): p. 1055-62.
136. Howard, E., et al., *PD-1 Blockade on Tumor Microenvironment-Resident ILC2s Promotes TNF- α Production and Restricts Progression of Metastatic Melanoma*. *Front Immunol*, 2021. **12**: p. 733136.
137. Moro, K., et al., *Innate production of T(H)2 cytokines by adipose tissue-associated c-Kit(+)/Sca-1(+) lymphoid cells*. *Nature*, 2010. **463**(7280): p. 540-4.
138. Qian, L., et al., *Suppression of ILC2 differentiation from committed T cell precursors by E protein transcription factors*. *J Exp Med*, 2019. **216**(4): p. 884-899.
139. Esensten, J.H., et al., *CD28 Costimulation: From Mechanism to Therapy*. *Immunity*, 2016. **44**(5): p. 973-88.
140. Eyquem, J., et al., *Targeting a CAR to the TRAC locus with CRISPR/Cas9 enhances tumour rejection*. *Nature*, 2017. **543**(7643): p. 113-117.
141. Ho, J.Y., et al., *Promoter usage regulating the surface density of CAR molecules may modulate the kinetics of CAR-T cells in vivo*. *Mol Ther Methods Clin Dev*, 2021. **21**: p. 237-246.

142. Hudecek, M., et al., *Receptor affinity and extracellular domain modifications affect tumor recognition by ROR1-specific chimeric antigen receptor T cells*. Clin Cancer Res, 2013. **19**(12): p. 3153-64.
143. Leick, M.B., et al., *Non-cleavable hinge enhances avidity and expansion of CAR-T cells for acute myeloid leukemia*. Cancer Cell, 2022.
144. Zhao, Z., et al., *Structural Design of Engineered Costimulation Determines Tumor Rejection Kinetics and Persistence of CAR T Cells*. Cancer Cell, 2015. **28**(4): p. 415-428.
145. Nishimura, T., et al., *Generation of rejuvenated antigen-specific T cells by reprogramming to pluripotency and redifferentiation*. Cell Stem Cell, 2013. **12**(1): p. 114-26.
146. Kawai, Y., et al., *Generation of highly proliferative, rejuvenated cytotoxic T cell clones through pluripotency reprogramming for adoptive immunotherapy*. Mol Ther, 2021. **29**(10): p. 3027-3041.
147. Minagawa, A., et al., *Enhancing T Cell Receptor Stability in Rejuvenated iPSC-Derived T Cells Improves Their Use in Cancer Immunotherapy*. Cell Stem Cell, 2018. **23**(6): p. 850-858.e4.
148. Elsaid, R., et al., *A wave of bipotent T/ILC-restricted progenitors shapes the embryonic thymus microenvironment in a time-dependent manner*. Blood, 2021. **137**(8): p. 1024-1036.
149. Miyazaki, M., et al., *The E-Id Protein Axis Specifies Adaptive Lymphoid Cell Identity and Suppresses Thymic Innate Lymphoid Cell Development*. Immunity, 2017. **46**(5): p. 818-834.e4.
150. Bennstein, S.B., et al., *Transcriptional and functional characterization of neonatal circulating Innate Lymphoid Cells*. Stem Cells Transl Med, 2021. **10**(6): p. 867-882.

151. Wang, L., et al., *TGF- β induces ST2 and programs ILC2 development*. Nature Communications, 2020. **11**(1): p. 35.
152. Xu, W., et al., *An Id2RFP-Reporter Mouse Redefines Innate Lymphoid Cell Precursor Potentials*. Immunity, 2019. **50**(4): p. 1054-1068.e3.
153. Wang, H.C., et al., *Downregulation of E Protein Activity Augments an ILC2 Differentiation Program in the Thymus*. J Immunol, 2017. **198**(8): p. 3149-3156.